The role of c-Jun in Schwann cell morphology and migration

Billy Ernest Jenkins

Thesis submitted for the degree of Doctor of Philosophy
University College London
May 2015

Declaration

I, Billy Jenkins, confirm that the work presented in this thesis is my own. Where information has been derived from other sources, I confirm that this has been indicated in the thesis.

Signed:

Date:

Abstract

Schwann cells of peripheral nerves undergo significant changes in morphology and gene expression during development and regeneration of the peripheral nervous system (PNS) after nerve injury. This plasticity is associated with the greater regenerative capability of the PNS compared with the CNS. The transcription factor c-Jun is highly expressed in Schwann cells following nerve injury and is required for the reprogramming of mature Schwann cells to become repair Schwann cells that promote regeneration. Mice with a Schwann cell-specific c-Jun deletion fail to generate these repair cells after nerve injury and consequently have a severe failure of axonal regeneration. One striking phenotype of Schwann cells lacking c-Jun is that in culture they lack normal bi- and tri-polar morphology and in the distal stump of injured nerve they form irregular and flattened profiles. I assessed whether the loss of c-Jun affected their ability to migrate, an important property of repair Schwann cells *in vivo* after nerve injury. Using two complementary *in vitro* assays, I revealed a significant reduction in cell migration and found that c-Jun deletion caused changes to the actin cytoskeleton and reduced the formation of focal adhesions. Nevertheless, performing quantitative polymerase chain reaction on a number of genes already known to regulate the cytoskeleton failed to reveal differences between RNA from c-Jun knockout Schwann cells and control RNA. I next investigated whether Schwann cell deletion of c-Jun leads to a reduction of Schwann cell migration and axonal outgrowth across the nerve bridge of the transected nerve. I developed an assay to create a nerve bridge that can be replicated easily in size and proximal-distal location. I achieved this by transecting the peroneal branch of the sciatic nerve while leaving the tibial branch intact to support the two nerve stumps. This method provides a useful model of nerve transection. The results reveal that in the c-Jun cKO mouse at 7 days after injury Schwann cells succeeded in migrating across the nerve bridge, but axons show poor re-entry into the distal nerve stump. This requires further investigation.

Acknowledgements

This thesis is dedicated to the memory of my mother, Safiye, who encouraged my love of science as a child. I am certain that I would not have undertaken this project had it not been for her inspiration and support. It brings me great sadness that she could not see the end of my work.

I thank my supervisors, Prof Kristjan Jessen and Prof Rhona Mirsky. This work would not have been possible without their support, guidance, teaching, and endless patience and understanding.

There are many colleagues who have given me valuable advice, support and knowledge during my time at UCL. In particular, I would like to thank Kristina, Shaline, Laura, José and Cristina for their humor, kindness and friendship.

I thank James for his immense support and understanding, without which, my work would have been so much harder.

I also thank my grandmother Munuse, for her endless love and support.

Finally, I thank the Wellcome Trust for providing the funding for my studentship.

Table of Contents

List of Figures

Abbreviations

ADS	Antibody diluting solution
AP-1	Activator protein-1
Ara-C	Cytosine arabinoside
ATF	Activating transcription factor
ATP	Adenosine triphosphate
BDNF	Brain-derived neurotrophic factor
BSA	Bovine serum albumin
BMP	Bone morphogenic protein
CAM	Cell adhesion molecule
cDNA	Complementary DNA
CMT	Charcot-Marie-Tooth disease
CNS	Central nervous system
CP	Capping protein
cyclicAMP	Cyclic adenosine monophosphate
dbcAMP	2'-O-dibutyryladenosine 3':5'-cAMP
DM	Defined medium
DMEM	Dulbecco's modified Eagles medium
DRG	Dorsal root ganglion
DNA	Deoxyribonucleic acid
ECM	Extracellular matrix
E day	Embryonic day
ERK	Extracellular signal-related kinase
FAK	Focal adhesion kinase
FCS	Fetal calf serum
FGF	Fibroblast growth factor
GAP	GTPase activating protein
GAPDH	Glyceraldehyde-3-phosphate dehydrogenase
GDI	Guanine dissociation inhibitor
GDNF	Glial derived neurotrophic factor
GFP	Green fluorescent protein
GEF	Guanine exchange factor
GTP	Guanosine triphosphate
HS	Horse serum
ICC	Immunocytochemistry
IF	Intermediate filament
IGF	Insulin growth factor
IHC	Immunohistochemistry
IL	Interleukin
JNK	c-Jun N-terminal kinase
KO	Knockout
LIMK	LIM kinase
MAG	Myelin associated glycoprotein
MAPK	Mitogen-activated protein kinase
MEF	Mouse embryonic fibroblast
MBP	Myelin basic protein
MLC	Myosin light chain
MMP	Matrix metalloprotease

NCAM	Neural-cell adhesion molecule
NGF	Nerve growth factor
NMJ	Neuromuscular junction
NRG1	β Neuregulin 1
NT	Neurotrophin
P0	Myelin protein zero
P75NTR	P75 neurotrophin receptor
PBS	Phosphate buffered saline
PCR	Polymerase chain reaction
P day	Postnatal day
PDGF	Platelet derived growth factor
PDL	Poly-D-lysine
PFA	Paraformaldehyde
PLL	Poly-L-lysine
PNS	Peripheral nervous system
RAG	Regeneration associated gene
ROCK	rho-associated, coiled-coil-containing protein kinase
RT-qPCR	Reverse transcription quantitative PCR
SCP	Schwann cell precursor
SEM	Standard error of the mean
SLI	Schmidt-Lanterman incisure
SRF	Serum response factor
TGF	Transforming growth factor
WASP	Wiskott Aldrich syndrome protein
WB	Western blotting
Wld^S	Wallerian degeneration slow
WT	Wildtype

bp	base pair
˚C	degrees Celsius
kb	kilobase
kDa	kilo Dalton
s	second
g	gram
mg	milligram
µg	microgram
L	litre
ml	milliliter
µl	microliter
mm	millimeter
µm	micrometer
M	molar
mM	millimolar
µM	micromolar

Chapter 1: General introduction

1.1 Schwann cells, the major glial cells of the peripheral nervous system

Schwann cells are the major glial cell type found in the peripheral nervous system (PNS). The term 'Schwann cell' encompasses several functionally distinct vertebrate glial cell types of common origin. Mature Schwann cells classically function to support motor and sensory neurons by facilitating the transmission of action potentials from sensory receptors to the central nervous system (CNS), or from the CNS to muscle fibers. The importance of this supporting role is most apparent when it is perturbed in neuropathies such as Charcot-Marie-Tooth disease, where mutations in Schwann cells can severely impair motor and sensory function. Although restricted to vertebrates in the literal sense, many invertebrates such as *Drosophila* possess peripheral glia that share many of the functions and characteristics of Schwann cells. This long evolutionary history hints at the essential functions these glial cells provide in the PNS, which are necessary for complex multicellular life.

1.1.1 Schwann cell subtypes.

Mature Schwann cells exist as myelinating and non-myelin-forming cell types. Myelin, a complex substance composed of a layered arrangement of proteins and lipids, provides electrical insulation along axons and accelerates action potentials by enabling saltatory conduction. Myelin is also synthesised by oligodendrocytes, the Schwann cell counterpart in the CNS. Myelinating Schwann cells are found in spinal nerves and nerve roots, where they each ensheath one large calibre axon (greater than 1 μm in diameter). Non-myelin-forming Schwann cells can be classified into several subtypes based on their location and function: Remak

Schwann cells, terminal Schwann cells and satellite Schwann cells. However, the term 'non-myelinating Schwann cell' is often applied to only the Remak Schwann cells. These are found in spinal nerves and nerve roots, and small-diameter axons are enveloped within invaginations of the Remak Schwann cell membrane, with the number of axons per cell ranging from one to over ten. Terminal Schwann cells are located at skeletal neuromuscular junctions (NMJ) and surround both the nerve terminal and synaptic cleft. Each NMJ typically contains one to three terminal Schwann cells, a number that varies with species and synapse size. Satellite Schwann cells of the sensory, sympathetic and parasympathetic ganglia are large, flattened cells covering the soma of sensory neurons (Armati 2007; Jessen & Mirsky 2005).

The PNS is also home to a number of other glial cell types (Fig. 1.1), which include olfactory ensheathing cells of the olfactory nerve, the enteric glia of the enteric nervous system and glia that reside at specialised sensory receptor nerve endings, such as the Pacinian corpuscle (Jessen & Mirsky 2005).

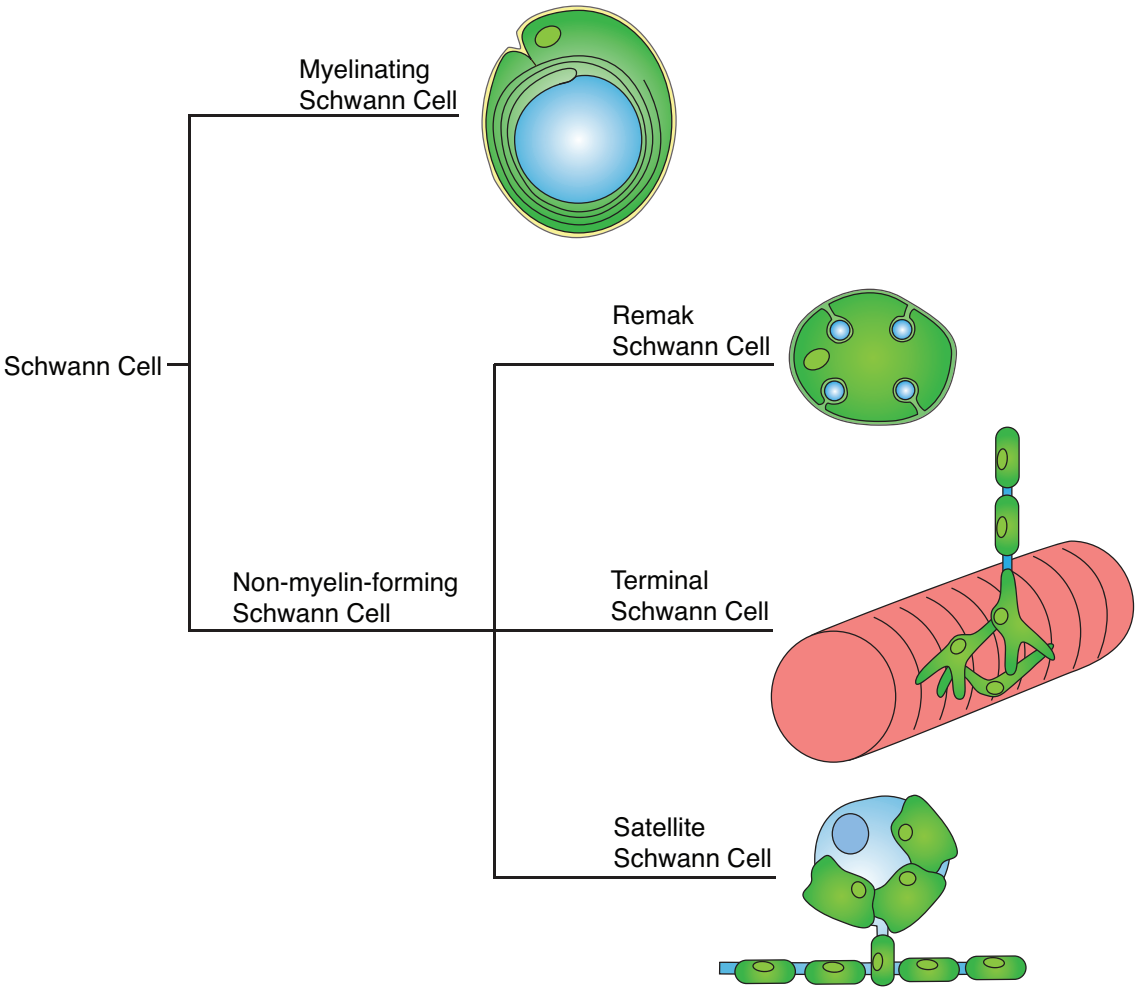

Figure 1.1: Schwann cell subtypes

The adult PNS is home to four specialised Schwann cell subtypes. Myelinating Schwann cells and Remak Schwann cells reside within spinal nerves and roots and associate intimately with axons. Terminal Schwann cells surround the synapses of skeletal muscle fibers and nerve terminals - the neuromuscular junction (NMJ), and satellite Schwann cells cover the soma of neurons in the PNS ganglia.

1.2 Schwann cell embryonic and postnatal development

All Schwann cells of the adult PNS are generated during development from the neural crest. Neural crest cells delaminate from the neuroepithelium and migrate along set pathways (Le Douarin & Kalcheim 1999). The Schwann cells of the nerve trunk originate from the neural crest cells that embark upon a ventral migration pathway, whereas Schwann cells of the dorsal and ventral roots and satellite Schwann cells of the dorsal root ganglia (DRGs) derive from both migrating neural crest cells and boundary cap cells. Boundary cap cells are the origin of the majority of glial cells in the nerve roots, and DRGs and are themselves derived from the neural crest (Jessen & Mirsky 2005; Maro et al. 2004).

Mature myelinating and Remak Schwann cells are generated from the neural crest via two intermediate cell types, the Schwann cell precursor (SCP) and the immature Schwann cell. The neural crest cell to SCP transition begins at E12-13 in the mouse (E14-15 in rat). Immature Schwann cells appear from E13-15 (E15-17 in rat) and persist until birth (Jessen et al. 1994; Dong et al. 1995; Dong et al. 1999). The cells of each stage differ widely in respect of their antigenic markers, cell morphology, motility, association with axons, interactions with the extracellular matrix (ECM) and their requirement for survival factors (Jessen & Mirsky 2005). The embryonic and postnatal development of boundary cap-derived Schwann cells, satellite Schwann cells and terminal Schwann cells has yet to be fully elucidated.

1.3 Schwann cell morphology and migration

1.3.1 Schwann cell precursor

1.3.1.1 Schwann cell precursor migration

'Primitive sheath cells', or Schwann cell precursors as they later became known, were first described in the tadpole fin owing to the easy visualisation of developing nerves within the embryo by light microscopy. These observations revealed an important characteristic of Schwann cell precursors *in vivo* is their ability to migrate - almost always in a proximal to distal manner, moving at an average rate of 60 μm/day and thus populating the entire nerve length with Schwann cells (Speidel 1932). In agreement with this, rat Schwann cell precursors exhibit a migration rate of 105 μm/hour *in vitro* (Jessen et al. 1994). As with the tadpole fin, the lateral line of the zebrafish has proven conducive for studying Schwann cell precursors *in vivo*. Live imaging using transgenic zebrafish expressing zFoxD3-GFP to label neural crest-derived cells, and the lipophilic dye DiD to label axons, reveals that as the axons extend along the lateral line, Schwann cell precursors migrate at the same rate, and at a distance of no more than 20 μm behind the axonal growth cone. In this study, Schwann cell precursors co-migrating with the growth cone were always observed to follow, not lead (Gilmour et al. 2002). Furthermore, additional studies have shown that and embryonic nerves are capable of reaching their final targets in the absence of Schwann cell precursors (Grim et al. 1992; Riethmacher et al. 1997; Woldeyesus et al. 1999).

Schwann cell precursors are also intimately associated with the growing peripheral nerve fronts in the mouse. Here, they are seen in contact with growth cones in the extreme periphery, close to the axonal targets. Schwann cell

precursors are even found to extend in front of the growth cone, providing a potential substrate for the growth cone to follow (Wanner, Mahoney, et al. 2006b). Genetic labelling of actin of the peripheral glia in Drosophila shows these cells also migrate with axons, as a continuous chain in the developing nerve. The leading cells of the chain extend filopodia, similar to those seen in the zebrafish, composed of actin and microtubules (Sepp et al. 2000; Sepp & Auld 2003).

The studies described above show that while the role of Schwann cell precursors in growth cone guidance remains unclear, they are integral to the growing nerve and co-exist with axons along their entire length during development. Although axons are capable of growing into the periphery in the absence of Schwann cell precursors, they are defasciculated and fail to innervate distal targets correctly (J. K. Morris et al. 1999).

For Schwann cell precursors to populate the entire nerve length, they must be either increasing in number by mitosis, continually differentiating from the neural crest, or a combination of the two, whilst concurrently keeping pace with the axons growing into the periphery. The progression from neural crest to Schwann cell precursors is poorly understood, but it is known that motor neurons arrest the migration of the Schwann cell precursor, as ablation of the ventral neural tube (and thus motor neurons) causes Schwann cell precursors to disperse from the ventral root area. Neural crest cell migration is not affected by the absence of motor neurons. The precise timing and location of Schwann cell precursor generation is not well characterised, but the observation that a subset of neural crest cells express myelin protein zero (MPZ) indicates that Schwann cell precursor differentiation begins before their association with axons at the ventral roots (Bhattacharyya et al. 1994; Bhattacharyya et al. 1991). It is suggested that the subset of neural crest cells destined to become Schwann cell precursors are

attracted to axons by contact or a diffusible cue (Bhattacharyya et al. 1994) and once they are at the nerve roots, these neural crest cells feed into chains of Schwann cell precursors that co-migrate with growth cones into the periphery (Klämbt 2010). Schwann cell precursors actively proliferate by mitosis whilst they are migrating along the growing axons (Speidel 1932). Thus, Schwann cell precursors achieve complete coverage of the nascent peripheral nerves by a combination of differentiation from the neural crest and cell division, while moving along the axons to settle in the periphery. The relative contributions of migration and proliferation to achieve complete coverage of the nerve are unclear. If proliferation is blocked, co-migration of peripheral glia and growth cones along the zebrafish lateral line is unaffected (Lyons et al. 2005), indicating that proliferation is not critical in this animal model.

1.3.1.2 Molecular control of Schwann cell precursor migration

Neuregulin 1 (NRG1) is critical for Schwann cell precursor generation and their migration, proliferation and survival (Jessen & Mirsky 2005). In mice deficient in NRG1 signalling (by knocking out NRG1, ErbB2 or ErbB3), neural crest cells fail to migrate past the level of the dorsal aorta along the ventromedial migration pathway, to the location of sympathetic ganglia formation (Britsch et al. 1998). These NRG1 mutants die from cardiac defects at embryonic day 11, however if this cardiac defect is rescued the mice can live until birth and the effect of NRG1 on Schwann cells may be determined. This reveals a severe depletion of Schwann cells in the peripheral nerve trunk (Riethmacher et al. 1997; Woldeyesus et al. 1999; J. K. Morris et al. 1999). As NRG1 signalling is critical to Schwann cell precursor survival and proliferation, it is difficult to tease out its role in cell migration using genetic mutants. In the zebrafish, it is possible to use pharmacological inhibitors of

ErbB3 to disrupt NRG1 signalling for a short period without inducing significant cell death. The effect of this is a dramatic decrease in Schwann cell precursor migration and an uncoupling of their co-migration with axonal growth cones. Cell migration along the lateral line resumes once the inhibitor is removed. NRG1 signalling inhibition also misdirects Schwann cell precursor movement in some cells, and Lyons et al. propose that NRG1 affects Schwann cell precursor directed migration and is continuously required for their motility, rather than simply allowing the cells to become competent at migrating (Lyons et al. 2005). In agreement with this, Schwann cell precursors deficient in ErbB3 have significantly reduced migration from DRG explants, but exogenous NRG1 does not enhance wildtype Schwann cell precursor migration (J. K. Morris et al. 1999). Recent work in zebrafish has shown that knocking down NRG1 type III directly leads to reduced migration along the pLL and overexpression of human NRG1 type III in neurons causes ectopic Schwann cell precursor migration (Perlin et al. 2011).

Dynamic remodelling of the actin cytoskeleton by the Rho family GTPases is crucial for cell motility (Raftopoulou & A. Hall 2004) and unsurprisingly, this holds true for the peripheral glia of Drosophila. Expression of constitutively active RhoA and Rac1 in these cells results in abrogated cell migration, however the over-expression or deletion of Cdc42 causes no migration phenotype (Sepp & Auld 2003). Rac1 and Cdc42 appear not to control Schwann cell precursor migration in the mammalian PNS, since genetic deletion of these proteins in Schwann cells at E12 does not lead to a deficit of Schwann cell numbers at E17.5 or affect their movement along axons (Benninger et al. 2007; Nodari et al. 2007).

1.3.1.3 Schwann cell precursor morphology and cytoskeletome

In vivo, Schwann cell precursors have extensive sheet-like processes that are in contact with compact axon bundles and other precursor cells. Electron microscopy observations have revealed the developing peripheral nerve contains very little extracellular matrix (ECM) at this point, although it is possible that some ECM is present. Schwann cell precursors lack a basal lamina and therefore make contact with axons and other precursors via their plasma membrane. Schwann cell precursors extend their sheet-like processes around the compact axon bundles and also within them, separating the bundles into smaller domains (Jessen et al. 1994). These flattened sheets are very elongated, longitudinally along the axon bundle (Wanner, Guerra, et al. 2006a). The pioneer Schwann cell precursors that follow closely behind axonal growth cones of the zebrafish lateral line have a dynamic and polarised shape, with filopodia at the front of the cell, characteristic of migrating cells (Gilmour et al. 2002). Similarly, at the nerve front of the developing mouse PNS, Schwann cell precursors extend lamellipodia and filopodia. These are observed both in contact with, and ahead of growth cones (Wanner, Mahoney, et al. 2006b). In culture, Schwann cell precursors are highly motile and form groups of highly flattened cells with many cell-cell contacts (Jessen et al. 1994).

Schwann cell precursors express vimentin, an intermediate filament (IF) that is often used as a marker of mesenchymal cells and is expressed throughout the Schwann cell lineage (Mirsky et al. 2001). Vimentin is known to induce cell migration in numerous cell types (Vuoriluoto et al. 2010; Gilles et al. 1999). Another IF protein, nestin, is expressed by Schwann cell precursors and this is also strongly associated with cell migration. GAP-43, which is expressed at high levels in growth cones and axons where it is involved in axon elongation and neurite

outgrowth, is also expressed by Schwann cell precursors (Curtis et al. 1992; Jessen et al. 1994; Dong et al. 1999). To date, the only Schwann cell precursor-specific marker is the cell adhesion molecule (CAM) N-cadherin. The absence of endoneurial space between the Schwann cell precursors is correlated with N-cadherin expression and the presence of extensive cell-cell contacts. N-cadherin expression is especially high in the Schwann cell precursors at the growing nerve front, in close proximity to the axonal growth cones (Wanner, Guerra, et al. 2006a).

1.3.2 Immature Schwann cell

The transition from Schwann cell precursor to immature Schwann cell takes place between E13-E15 in the mouse (and E15-E17 in rat). At this time, significant events in nerve organogenesis are taking place, such as increased production of ECM, vascularisation and establishment of the perineurium surrounding the nerve (Jessen & Mirsky 2005). The nature of the Schwann cell-axon relationship changes dramatically when Schwann cell precursors differentiate. Innervation of axonal targets is complete by this stage, and thus the requirement for Schwann cell colonisation of additional axonal territory and therefore longitudinal Schwann cell migration, is unnecessary. The most striking changes in immature Schwann cell spatial behaviour initially occur in the transverse plane of the nerve, in contrast to the longitudinal (proximal-distal) movement of Schwann cell precursors. Immature Schwann cells become arranged into groups or 'families' that share a common basal lamina and ensheath large bundles of axons. Surrounding these axon-Schwann cell families are endoneurial fibroblasts, blood vessels and ECM (Jessen & Mirsky 2005). Following this, another change in Schwann cell behaviour occurs, when Schwann cells start to elongate longitudinally to establish the presumptive myelin internode. Schwann cell elongation is necessary to maintain

coverage of the axon since the embryonic/neonatal nerve is continuously growing in length but the number of Schwann cells does not increase.

1.3.2.1 Radial sorting

Shortly after Schwann cell families are established, a process occurs whereby individual large diameter axons are isolated and ensheathed by a single Schwann cell. This has been termed 'radial sorting' and requires immature Schwann cells to extend radial lamellipodia into the axon bundle and segregate large diameter axons (Webster & Favilla 1984). The rearrangement of axon bundles by immature Schwann cells to form a 1:1 ratio of large diameter axons and Schwann cells, and also the generation of Remak Schwann cells containing multiple small diameter axons, requires remarkable precision and control over the Schwann cell cytoskeleton. The signals that control this process have slowly been revealed, and initial insights were gained from studying mouse models with axonal sorting phenotypes. Correct radial sorting is highly dependent on there being a sufficient number of Schwann cells in the nerve to segregate the axons, therefore proteins that have an effect on cellular proliferation, but not process extension can also perturb the sorting of axons.

The first axonal sorting phenotype identified was in dystrophic mice that have mutations in the basal lamina protein laminin 211, causing muscular dystrophy. Congenital muscular dystrophy 1A patients also lack the gene encoding the laminin $\alpha 2$ chain. Dystrophic mice have a sorting defect, in which bundles of naked axons remain, with no ensheathment by Schwann cells (Bradley & Jenkison 1973). Immature Schwann cells express the laminin receptor $\beta 1$-integrin, and its inactivation provides an almost complete block on myelination. Using mice in

which β1-integrin is conditionally deleted in Schwann cells, the block on myelination was shown to be due to a failure in radial sorting to generate pro-myelinating Schwann cells. These mice display a similar phenotype to dystrophic mice (Fernandez-Valle et al. 1994; Feltri et al. 2002). Additional radial sorting phenotypes have been found in mice with conditional deletions of genes encoding proteins downstream of laminin-integrin signalling, such as focal adhesion kinase (FAK) (Grove et al. 2007), Rac1 (Nodari et al. 2007) and integrin-linked kinase (ILK) (Pereira et al. 2009). Rac1 specifically has been linked to the extension of radial lamellipodia by Schwann cells that are necessary for the sorting of axons. Immature Schwann cells of the Rac1 cKO mouse have shorter processes and almost no radial lamellipodia. The presence of large-diameter axons within Remak bundles indicates a reduced ability for Rac1 KO Schwann cells to sort axons. Expression of a mutated form of the protein NF2 (also called merlin or schwannomin) from a gene in which exons 2 and 3 are deleted, to mimic the muted gene in NF2 patients, can partially rescue the defects in axial process length and myelination in Rac1 KO Schwann cells, but does not restore the normal abundance of radial lamellipodia (Guo et al., 2012). This finding suggests that Rac1 mediated axial process extension is somewhat dependent on NF2. It seems that NF2 is not involved in Rac1-dependent radial sorting, since the sorting defects observed in the Rac1 cKO mice are unchanged in the Rac1 cKO&NF2-del mice. There are now several interconnected pathways that have been identified in regulating Schwann cell-mediated radial sorting of axons (Figure 1.2).

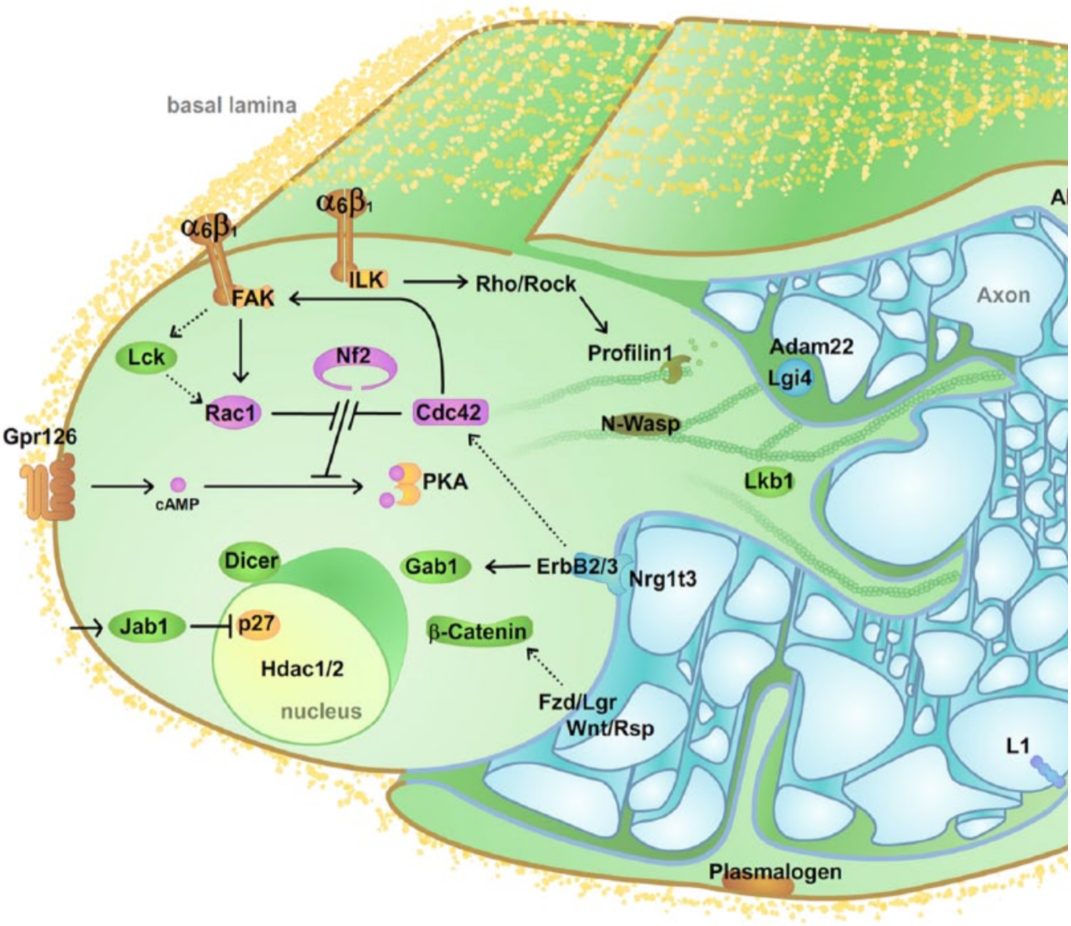

Figure 1.2: Radial sorting involves a number of molecular pathways.

An illustration of the molecular pathways involved in radial sorting of axons, adapted from Feltri et al, 2015. Depicted are two immature Schwann cells, inserting processes into an axon bundle. Cyclic AMP (cAMP), Dystroglycan (DG), Focal adhesion kinase (FAK), Grb2-Associated Binder (Gab), Gpr (G protein-coupled receptor), Histone deacetylase (Hdac), Integrin (α6β1, α7β1), Integrin-linked kinase (ILK), Jun activation domain–binding (Jab), lymphoid cell kinase (Lck), Leucine-rich-glioma inactivated (Lgi), Liver Kinase B (Lkb), Neurofibromin (Nf), Neural Wiskott–Aldrich syndrome protein (N-Wasp) and Protein Kinase A (PKA)

1.3.2 Myelinating Schwann cell

An immature Schwann cell that has become associated with a solitary large-diameter axon is termed a pro-myelinating Schwann cell. This is a transient stage, occurring before the onset of axonal ensheathment in the days following birth. Myelination begins when the leading edge of the Schwann cell inner-mesaxon starts to extend and wrap spirally around the axon. This extensive membrane synthesis and spiral wrapping of the axon generates the multi-lamella structure of myelin (Bunge et al. 1989). Parallels between the two morphological processes of myelination and cell migration can be seen, such as the requirement for actin polymerisation for membrane extension and the involvement of the RhoGTPases and other modulators of the actin cytoskeleton.

1.3.2.1 Cytoskeletal control of myelination

Actin polymerisation is required for myelination, as its inhibition in Schwann cell-neuron cocultures by cytochalasin D provides a complete block on myelination (Fernandez-Valle et al. 1997). Myosin II, an actin cross-linking protein that enables contraction of actomyosin bundles is also crucial for myelination, since its inhibition similarly blocks myelin formation *in vitro* (Wang et al. 2008). Thus it appears that in order for a Schwann cell to elaborate its myelin sheath around an axon, both actin polymerisation and actomyosin contraction are required. In support of this, several regulators of actin microfilament assembly/disassembly and myosin II activity described below are also regulators of myelination. An important caveat in studying the involvement of the cytoskeleton in myelination is the complication of the signals that drive membrane protrusion involved in ensheathment are similar to those required for the extension of radial lamellipodia

during radial sorting, as described earlier. To correctly implicate the involvement of specific cytoskeletal regulators in controlling myelination, radial sorting must first proceed normally and this makes *in vivo* evidence hard to obtain.

The actin-regulating RhoGTPases Cdc42 and Rac1 are both required for correct radial sorting (Benninger et al. 2007; Nodari et al. 2007), however some Schwann cells in these conditional knockout mice do progress to the pro-myelinating stage. These cells are arrested and do not go on to myelinate, indicating an involvement in both ensheathment and radial sorting for these two proteins (Feltri et al. 2008; Guo et al. 2012).

1.3.3 Bungner/denervated Schwann cell

The Bungner Schwann cell (also referred to as a denervated or dedifferentiated Schwann cell) is generated from both myelinating and non-myelinating Schwann cells of the mature nerve when they lose contact with axons. A nerve injury such as crush or transection will cause an axon to become separated from the perikaryon and then degenerate. The accompanying Schwann cells will lose contact with the axonal membrane. An unknown signal causes the Schwann cell to switch from a phenotype that can support the intact axon, for example by maintaining the myelin sheath and nodes of Ranvier, to a phenotype that is supportive of nerve repair. This repair program enables Bungner cells to provide an environment that is permissive for axon regrowth through the regenerating nerve; by secreting trophic factors, expressing surface molecules that interact with axons, recruiting macrophages to clear debris from the nerve, remodelling the extracellular matrix and forming guidance conduits called Bands of Büngner. (Arthur-Farraj et al. 2012). These functions are distinct from those of the immature Schwann cell, which share similar antigenic markers and the process of generating Bungner

Schwann cells has been referred to as 'transdifferentiation' rather than 'dedifferentiation'. Another important difference is that Bungner Schwann cells are for the most part without any axonal contact. All other cells of the Schwann cell lineage are in constant association with axons. The Bungner Schwann cell will quickly re-differentiate into a myelinating or non-myelinating Schwann cell when contact is re-established.

1.3.3.1 Bungner/denervated Schwann cell migration

Bungner Schwann cells are highly motile, a characteristic that is important for effective nerve regeneration, for example in bridging the gap between two transected nerve stumps. The first observations of Schwann cell motility were of Bungner/denervated Schwann cells spreading out from explants of degenerating peripheral nerves – the observations of migrating Schwann cell precursors by Speidel were made some time later. Ingebrigtsen recorded cells migrating from the nerve explant approximately five days after being in culture and hypothesised the same behaviour might take place *in vivo* following nerve transection (Ingebrigtsen 1913). To date, the vast majority of studies that consider the molecular control of Schwann cell migration have utilised cultured Bunger/denervated Schwann cells, and many of these have wrongly been used as an *in vitro* model to understand Schwann cell precursor migration during development. For this reason, *in vitro* studies for Bungner Schwann cell migration are plentiful, but there are few *in vivo* studies of the molecular control of their migratory behaviour during nerve regeneration.

1.3.3.2 Molecular control of Bungner/denervated Schwann cell migration

1.3.3.2.1 Neuregulin

NRG1 stimulation of ErbB2/3 is required for the persistent and directed migration of Schwann cell precursors, as discussed previously (Section 1.3.1.2). Some studies have used denervated Schwann cell cultures to provide indirect *in vitro* evidence for the role of NRG1 in Schwann cell precursor migration, since the precursor requires NRG1 for its survival. Expression of NRG1 isoforms and ErbB2/3 in the distal nerve stump increases following injury, first detectable at 3 days (Fricker et al. 2013). Mahanthappa et al. found that secreted NRG1 (also known as Glial Growth Factor 2) increases the motility of denervated Schwann cells at concentrations insufficient to induce proliferation (Mahanthappa et al. 1996). Later studies have implicated several signalling pathways in NRG-ErbB2/3 induced Schwann cell migration; these include MAPK, Rac1/Cdc42-JNK and Shp2-Src-FAK (Meintanis et al. 2001; Yamauchi et al. 2008; Grossmann et al. 2009). Expression of the fibronectin receptor integrin $\alpha5\beta1$ is increased in the Bungner Schwann cell after nerve crush. Integrin $\alpha5\beta1$ forms a protein complex with ErbB2 and FAK after both crush (*in vivo*) and stimulation with NRG (*in vitro*). siRNA knockdown of the integrin $\alpha5$ subunit is sufficient to significantly reduce the pro-migratory effect of NRG on denervated Schwann cell cultures grown on laminin, collagen and fibronectin substrates (Wakatsuki et al. 2013).

Terminal Schwann cells, which are of the same origin as the myelinating and non-myelinating Schwann cells also respond to activation of NRG1-ErbB2 by becoming motile. Hayworth et al. show that inducible expression of a constitutively active ErbB2 receptor in terminal Schwann cells results in them

developing extensive sprouts and migrating away from motor endplates, as seen following nerve injury (Hayworth et al. 2006).

1.3.3.2.2 Neurotrophins

Neurotrophins are a class of secreted growth factors that support the growth, development and function of neurons, expression of many members is increased as part of the regenerative process that occurs following nerve injury. Specifically, expression of nerve growth factor (NGF), brain derived neurotrophic factor (BDNF), neurotrophin-4 (NT-4) and the receptors p75NTR and TrkC are upregulated in the distal nerve stump after injury (Heumann et al. 1987; Meyer et al. 1992; Funakoshi et al. 1993).

Schwann cells show enhanced migration from nerve explants in the presence of NGF (Anton, Weskamp, et al. 1994b). Another study has shown that deletion of Schwann cell p75NTR, the binding partner of NGF, has negligible effect on the migration of Schwann cell precursors (Bentley & Lee 2000). Yamauchi et al. have shown that BDNF inhibits Bungner Schwann cell migration by binding to p75NTR and initiating a signalling cascade involving Src, Vav2 and Rho A (Yamauchi et al. 2004). They have also found that neurotrophin-3 (NT-3) stimulates migration of cultured Schwann cells via TrkC, although the relevance of this to nerve regeneration is unclear, since NT-3 expression decreases within the weeks following nerve injury (Yamauchi et al. 2003; Funakoshi et al. 1993).

1.3.3.2.3 Extracellular matrix

Mature Schwann cells of the nerve reside within endoneurial tubes (also called the endoneurium), which is the innermost layer of connective tissue surrounding the

nerve fiber. The Schwann cell basal lamina is composed of proteins such as laminin, fibronectin and collagen. These proteins are currently used in nerve guidance repair conduits, partly due to their ability to enhance Schwann cell and neuronal growth cone migration.

Upon nerve transection, Schwann cells have been observed to crawl along the tubes in the distal stump and migrate out of the proximal end (Holmes & Young 1942; Holmes et al. 1940). At the inter-stump gap, Schwann cells migrate across a cellular bridge formed by inflammatory cells and fibroblasts of the perineurium (Rexed 1942). Fibronectin is strongly expressed in the nerve bridge and enhances denervated Schwann cell migration via α5-integrin (Lefcort et al. 1992; Baron-Van Evercooren et al. 1982). Collagens V and IV are major constituents of the endoneurial and perineurial basal laminae and promotes migration of cultured Bungner Schwann cells. Binding of syndecan 3 on the Schwann cell membrane to collagen V induces Erk1/2 activation and Schwann cell migration (Erdman et al. 2002).

The predominant laminin isoforms present in the Schwann cell basal lamina are laminins 2 and 8 (Feltri & Wrabetz 2005). Blocking of laminin 2 inhibits Schwann cell migration, and both laminin 1 and 2 enhance Schwann cell migration in *vitro* through interactions with β1-integrin (Anton, Sandrock, et al. 1994a; Milner et al. 1997).

1.4 The cytoskeleton

In common with many other fundamental components of cell biology, the cytoskeleton was first described from observations made in the nervous system. The first illustration of the cytoskeleton was made by Robert Remak in 1844, where he noted delicate fibrils within the ganglion cell of the crayfish (Remak, 1844). The significance of this observation went largely unrealised in the proceeding decades, and was even contradicted by Thomas Huxley, who described the content of the crayfish ganglion as "perfectly pellucid, and without the least indication of structure" (Huxley, 1880). This ambiguity was removed when Sigmund Freud reported identical observations to Remak, "The nerve cells in the brain and in the ventral ganglionic chain consist of two substances, one of which is arranged as a network in the fibrils of the nerve fibers, and the other is homogeneously continuous in between" (Freud, 1882). The structures observed by Remak and Freud were later termed neurofibrils by Apáthy and Bethe (Frixione, 2000).

The first questions this finding posed to these early cell biologists was that of the function of the filaments within the neuron, and whether they are present in other cells. Ramón y Cajal correctly predicted that neurofibrils did not have a specific role in the conduction of nerve impulses, a conclusion he came to as similar filaments had been discovered in many other cell types, such as epithelial and egg cells (R. Cajal, 1903). Around the same time, Walther Flemming provided another example of intracellular filaments and significantly, observed their first known function within the cell, describing the involvement of "pale threads" in the transport of chromosomes during cell division (Flemming, 1880). By the turn of the 20th Century, biologists had observed what we now know as intermediate filaments and microtubules, and found at least one role for these structures.

The evolving view of the cytoplasm as an environment of great biochemical complexity, playing host to the multitude of metabolic processes being discovered at that time, led Rudolph Peters to postulate that an intracellular three-dimensional protein network might provide the necessary structure to allow complex metabolism in the cell (Peters 1930). The French embryologist Paul Wintrebert coined the term cytoskeleton, or "cytosquelette" to describe an idea shared with Edwin Conklin, that 'there must be in existence a network within the cell that will properly redistribute intracellular contents following mechanical disorganisation' (Conklin 1917, Frixione, 2000).

The advent of electron microscopy enabled further examination of the neurofibrils described by Remak. Studies of disrupted nerves allowed the visualisation of long, tubular structures within the axon, termed "neurotubules" and today known as microtubules (De Robertis & Schmitt 1948) and thin intra-axonal filaments (Schmitt & Geren 1950) which were later termed neurofilaments (Gray & Guillery 1961). The cytoskeleton as we know it today is composed of three types of filaments; microtubules, intermediate filaments and microfilaments (F-actin). The latter had not been visualised during this early era of cell biology, however the discovery of myosin in contractile muscle led scientists to find its binding partner, actin (Straub 1943).The finding that myosin decorated actin filaments with a characteristic 'arrowhead' configuration allowed researchers to detect the presence of F-actin in many other cell types (Moore et al. 1970; Ishikawa et al. 1969)

The three filament types that form the cytoskeleton often span tens or hundreds of micrometres and are formed by the repetitive assembly of many tiny subunits. Rapid assembly and disassembly of these subunits allows the cell to quickly form or break the cytoskeletal structures necessary for organelle transport

and cell motility. An array of accessory proteins regulate the spatial distribution and behaviour of the cytoskeleton subunits or polymers, allowing the cell to integrate extracellular or intracellular signals to trigger dynamic transformations of the cytoskeleton for events such as phagocytosis, organelle transport and cell movement. In the following sections, I will describe the molecular biology of these cytoskeletal proteins, with an emphasis on their role in cell migration.

1.4.1 The actin cytoskeleton

Proteins belonging to the actin family are capable forming filaments (F-actin), which can assemble and disassemble as required by the cell. There are six highly conserved actin isoforms, however only two (β-actin and γ-actin) are expressed in the majority of cells. Actin monomers are also referred to as G-actin due to their globular form, and to distinguish them from their polymerised form, F-actin. Actin has a molecular weight ~42 kDa. Actin polymerisation at the leading edge of a migrating cell provides the force that allows the cell membrane to extend forward. This protrusion at the front of the cell is called the lamellipodium and its extension is driven by the assembly of actin monomers into filamentous actin, in a process known as treadmilling (Pollard & Borisy, 2003).

β-actin is the isoform of actin most implicated in cell migration and morphology. It is extremely well conserved across most species, with approximately 80% similarity between the yeast and human forms of the protein. The reason for this is probably due to the very large numbers of proteins that interact with actin, thus limiting the variability of actin binding sites. It is the most abundant protein in the cell cortex, and the most abundant protein overall in many cell types (Pollard & Borisy 2003). An important feature of actin is its ability to

hydrolyse ATP, which acts as a timer for the stability of F-actin (Bugyi & Carlier 2010).

1.4.1.1 Actin nucleation

Most ATP-bound actin monomers in the cell exist in a complex with the accessory protein profilin, which catalyses the exchange of ADP to ATP. This act of sequestering the ATP-actin available for polymerisation into F-actin is an important step in the temporal and spatial control of actin filament growth. Thymosin β4 is another protein that helps to sequester actin monomers in the cytoplasm, and both these actin-binding proteins suppress the spontaneous nucleation of actin monomers that generates F-actin (Chesarone & Goode 2009).

In order to overcome the barriers that prevent the dynamic formation of F-actin, cells express an array of factors that act as a seed for the polymerisation of an actin filament, these are called 'nucleation factors' and exist as 3 classes, based on the mechanism by which they enable filamentous actin assembly. Class 1 nucleation factors include the Arp2/3 complex and N-WASP/SCAR. These proteins mimic G-actin monomers, providing part of the nucleus from which F-actin can elongate (Fig. 1.3). Importantly, Arp2/3 can only initiate F-actin polymerisation when bound to an already present actin filament, and results in the nascent actin filament growing out at an angle of 70° to generate a branch (Chesarone & Goode 2009).

Formins are the protein family that form class 2 of the actin nucleation factors. They catalyse the formation of F-actin by capturing spontaneously formed actin dimers and trimers via their FH2 domains. Unlike Arp2/3, which remains associated with the pointed end of the growing actin filament, formins move with

the growing barbed end, ready to insert additional actin subunits (Pring et al. 2003). Unlike Arp2/3, formins do not require an existing actin filament to induce actin polymerisation.

The third class of actin nucleation factors includes Spire, first identified in Drosophila. Spire has four WASP homology 2 (WH2) domains, each of which recruit an actin monomer and align them to form the F-actin nucleus (Quinlan et al. 2005).

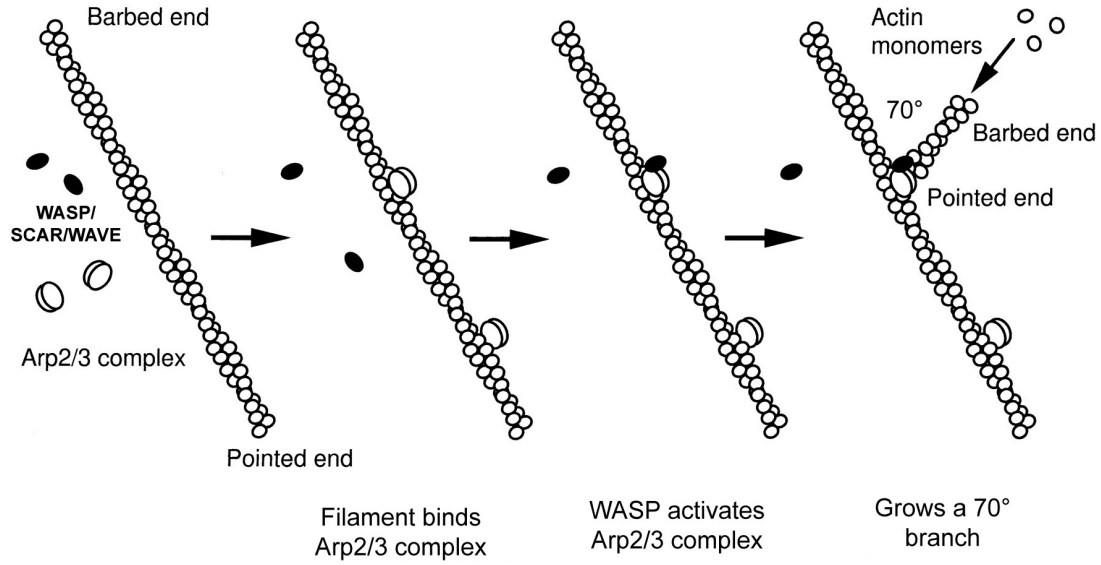

Figure 1.3. Arp2/3 interacts with F-actin

Arp2/3 nucleates a new actin filament after activation by members of the WASP/SCAR/WAVE family. The new actin filament is capped at its pointed end, and grows from its barbed end at an angle of 70° from the existing actin filament. Adapted from (Machesky et al. 1999).

1.4.1.2 Actin elongation, treadmilling and disassembly

Once actin filament polymerisation is initiated, F-actin continues to extend at its barbed end until it is either abrogated by a capping protein, or the pool of free ATP-actin is exhausted. The cell expresses a class of proteins, referred to as actin elongation proteins, which shield the barbed end from these capping proteins and allowing the barbed end to continue extending. Formins constitute one member of this class, since they remain attached to the barbed end of the F-actin via their FH2 domains. Another member is Ena/VASP, which seems to have a less potent anti-capping ability than formin. There are conflicting reports on the protection it offers to the barbed end, although it seems to depend on Ena/VASP concentration (Bear & Gertler 2009). It is clear, however, that both formins and Ena/VASP accelerate the rate of F-actin elongation, up to 5-fold and 7-fold respectively (Chesarone & Goode 2009).

Treadmilling refers to the scenario where each end of the actin (and microtubule) filament possesses a different affinity for addition of subunits (Critical concentration, C_c). The barbed end of F-actin has a lower C_c than the pointed end, meaning that ATP-actin-monomers bind more easily. If the concentration of cytosolic free ATP-actin is higher than the C_c of the barbed end and pointed end, polymerisation will occur at both. If it is less, then disassembly will take place at both ends. In reality, the presence of actin-binding proteins such as Arp2/3, formins and capping proteins will prevent the free association of G-actin at either the pointed or barbed end. Actin treadmilling takes place when actin monomers are being added to the barbed end, whilst being removed at the pointed end. If the rate of these is the same, it is called 'steady state treadmilling'. As actin will slowly hydrolyse ATP into ADP, there exists a gradient along the actin

filament, with the barbed end containing ATP-bound actin monomers and the pointed end composed of mostly ADP-bound actin (Bugyi & Carlier 2010).

In order for actin treadmilling to proceed, a constant supply of ATP-actin is required. As mentioned previously, the G-actin binding protein profilin captures ADP-actin monomers, catalyses the transfer of ADP to ATP and delivers them to the barbed end of the growing actin filament. This process requires the supply of ADP actin, which is removed from the pointed end of F-actin by ADF/Cofilin, which speeds up F-actin disassembly and therefore the liberation of ADP-actin. Cofilin does this by increasing actin disassembly at the pointed end, and also by severing F-actin and exposing more pointed ends from which ADP-actin can disassemble. Gelsolin is another F-actin severing protein that promotes disassembly (Bugyi & Carlier 2010).

1.4.1.3 Capping protein

F-actin Capping Protein (CP) is a heterodimeric protein that binds tightly to the barbed end of F-actin, preventing the addition or subtraction of any actin monomers. CP is associated with lamellipodia protrusion and cell migration, since it prevents excessive elongation of F-actin and promotes Arp2/3 induced actin nucleation and branching. Lack of CP leads to the formation of filopodia (Takeda et al. 2010).

1.4.1.4 Actin cross-linking/bundling proteins

There are several classes of actin-binding proteins that can bind and cross-link two or more actin filaments. These can be classified depending on the type of macrostructure they form and are often associated with certain cellular

specialisations (Fig. 1.4). Filopodia and microvilli require actin bundling proteins, such as villin and fimbrin to extend parallel, unbranched bundles of F-actin away from the plasma membrane. These are found in many cell types, including intestinal epithelial cells and Schwann cells. In contrast, lamellipodia require a branched actin network, where cross-linking proteins such as Arp2/3, filamins and spectrins hold two F-actins at angles of up to 90 degrees. This creates the 3-dimensional mesh of actin filaments found in the cell cortex and is required for the extension of lamellipodia for cell migration, or other cell morphogenetic events such as radial sorting by Schwann cells.

Actin bundles can be further divided between those that allow/disallow the binding of another actin-binding protein, myosin II. Myosins are a superfamily of motor proteins that hydrolyse ATP, bind actin and can exert mechanical force. They are classically known to be involved in muscle fiber contraction, but are also important in cell motility (Cramer 2013). The presence of myosin II in actin bundles allows them to become contractile by sliding actin filament across one another. Contractile bundles are formed by F-actin cross-linking proteins such as α-actinin and are found in actin stress fibers. The role of myosin II and actin stress fibers in cell migration will be discussed later.

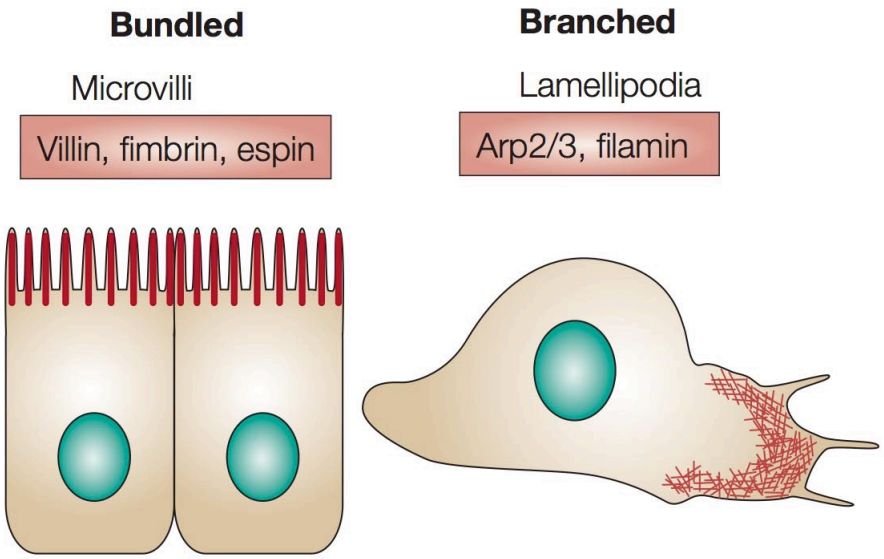

Figure 1.4. Actin macrostructures.

Actin filaments can be arranged into macrostructures that consist of either bundled, parallel filaments, e.g. microvilli, or as branched networks such as lamellipodia. Each structure is generated by a specific actin cross-linking protein. Adapted from (Revenu et al. 2004),

1.4.1.5 Rho GTPases

The Rho family of GTPases are small G proteins that cycle between active (GTP-bound) and inactive (GDP-bound) states, acting as molecular switches (Fig. 1.5). The active 'on' and inactive 'off' states are controlled by two classes of proteins: Guanine Exchange Factors (GEFs) and GTPase Activating Proteins (GAPs). There are 20 members of the Rho family in mammals, the most studied of these being RhoA, Rac1 and Cdc42 (A. Hall 1998).

The Rho GTPases are primarily known for their role in actin cytoskeleton remodelling, but have numerous other functions in the cell, including promoting gene transcription, cell polarity and microtubule dynamics (Etienne-Manneville & A. Hall 2002). They play a critical role in integrating intracellular and extracellular signals to control the cytoskeleton, and thus cell morphology and migration.

It has been uncovered through the use of dominant negative and constitutively active forms of RhoA, Rac and Cdc42 these three GTPases control different aspects of actin dynamics. RhoA regulates the formation of contractile actin-myosin stress fibers, Rac promotes the polymerisation of actin to form lamellipodia, and Cdc42 promotes actin polymerisation to form filopodia. The signals that regulate these proteins, and their downstream effectors are too numerous to go into detail here, but these will be further discussed in the context of cell migration.

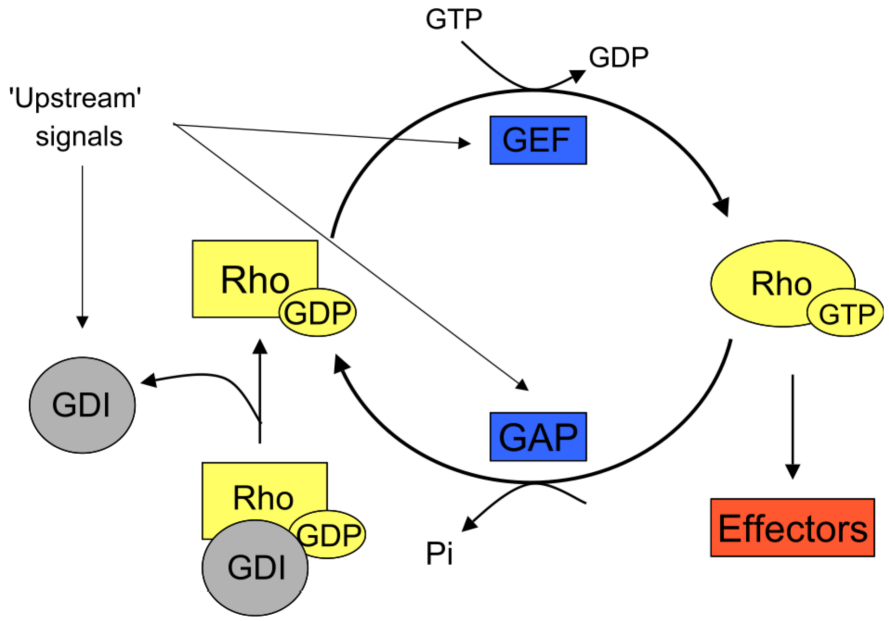

Figure 1.5. Rho GTPases act as molecular switches

The RhoGTPases cycle between an active (GTP-bound) state and inactive (GDP-bound) state. This cycle is controlled by Guanine Exchange Factors (GEFs), GTPase Activating Proteins (GAPs) and Guanine Dissociation Inhibitors (GDIs). Adapted from (Raftopoulou & A. Hall 2004)

1.5 Regulation of cell migration

Motility is a fundamental cellular process, necessary for development, tissue regeneration and wound healing, formation of neuronal connections and immune responses. The mechanism by which most cells migrate remains the same amongst organisms as diverse as protozoa and mammals, and involves (i) the protrusion of the cell front and forward displacement of cytoplasm through rapid branched actin polymerisation, (ii) attachment of the advancing plasma membrane to a substrate, (iii) contraction of actin-myosin stress fibers to translocate the cell body, (iv) release of focal adhesions at the cell rear, and finally (v) the recycling of cell membrane and proteins from the cell rear.

Cells migrate in response to a number of external signals, including chemical and mechanical factors. Mechanotaxis refers to the directed motility of cells in response to cues such as fluidic shear stress and substrate rigidity (Lo et al, 2000). Chemotactic signals are diffusible chemicals that form a gradient in the medium, and include an array of proteins and lipids that affect cell motility. Perhaps the best known are chemokines, a subset of cytokines that induce chemotaxis. Examples of these include Interleukin-1 and CCL5. These diffusible signals bind to an array of complementary receptors on cells and activate intracellular cell signalling pathways that lead to rearrangement of the actin and microtubule cytoskeletons. ECM is a further cue for directed cell migration, and the induction of cell motility by adherence to a gradient of chemoattractants is referred to as haptotaxis, and plays a major role in successful wound healing. In addition to the aforementioned types of cell migration, contact inhibition of locomotion provides another means for directed cell movement. In this case, a group of cells collide and cease movement in the direction of collision. Contact

inhibition of locomotion is regulated by a number of cell surface proteins, such as cadherins, delta-notch, integrins, ephrins and nectins, and these signal to a number of cytoskeletal regulatory proteins, including RhoA and ROCK (Mayor and Carmona-Fontaine, 2010).

The initial polymerisation of actin and extension of lamellipodia and filopodia results from signal transduction, normally from an extracellular cue such as a chemoattractant or the extracellular matrix. These signals are integrated into the RhoGTPases Rac1 and Cdc42, probably through their activation by GEFs, which in turn activate effector proteins (Fig. 1.6). Activated Rac1 and Cdc42 localise to the leading edge of the cell and activates the Ser/Thr kinase p65PAK and LIM kinase, which then phosphorylates and inactivates Cofilin, an actin-depolymerising protein and therefore allows increased accumulation of polymerised actin at the leading edge. Both Rac1 and Cdc42 also activate the Arp2/3 complex through members of the WASP/SCAR/WAVE family, enhancing actin nucleation, F-actin extension and branching (Raftopoulou & A. Hall 2004).

Another important function of Rac1 in promoting extension of the leading edge of the cell is to inhibit RhoA. RhoA activation at the leading edge of the cell would be detrimental to cell migration, since it promotes the formation of actin-myosin stress fibers and focal adhesions. It does this by activating Rho kinase

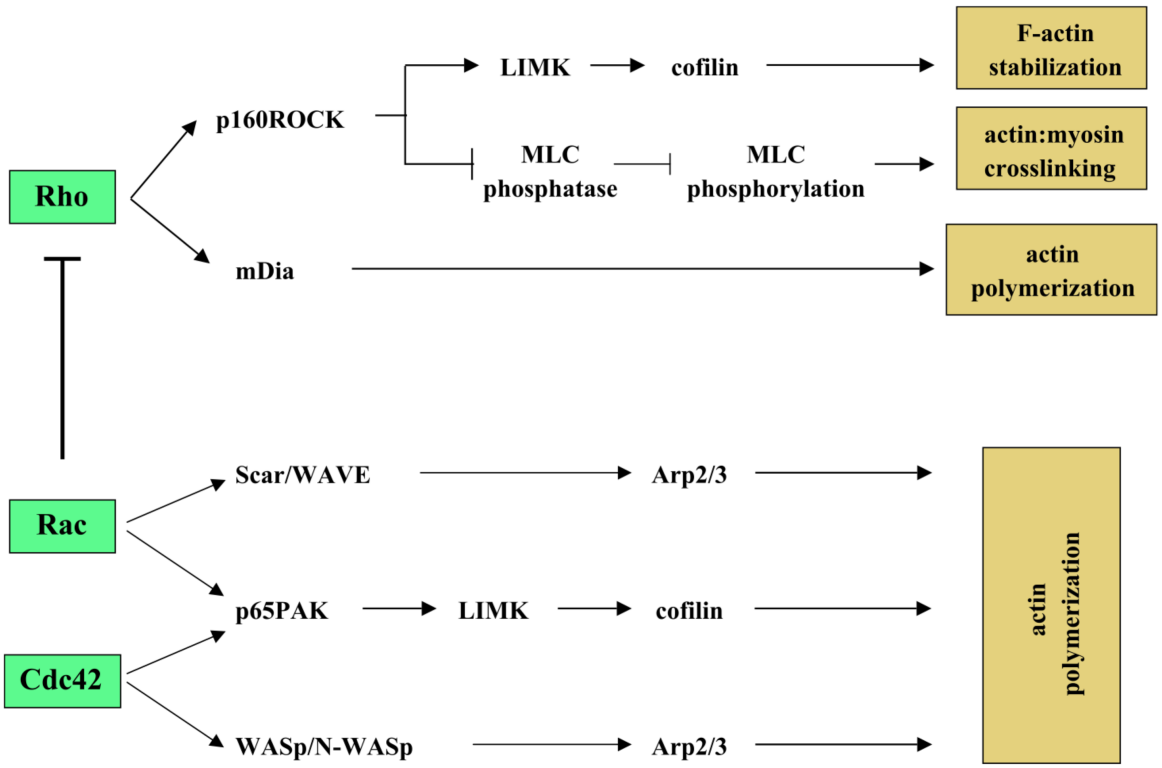

Figure 1.6. Rho GTPase effector molecules

The RhoGTPases activate distinct effectors that mediate actin polymerisation and stress fiber formation. Adapted from (Raftopoulou & A. Hall 2004).

(ROCK), which activates LIMK and stabilises F-actin in the same manner as Rac1/Cdc42, via Cofilin. ROCK additionally inhibits the phosphorylation of myosin light chain (MLC), which allows actin-myosin cross-linking and formation of stress fibers. In addition to this, RhoA activates mDia, a member of the formin family, which nucleates and promotes actin polymerisation at focal adhesion sites (Raftopoulou & A. Hall 2004).

The protrusive force of actin polymerising against the leading edge of the cell is important for initial stages of cell migration, but another force is needed in order to move the remainder of the cell along. This force is generated mostly by contraction of actin-myosin stress fibers, which as mentioned are induced by activation of RhoA. Stress fibers, whilst required for cell migration, are typically thinner and more dynamic in motile cells than stationary cells (Pellegrin & Mellor 2007). Stress fiber role in cell migration is rather confused, since they are absent in many motile cells such as leukocytes and *Ameoba* (Valerius et al. 1982; Rubino et al. 1984) but they are strongly associated with the regulation of focal adhesion size and turnover, which does affect the rate of cell migration (Tojkander et al. 2012).

1.6 c-Jun regulation of cell morphogenesis

The transcription factor c-Jun is known to control cell shape and motility through a number of different mechanisms, it is required for tissue morphogenesis during both mouse and Drosophila development and also promotes the invasiveness of cancer cells.

1.6.1 Dorsal closure

Dorsal closure of the Drosophila embryo occurs during mid-embryogenesis and involves the concerted movement and elongation of the cells of the ventral and lateral epidermis, in the absence of cell division, so the two epithelia meet and fuse at the dorsal midline. Drosophila mutants that show a failure in epidermal closing at the dorsal midline are said to possess the "dorsal open" (DO) phenotype. Molecular analysis of these mutants reveals two main classes of genes involved in dorsal closure; those encoding structural proteins such as myosin and components of focal adhesions, and those encoding proteins likely to regulate and trigger cell morphogenesis (Hou et al. 1997). Basket and hemipterous are Drosophila mutants that represent such regulatory proteins, and encode *Drosophila JNK* (*DJNK*) and *DJNK kinase* (*DJNKK*). The *Drac* mutant, which is the homologue of the mammalian small GTPase Rac1 also displays a DO phenotype (Riesgo-Escovar & Hafen 1997b). In cells of the leading edge of the ventral and lateral epidermis, an unknown signal activates the Rac1-JNK pathway and in turn, the downstream targets *DJun* and *DFos* (homologs of c-Jun and c-Fos, which together form the AP-1 complex). *DJun* regulates the expression of the TGF-β homologue, *decapentaplegic* (*dpp*), which binds to its receptors *punt* and *tkv* and leads to SMAD translocation to the cell

nucleus (Fig. 1.7), and subsequent gene expression that initiates the cell morphological changes necessary to drive leading cell elongation, and thus closure of the dorsal midline of the embryo (Hou et al. 1997; Riesgo-Escovar & Hafen 1997a; Riesgo-Escovar & Hafen 1997b)..

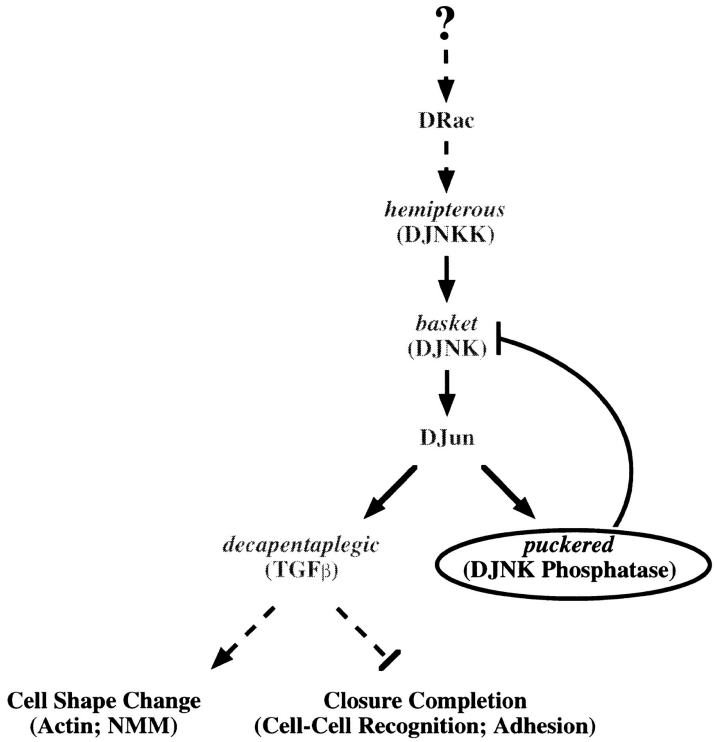

Figure 1.7. Activation of the *DJNK* pathway in cells of the leading edges of the ventral and lateral epidermis of the Drosophila embryo leads to expression of *DJun* and *dpp*, which mediates the cytoskeletal changes necessary for cell elongation and dorsal closure. Adapted from (Martín-Blanco et al. 1998).

1.6.2 Mouse eyelid closure

Eyelid closure in the mouse takes place between E15-E16 and is analogous to dorsal closure in Drosophila as both processes involve the extension and fusion of two epithelia, which requires cell morphogenesis. Failure of eyelid closure is referred to as the eye-open-at-birth (EOB) phenotype. The molecular control of this morphogenetic event is also comparable to that of dorsal closure as c-Jun lies downstream of JNK signalling, and induces the expression of genes that affect cell shape and migration. Activin B initiates MEKK1-MKK4 signalling, which activates the JNK1/2 pathway and culminates in the phosphorylation of c-Jun (Takatori et al. 2008). Conditional deletion of c-Jun and other proteins in this pathway causes the EOB phenotype. Keratinocytes are the cells that compose the eyelid epidermis, and deletion of c-Jun in these cells reduces their expression of another EOB protein, EGF receptor (Zenz et al. 2003).

1.6.3 Cellular invasiveness

c-Jun was the first oncogenic transcription factor to be discovered and is over-expressed in many cancers. In contrast to the deficient migration of c-Jun$^{-/-}$ keratinocytes that causes the EOB phenotype in mice, high expression of c-Jun is seen in malignant keratinocytes derived from squamous cell carcinoma (Lohman et al. 1997). Cellular invasion occurs during normal development as well as cancer metastasis, for example during angiogenesis and organogenesis (Egeblad & Werb 2002). Deletion of c-Jun in mouse embryonic fibroblasts (MEFs) causes a significant reduction in cell motility and causes cell flattening and induction of actin stress fibers and focal adhesions. Lack of c-Jun is found to increase the

activity of RhoA-activated kinase (ROCK II) through the reduction of c-Src expression (Jiao et al. 2008), this pathway is shown in Fig. 1.8.

Another pathway implicated in c-Jun dependent cell invasiveness and cytoskeleton remodelling is that of TGF-β, which as mentioned previously (Fig. 1.6), is also active in the dorsal closure of the Drosophila embryo and is dependent on JNK/c-Jun. The response by 3T3 cells to TGF-β causes an increase in nuclear and cytosolic Ca^{2+} and increased cell migration. The increase in Ca^{2+} and migration in response to TGF-β requires c-Jun, as both are abolished when c-Jun is deleted from the cells (Janowski et al. 2011). Since TGF-β induced cell migration requires RhoA, a GTPase known to be regulated by c-Jun, this may be a common mechanism linking the c-Jun-Src-ROCKII pathway (Jiao et al. 2008).

Stem cell factor (SCF) and its receptor kit are involved in cell migration, differentiation and proliferation in a diverse set of cell types, including neural stem cells and endothelial cells. SCF can be secreted from the cell, and Katiyar and colleagues have shown that conditioned medium from cultured MEFs can rescue the migration phenotype of c-Jun $^{-/-}$ MEFs. Indeed, it turns out to be the case that c-Jun regulates the expression of SCF, and SCF can rescue the morphological and migratory phenotype of c-Jun deleted MEFs (Katiyar et al. 2007). This suggests that SCF can signal through its receptor Kit normally in the absence of c-Jun. Since SCF expressing tumour cells are mostly found at the tumour border, where infiltration occurs and also where c-Jun expression is highest, this pathway may also contribute to c-Jun dependent cell invasiveness and tumour progression (Vleugel et al. 2006).

ErbB2, a member of the epidermal growth factor receptor family plays a significant role in both Schwann cell development and migration, and in the induction of mammary tumour cell invasion. Both c-Jun and ErbB2 are over-

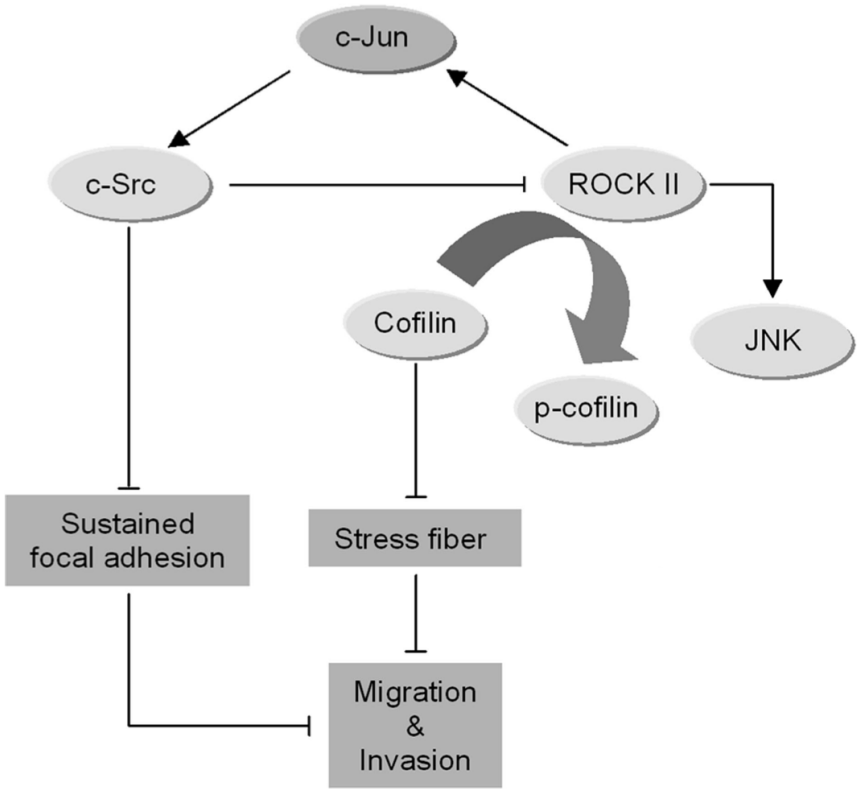

Figure 1.8. The transcription factor c-Jun regulates cell shape and motility through the expression of c-Src and the inhibition of ROCK II activity. Deletion of c-Jun causes decreased c-Src activity, increased ROCK II activity and therefore increased focal adhesions, actin stress fibers and reduced cell migration.

expressed in breast cancers, and both play a role in Schwann cell biology during nerve regeneration, so it seems likely they are part of an overlapping regulatory network of activating and effector proteins. ErbB2 is known to induce the expression the secreted proteins SCF, which is also regulated by c-Jun, as discussed above (Katiyar et al. 2007; Jiao et al. 2010). ErbB2 induces the expression of another soluble protein, CCL5, also known as RANTES. CCL5 is upregulated in the distal nerve stump following transection, at the same time as c-Jun upregulation in Schwann cells (Taskinen et al, 2000). CCL5 is regulated at the transcriptional level by c-Jun. In contrast to the MEF cells of the previous studies, c-Jun dependent migration of the mammary epithelial tumour cells (METs) is not induced by SCF, but instead by CCL5 (Jiao et al. 2010).

1.7 Peripheral nerve injury and regeneration

The mammalian PNS has the capacity to regenerate following nerve injury, an ability that provides a contrast with the limited regenerative capability of the CNS. This difference was first observed by Ramon y Cajal, who showed that peripheral nerves could not regenerate through central nerve graft tissue (R. Y. Cajal 1928). It was later shown that nerve fibers from the CNS, which are not capable of regenerating in their native environment, are able to grow through transplanted peripheral nerve (David & Aguayo 1981; Richardson et al. 1980). The results of these studies indicate that both PNS and CNS neurons possess the ability to regenerate, but only the PNS provides the necessary conditions to enable axonal regrowth. DRG sensory neurons exist in a unique configuration, containing a single, branched axon (referred to as pseudobipolar) that extends into and connects both sensory receptors in the periphery and neurons in the brain (via the spinal column). The two axon branches exhibit different responses to injury. Injury to the peripheral branch results in spontaneous regeneration with some recovery of sensory function, whereas injury to the central branch does not lead to regeneration. Significantly, if the peripheral branch lesion is followed by similar injury to the central branch, the central nerve does show signs of regeneration into the normally inhibitory environment of the spinal cord. Richardson & Issa performed an *in vivo* experiment, in which the dorsal column of the rat spinal cord was incised bilaterally and a sciatic nerve graft (from the right leg) was transplanted into the midline of the spinal cord. DRG neurons growing into the nerve graft were labeled and counted, and the results demonstrated that DRGs ipsilateral to the sciatic nerve transection were labeled positive, demonstrating that spinal axons from the DRG neurons had regenerated, however, no axonal regeneration into the CNS was observed from DRGs of the left side that did not experience peripheral injury (Richardson & Issa, 1984).

Pre-degeneration of the peripheral nerve graft promotes an even greater regenerative response from injured central axons, however, this effect is only seen in response to sciatic nerve crush (Oudega et al, 1994). Chong *et al*. demonstrated increased expression of GAP-43 mRNA in L4 DRG sensory neurons in the weeks following sciatic nerve crush, highest at 3 weeks following the conditioning injury, and persisting for at least 19 weeks (Chong et al, 1996). GAP-43 is a major protein kinase C (PKC) substrate and plays a role in neurite formation and regeneration (Benowitz et al, 1997) and therefore its expression is a measure of the intrinsic growth capacity of sensory neurons. Chong *et al* also reported an increase in the number of myelinated axons that had grown into the nerve graft from the axons of the dorsal root compared to grafts without crush injury, at all following time points. (Chong et al, 1996).

Neumann and Woolf conducted an experiment in which a peripheral lesion (sciatic nerve transection) was made at the same time as the central lesion, and observed sprouting of neurites proximal to the transected dorsal column, as well as neurites growing into and through the lesion. This contrasted with an absence of regenerating nerve fibers when no peripheral lesion was made. Peripheral lesions were also made 1 week and 2 weeks prior to the central lesion, and these led to greater neurite outgrowth, including beyond the lesion site (Neumann & Woolf, 1999). Chong *et al* performed a similar experiment, in which the left dorsal roots L4, L5 and L6 were transected, with or without a simultaneous crush injury to the ipsilateral sciatic nerve. The results of this study demonstrated little regeneration of neurites into the spinal cord in animals that did not have the conditioning sciatic nerve crush injury. In rats that did experience the conditioning lesion, most regenerating axons were found stalled at or near the dorsal root entry zone, however, in all cases a subpopulation of axons were observed to enter the spinal cord and penetrate into the grey matter of the dorsal horn.

The existence of this 'conditioning lesion' effect implies that whilst the local environments of injured central and peripheral DRG axons have a large affect on their regenerative potential, there exists an intrinsic capacity for growth in these neurons, and this is sufficient to overcome the less favourable regenerative environment of the CNS.

1.7.1 Initial events of nerve regeneration

Immediately following nerve injury, the cells of the peripheral nerve respond to this trauma by activating their regeneration programme. The precise trigger for this is unknown, although it is likely to be a combination of cellular mechanical stress such as disruption to cell membranes, and the loss of signals such as action potentials that are normally present in the uninjured nerve.

1.7.1.1 The axonal response to nerve injury in distal stump

The axonal response to nerve injury occurs rapidly following crush or transection. The transected axons in the proximal stump quickly seal their ends to prevent further escape of axoplasm. The axons in the distal stump start to disintegrate within hours of injury, as part of the process of Wallerian degeneration. This process culminates in the removal or myelin and axonal debris from the distal stump (Chen et al. 2007; Waller 1850). The axons do not breakdown straight away, there is a lag of 24-48 hours in rodents (Lubinska 1977) and several days in humans (Chaudhry & Cornblath 1992) and remain electrically excitable during this time. There is evidence that degeneration in crush injuries is delayed by 2-3 hours compared to complete transection, and this occurs in a retrograde direction, compared to the anterograde degeneration seen in nerve transection injuries (Beirowski et al. 2005). Axonal beading and swelling, accompanied with the disintegration of the axonal cytoskeleton is seen at the start of axonal degeneration, and is known to be dependent on calcium and the activation of calpain and ubiquitin, which

suggests this is an active, rather than passive process of axonal breakdown (Gaudet et al. 2011). This point is further supported by the Wallerian degeneration slow, or Wld^S mouse, which has much slower axonal degeneration (Lunn et al. 1989; Perry et al. 1991). Axons in the distal stumps of Wld^S mice degenerate with a delay of 2-3 weeks. The exact nature of the Wld^S mutation, identified by positional cloning, consists of an 85 Kb tandem triplication on chromosome 4 (Lyon et al. 1993; Coleman et al., 1998). As a result, a chimeric protein is overexpressed in neurons that consists of the first 70 amino acids of multi-ubiquitination factor, Ufd2 fused to the coding sequence of D4Cole1e/Nmnat1 (nicotinamide mononucleotide adenyltransferase1) (Conforti et al., 2000; Mack et al., 2001). Nmnat1 enzymatic activity is known to be necessary for Wld^S mediated axonal protection (Araki et al. 2004).

1.7.1.2 The axonal response to nerve injury in the proximal stump

As mentioned above, the severed ends of the axons in the proximal stump of the transected nerve are quickly sealed to prevent excessive egress of axoplasm. Similar to the distal stump, there is some axonal degeneration but this is restricted to the first node of Ranvier proximal to the site of transection (Zochodne, 2003). Within several hours the axonal cytoskeleton is rearranged, with microtubules in the most distal end of the axon reorganized to form traps for anterogradely transported vesicles that help to form the growth cone organising complex (Erez et al. 2007).

Another early event in the axonal response to injury is the activation of signals that are transported retrogradely to the neuronal cell body. One of the first signals is the influx of Calcium ions into the axon, as mentioned previously in the context of calcium-dependent axonal degeneration. This wave of calcium can travel up to 1mm per minute and occurs immediately proceeding nerve injury (Mandolesi et al. 2004). The transient increase in axonal Ca^{2+} ions returns to resting levels within hours in mammalian

neurons *in vivo* (Howard et al. 1999). Recent data has shown that retrograde Calcium signaling can induce the export of histone deacetylase 5 (HDAC5) via protein kinase Cμ from the neuronal nucleus, which accumulates at the site of axonal injury, and is able to deacetylate tubulin and promote axonal regeneration (Cho et al. 2013).

Another retrograde signaling phase occurs later and these are trafficked from the injury site to the soma via dynein motors. JNK3 and JIP3 are involved in the formation of retrograde signaling complexes and knockout of the JNK homologue DNK in Drosophila shows that it is required for the upregulation of p-Jun and p-STAT3 in sensory neuron soma (Shin et al. 2012).

Dynein motors are also used to convey a separate retrograde signaling complex that consists of importin-α and importin β1 bound to cargo that recognise their nuclear localization signal binding sites. This cargo includes p-ERK-vimentin and p-STAT3 (Rishal & Fainzilber 2014).

Whilst the exact molecular pathways that switch on the motor and sensory neurons of the peripheral nerve to respond to injury by acquiring a regeneration-permissive phenotype are not fully understood, changes to the cellular architecture of both the proximal and distal stumps, and to the injury site are well characterized, particularly by electron microscopy studies in the 1960s. This early work has since been refined using transgenic mice expressing fluorescent markers in axons and Schwann cells.

Within 1-2 days of nerve transection, the axons of the proximal stump develop swellings called axon endbulbs (also referred to as boutons), which may influence nerve regeneration by releasing molecules such as CGRP and nitric oxide (Zochodne 2008). At the same time as endbulbs are forming at the axon terminals, axonal sprouts appear as membrane outgrowths from the parent axon. Myelinated axons normally develop sprouts from either the first or second node of Ranvier (Friede & Bischhausen 1980).

Extensive sprouting takes place, with each axon developing multiple daughter sprouts. Nerve crush injuries also produce axonal sprouts, and these can grow relatively easily into the distal stump, as the endoneurial tubes are intact and the Schwann cells that line these structures form the Bands of Büngner, which are permissive substrates for axons to regenerate on. In contrast, sprouts from the proximal stump of the transected nerve must advance across newly formed tissue, referred to as the 'nerve bridge', composed primarily of fibroblasts from the epineurium, and Schwann cells from the nerve stumps. This structure is not very favourable for axonal regrowth, and very few of the sprouts successfully cross the bridge (Zochodne 2008).

1.7.1.3 Initial changes to Schwann cells during nerve regeneration

In the distal stump and at the very end of the proximal stump of the injured nerve, Schwann cells undergo the process of demyelination. Myelin fragmentation begins at the Schmidt-Lanterman Incisures (SLIs) just minutes after injury (Williams & S. M. Hall 1971) and by 1-2 days the myelin sheath has started to break up into ovoid structures. Myelin ovoids form more slowly in thicker fibers (Lubinska 1977). It is not clear how myelin is broken down in the nerve, but it is known that both Schwann cells and macrophages make a contribution. Elimination of infiltrating macrophages by whole body irradiation prior to nerve injury shows that myelin breakdown occurs normally for the first 5 days and then slows down. This shows that the initial breakdown of myelin is probably carried out by Schwann cells and resident macrophages (Perry et al. 1995). This is supported by Arthur-Farraj et al. who show that deleting Schwann cell c-Jun, and thus preventing these cells from becoming activated repair cells also slows the rate of myelin breakdown (Arthur-Farraj et al. 2012). Recent data suggests these Schwann cells are not able to process myelin through the autophagy pathway, in contrast to wildtype Schwann cells (Carty et al, unpublished data).

A further response of Schwann cells to nerve injury is their re-entry into the cell cycle. Schwann cell proliferation is negligible in the adult nerve, but is strongly increased following injury (Abercrombie, 1946). The significance of the increased cellular proliferation is unclear, since inhibiting Schwann call proliferation by disrupting the cyclin D1 gene does not lead to a deficiency in regeneration of remyelination (Yang et al. 2008). The authors of this study only considered nerve crush injury, so it is unknown whether Schwann cell proliferation is necessary for the successful bridging of the inter-stump gap created by nerve transection injury.

Following demyelination, Schwann cells in the distal stump are found aligned within their basal lamina tubes, where they proliferate and secrete neurotrophic factors. The attraction of regenerating axons to the distal nerve stump has been well documented (Politis et al. 1982).

1.7.2 Schwann cell migration during nerve injury and regeneration

I have discussed the migratory behaviour of Schwann cells in detail in the first section of this introduction, but only briefly touched on their migration during peripheral nerve regeneration. Abercrombie conducted a series of experiments that revealed the motile behaviour of Schwann cells in the degenerating nerve. He observed Schwann cells in pre-degenerated nerves 'outwander' from a nerve explant at rate proportional to the length of time they were degenerated *in vivo*, peaking at 19 days. In this study, Schwann cells only emigrated from the cross-section of the nerve explant (i.e. not through the epineurium) and there was a latency period of 4-5 days before emigration occurred, Abercrombie suggested this is the time taken for Schwann cells to fully demyelinate and become mobile. Very little emigration was observed from nerves that had not been predegenerated (Abercrombie, 1942). In later studies, Abercrombie allowed the distal portions of transected nerves to become reinnervated and then

measured Schwann cell outwandering, finding that reinnervation largely diminished emigration from the nerve of Schwann cells, but not fibroblasts, showing that Schwann cells lose their ability to migrate once they become re-associated with regenerating axons (Abercrombie et al, 1949).

In vivo evidence of Schwann cell migration during regeneration was first reported by Nageotte, who described the outgrowth from a transected nerve as a 'peripheral glioma' (Frixione, 2000) and this was also described by Masson (Masson 1932). Holmes and Young described the *in vivo* migratory properties of Schwann cells in the distal stump of the transected nerve. They observed Schwann cells migrating within the intact endoneurial tubes and forming an outgrowth at the end of the distal nerve stump. Both proximal and distal stumps formed outgrowths, however the distal outgrowth was much larger and more rapid. The outgrowth is progressive for several weeks after transection but does not continue indefinitely. Schwann cell mitoses were observed in cells leaving the stump so it is possible that proliferation in addition to migration contribute to the size of the Schwann cell outgrowth. The authors also noted the outgrowth of fibroblasts from the epineurium and perineurium was significant, and sometimes greater than the outgrowth of Schwann cells (Holmes & Young 1942; Holmes et al. 1940). Rexed found the Schwann cell outgrowth proceeded at a rate of up to 0.3mm/day, starting from the third day following transection. In the first day, the inter-stump gap filled with an exudate containing macrophages, fibroblasts and capillaries, followed by Schwann cell outgrowth at 3 days. Transection of an already degenerated distal stump formed two nerve stumps from which the outgrowths were equally intense (Rexed 1942). The asymmetry of outgrowth from the proximal and distal stumps following a single transection correlates with the extent of Wallerian degeneration that takes place. In the proximal stump, axonal degradation and Schwann

cell denervation is limited to 1-2 mm from the cut site in rat, limiting the pool of cells that can proliferate and emigrate into the gap.

Thomas later confirmed the findings of Young and Rexed using electron microscopy of sections of the 'nerve bridge'. He found that Schwann cells emigrated from the distal stump in columns, continuous with the Bands of Büngner. Cells of perineural origin, resembling fibroblasts, come to surround these Schwann cell columns. This leads to the formation of multiple small fascicles in the nerve bridge, each surrounded by a perineurium (Thomas 1966). This had been noted previously by Cajal and later by Morris, who applied the term 'compartmentation' to the formation of mini-fascicles in the nerve bridge and the proximal/distal stumps. Morris found that compartmentation only takes place in the presence of regrowing axons (J. H. Morris et al. 1972).

1.7.3 The role of c-Jun in peripheral nerve regeneration

c-Jun is a key regulator of the Schwann cell response to nerve injury. c-Jun is upregulated rapidly, within an hour following nerve injury (Shy et al. 1996) and its deletion in mouse Schwann cells prevents recovery of motor and sensory function (Arthur-Farraj et al. 2012). c-Jun is expressed in immature Schwann cells before birth (Stewart et al. 1995; Parkinson et al., 2008), however, its expression is downregulated when Schwann cells begin myelination. Thus, c-Jun is only expressed in non-myelinating Schwann cells in the adult, at low levels (Shy et al, 1996; Parkinson et al, 2008). Furthermore, c-Jun is also upregulated in peripheral neurons following nerve injury and is required in these cells for in vivo regeneration (Behrens et al, 2002; Raivich et al, 2004). c-Jun regulates the transdifferentiation of mature myelinating and non-myelinating Schwann cells to repair cells, or 'Bungner Schwann cells' that promote nerve regeneration by controlling the expression of a number of genes. Following nerve

transection, there are 172 differentially regulated genes in the c-Jun cKO mouse compared to the control. These include genes such as GDNF, BDNF, Shh, Artemin and GAP-43, which fail to upregulate following injury and have been implicated in nerve regeneration and the trophic support of neurons. Furthermore, c-Jun protects sensory neurons from cell death following nerve injury, since its deletion leads to increased death of both large and small DRG neurons (Arthur-Farraj et al. 2012). The Wld^S mouse has limited nerve regenerative capability, in addition to the slow degradation of axons, as the Schwann cells remain in a differentiated state. Increased expression of c-Jun from the low level found in Wld^S nerves after injury significantly enhances nerve regeneration (Arthur-Farraj et al. 2012). These findings show that c-Jun controls many of the functions that Schwann cells carry out in their role as a repair cell in the regenerating nerve.

In agreement with the above work, Fontana et al show that conditional deletion of c-Jun in Schwann cells perturbs motor function of the mouse whisker following injury to the facial nerve and dramatically increases neuronal cell death. The neurotrophic factors GDNF and Artemin had reduced expression in the c-Jun knockout, and the authors identified these proteins, along with their receptor Ret as being important signals that mediate the regeneration-promoting ability of c-Jun in Schwann cells (Fontana et al. 2012).

Aims

The aim of this thesis was to characterise the effect of deleting c-Jun from Schwann cells to understand how this has such a large affect on their ability to promote regeneration of the peripheral nerve. I did this by analyzing the changes to Schwann cell morphology and migratory behaviour in the absence of c-Jun. I also wanted to uncover the molecular mechanism by which c-Jun controls Schwann cell morphology and cell migration. Finally, I wanted to see if the *in vitro* observations were also replicated in the regenerating mammalian peripheral nerve.

Chapter 2: Materials and methods

2.1 List of Reagents

2.1.1 Reagents for tissue culture

Cytosine arabinoside (AraC), dimethyl sulphoxide (DMSO), bovine serum albumin (BSA), transferrin, selenium, putrescine, triiodothyronine (T3), thyroxine (T4) progesterone, dexamethasone, insulin, poly-D-lysine (PDL), poly-L-lysine (PLL), laminin and 2'-0-dibutyryladenosine 3',5'-cyclicAMP (dbcAMP) were obtained from Sigma (Poole, UK). Collagenase was obtained from Worthington (Lorne Laboratories, Reading, UK). Dulbecco's modified Eagles medium (DMEM), Ham's F-12 medium and L-15 medium, horse serum and glutamine were obtained from Invitrogen Ltd (Paisley, UK). Trypsin, trypsin EDTA and penicillin/streptomycin were obtained from PAA (UK). Fetal bovine serum (FBS) was obtained from Perbio (UK). Forskolin was obtained from Calbiochem (CA, USA). NRGβ-1 was obtained from R&D Systems (Minneapolis, MN, USA). Tissue culture dishes, 24 well plates and centrifuge tubes were obtained from VWR. Round 13-mm coverslips were obtained from BDH (Lutterworth, UK). Transwell 6.5-mm inserts with 8 μm pores were obtained from Corning (New York, USA).

2.1.2 Reagents for molecular biology

EDTA disodium salt, ethidium bromide, sodium citrate, phenylmethylsulphonylfluoride (PMSF), sodium hydroxide, bromophenol blue and urea were purchased from Sigma (Poole, UK). 10B lysing matrix beads were from MP Biomedicals (USA). Hybond-N nitrocellulose membrane was from Amersham

Pharmacia Biotech (UK). Reblot plus strong stripping solution was from Millipore (MA USA). Super Signal West Dura kit was from Perbio (UK). Absolute ethanol, isopropanol, methanol, sodium dodecyl sulphate (SDS), sodium chloride (NaCl), Triton X-100 and glycerol were from BDH Lab. Supplies (Poole, UK). Kaleidoscope pre-stained standards were from Biorad (CA, USA). Tris Base, Tris-HCl, hydrogen peroxide, luminol and coumaric acid were from Sigma (Poole, UK). SeeBlue Plus2 pre-stained standards were purchased from Invitrogen Ltd (Paisley, UK). CL-XPosure film was from Thermo Scientific (UK). Taq DNA-polymerase, dNTPs, 1KB plus DNA ladder, 100mM dNTP set and Agarose were from Invitrogen Ltd (Paisley, UK).

2.1.3 Reagents for immunolabelling

Paraformaldehyde was obtained from Fluka Chemicals Ltd. (Buchs, Switzerland). Triton X-100, lysine and Hoechst dye H33258 were obtained from Sigma (Poole, UK). Citifluor was from Citifluor Ltd. (London, UK) HCl and glycerol were obtained from BDH (Lutterworth, UK).

2.1.4 Surgery

Surgical tools were purchased from Fine Science Tools (Germany). Vetinary autoclips were purchased from VET-TECH (UK). Sterile drapes, swabs and isofluorane were provided by the Biological Services Unit at UCL.

2.2 Mice

Wild-type C57BL/6 mice and wild-type Sprague-Dawley rats were obtained from the Biological Services unit at University College London.

P0-Cre mice

Transgenic mice expressing mP0TOT(Cre) transgene (P0-Cre) were driven by the mpz promoter. P0-Cre transgene activates Cre-mediated recombination specifically in Schwann cells between the ages of E13.5 and E14.5. Strong P0-Cre activity is only detected in the peripheral nerve, with slight activity in the occipital lobe of the cerebral cortex, Purkinje cell layer of the cerebellum and in the heart. The P0-Cre mice were provided by Dr L. Wrabetz and Dr M.L. Feltri (Hunter James Kelly Research Institute, Buffalo, NY, USA). P0-Cre mice have been used extensively in Schwann cell reports for the ablation of 'floxed' genes. P0-Cre mice were used in this study to generate Schwann cell specific ablation of c-Jun as described below.

c-Jun null mice

c-Jun null mice have been characterised extensively by members of the Jessen and Mirsky laboratory. c-Jun null mice were generated using transgenic mice in which loxP sites are present in the 5' untranslated region (UTR) of c-jun and in the 3' flanking sequence 2.5 kb downstream of the translation stop codon, known as c-Jun floxed mice (c-Jun$^{flox/flox}$). These mice were kindly provided by Dr Axel Behrens (Cancer Research UK). The c-Jun$^{flox/flox}$ mice were crossed with P0-Cre mice to produce P0-Cre;c-Jun$^{flox/wt}$ mice. These were subsequently crossed again with c-Jun$^{flox/flox}$ mice, generating P0-Cre; c-Jun$^{flox/flox}$ mice (c-Jun null mice).

2.3 Tissue Culture

2.3.1 Preparation of coverslips and tissue culture dishes

Substratum coating of Poly-D-lysine and Poly-L-lysine

Round 13-mm glass coverslips were baked in an oven for 4 hours at 140°C and were coated with 20 µg/ml Poly-D-Lysine (PDL) in distilled H2O for rat Schwann cells, or 20 µg/ml Poly-L-Lysine (PLL) in distilled H_2O for mouse Schwann cells, for 3 hours at RT. Coverslips and dishes were then washed 3 times, for 15 min each in sterilised water and dried overnight in a class I tissue culture hood before being stored in sterile and desiccated (in the presence of silica gel) conditions at RT. 35 mm and 60 mm tissue culture dishes were coated with PDL (20 µg/ml) or PLL (20 µg/ml) for 4 hours at RT. The solution was removed and the dishes rinsed once with distilled H_2O and allowed to air-dry overnight in a class I tissue culture hood.

Laminin

A 15-µl drop of laminin solution (diluted in DMEM, 20 µg/ml) was placed into the centre of each glass coverslip, or completely covering the culture dish and incubated for 30 min at RT. The laminin solution was removed immediately prior to plating cells onto the coverslip.

2.3.2 Tissue Culture Media

Defined supplemented Medium (DM)

This is a modification of the medium of Bottenstein and Sato (1979).

A 1:1 mixture of DMEM and Ham's F12 medium was enhanced with the following: bovine serum albumin (0.3 mg/ml), putrescine (16 µg/ml), transferrin

(100 μg/ml), thyroxine (400 ng/ml), progesterone (60 ng/ml), glutamine (1 mM), penicillin-streptomycin (100 U/ml), triiodothyronine (10.1 ng/ml) and selenium (160 ng/ml) and insulin (10^{-6} M).

2.2.3 Pharmacological Agents

The Rho Kinase II (ROCKII) inhibitor Y-27632 was purchased from Sigma Aldrich, dissolved in DMSO and used at a final concentration of 10 μM for all experiments. The c-Src inhibitor SU6656 was also purchased from Sigma, dissolved in DMSO and used at a final concentration of 2 μM for all experiments. Mitomycin-C was used to inhibit cellular proliferation in the migration assays. I purchased this from Sigma, and the compound was dissolved in H_20 and used at a concentration of 10 μg/ml.

2.3.4 Serum purified mouse Schwann cell cultures

Mouse Schwann cells were isolated using a protocol , as follows, adapted from previous studies that isolated rat and mouse Schwann cells (Brockes, 1979; Dong et al. 1995). The sciatic nerves and brachial plexuses were dissected from two postnatal day 6 (P6) mice and transferred to L15 medium (Life Technologies) on ice. Using a dissecting microscope, the epineurial sheath of each nerve was removed using no. 5 forceps. The desheathed nerves were then transferred to a 35-mm tissue culture dish containing 5% horse serum in DMEM + Pen/Strep and left overnight at 37˚C in 5% CO_2. The following day, the nerves were removed from the medium and transferred to a culture dish containing trypsin/collagenase, and left in the incubator for 30 min at 37˚C in 5% CO_2. The nerves were then triturated ten times with a blue pipette tip, and ten times with a yellow tip and then re-incubated for 10 min. Trituration was repeated to fully dissociate the cells and

then the 5% horse serum/DMEM was added to prevent further enzymatic digestion. The digested cells were then transferred to a 15-ml Falcon tube and centrifuged at 1,000 rpm for 10 min. The cell pellet was then resuspended in 2 ml of 5% horse serum + Pen/Strep and transferred to a laminin-PLL-coated 35-mm tissue culture dish. Ara-C was added to the dish at a final concentration of 10^{-5} M and the cells were incubated at 37˚C in 5% CO_2 for 3 days to eliminate proliferating fibroblasts. After 3 days, the cells were trypsinised and re-plated into a 35-mm dish containing Schwann cell expansion medium (Defined Medium containing 0.5% horse serum (1:200), 100 µM dbcAMP (1:500) and 10 ng/ml NRG1 (1:500). The cells were used for further experiments once the dish had become confluent (~7-10 days following purification), but were placed in DM without any mitogenic factors for 12 hours until experimental reagents were added.

2.3.5 Adenovirus constructs and preparation

The adenovirus expressing Cre recombinase, and its control expressing GFP were obtained as gifts from Dr Axel Behrens, made in the laboratory of Dr A Berns (Akagi et al. 1997). The HindIII fragment of PBS185, containing the Cre recombinase open reading frame under the control of human CMV immediate early promoter and the metallothionein polyadenylation signal was inserted into the HindIII site of pdE1spIA. This was co-transfected with pJM17 into 293 cells and adenovirus was obtained by plaque purification (Akagi et al. 1997).

Adenoviral supernatants were prepared and titred as described previously (Parkinson et al. 2001). HEK 293 cells were infected with the adenovirus, and once the cells had started to round and detach from the culture dish (~3 days), the cells were scraped and transferred to a 50-ml Falcon tube and centrifuged at 1,500 rpm for 5 min at 4˚C. The supernatant was discarded and the pellet resuspended in 1.5

ml of PBS. Three cycles of freeze-thawing using the -80˚C freezer and 37˚C water bath were completed, and the cell suspension was centrifuged at 3,000rpm for 5 min. The supernatant was passed through a 0.2 μm filter and the virus-containing solution was aliquoted and stored at -80˚C.

The viruses were then titred by infecting Ara-C purified Schwann cells with different volumes of the virus. The volume that resulted in >95% infection (as determined by immunolabelling Cre, or expression of GFP) and no cell death was chosen. Viral titration was carried out each time when preparing new adenoviral stocks.

2.3.6 Adenoviral infection

The adenoviruses were used to infect the expanded primary mouse Schwann cell cultured. Briefly, the medium of confluent 35-mm dishes was changed from expansion medium to DM containing 0.5% horse serum and 2 μM Forskolin and Insulin (10^{-6} M). A volume of adenovirus was added (determined by titration) and after 24 hours, the medium was exchanged with DM containing 0.5% horse serum and left for 2 days before being used in experiments.

2.4 Migration Assays

2.4.1 Transwell migration assay

Primary mouse Schwann cells were used in all Transwell migration assays, purified as described in section 2.3.4. Cells were detached from 35-mm culture dishes following adenoviral infection (omitted in the case of wildtype cells) and pre-incubation with mitomycin-C (2 hours) and then counted using a hemocytometer. Approximately 5,000 cells in a volume of 100 μl of DM were

pipetted into the top compartment of a Transwell (pores size of 8 μm, placed in a 24-well plate). The contents of the lower compartments were varied across different experimental conditions. Cells were allowed to migrate for 12 hours. At the end of the experiment, the Transwell membrane was fixed with 4% PFA for 10 min, washed three times with PBS and the upper side of the membrane was gently scrapped with a cotton bud to remove non-migrated cells. The membrane was stained with dapi, cut out of the Transwell supports and mounted onto slides. The total number of nuclei (representing migrated cells) were counted across the entire membrane using a fluorescent microscope.

2.4.2 Wound assay

Schwann cells were detached from 35-mm culture dishes following adenoviral infection (omitted in the case of wildtype cells) and counted using a hemocytometer. Approximately 200,000 cells were plated onto a laminin-coated coverslip and cells were allowed to adhere, in the presence of mitomycin-C to prevent cell proliferation. A scratch was made across the center of the coverslip using a yellow pipette tip (Fig. 2.1). The scratch was practiced beforehand in order to generate a consistent diameter, and this was determined to be approximately 220 μm wide. The coverslips were placed inside the wells of 24-well plates, and covered with 400 μl of medium prior to the wound being made. The assay was terminated at several time points (0, 6, 12 and 24 hours) in order to examine the rate of cell migration. The coverslips were immunolabelled with β1-integrin to visualise the migrating cells, the distance of the wound gap was measured at 8 equidistant positions and the average diameter of the wound was calculated.

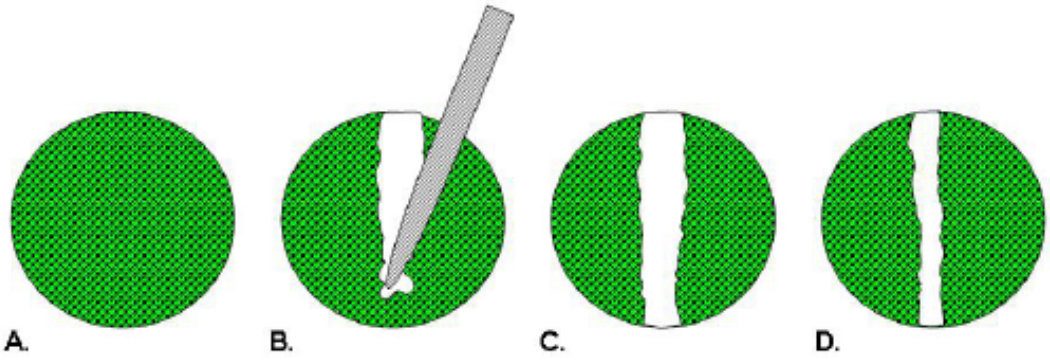

Figure 2.1 Scratch Assay
(A) a confluent layer of Schwann cells is maintained in culture on 35-mm glass coverslips. (B) a scratch is made across the diameter of the coverslip using a yellow 200µl pipette tip. (C) The denuded area is imaged to mark the area of the wound at 0 hours. (D) At the end of the time point, the gap is imaged again, and the average distance is calculated. Adapted from (Hulkower, 2011).

2.5 Sciatic nerve transection injury models

All surgical procedures were carried out under UK Home Office guidelines, using sterile surgical technique. Mice were shaved in the region of the leg and lower back and subsequently anaesthetized with 2% isofluorane. For the complete transection experiment, the sciatic nerve was exposed and transected at the mid-thigh level, approximately 1 cm above the point at which the nerve trifurcates into the tibial, peroneal and sural branches.. For the partial transection injury model, no. 5 forceps were used to gently part the tibial and peroneal branches to create a gap of sufficient size to insert the blades of the surgical scissors and then transect the peroneal branch. Care was taken to separate the two branches in small area so that following transection, the proximal and distal stumps were still attached to the tibial nerve and kept in close proximity to each other. The skin was closed using veterinary autoclips and animals were left to recovered in a heated box.

2.6 Genotyping

HotShot DNA extraction: Ear clips were collected from mice at P8-P12 and digested using HotShot lysis reagent (25 mM NaOH, 0.2 mM disodium EDTA, pH 12) for 1 hour at 95˚C. Samples were then vortexed and cooled to 4˚C and subsequently neutralised with 40 mM Tris-HCl. Samples were stored at -20˚C until use.

Semi-quantitative PCR: Polymerase chain reactions (PCR) were performed for each sample using 100-400 ng of DNA from the above extraction, in a total reaction volume of 25 µl. PCR was performed in an Eppendorf Mastercycler Gradient PCR thermalcycler. Specific conditions were used for each primer pair. 15 µl of the PCR

reaction was used for electrophoresis in a 2% agarose gel containing ethidium bromide, immersed in 1x Tris Acetate EDTA (TAE) buffer (Horizon 58 gel apparatus, BRL- Life Technologies, Gaithersburg, MD). Samples were run alongside 10µl of 1kb DNA ladder (Invitrogen).

2.6.1 Primers and PCR conditions for genotyping

c-Jun flox mice:

Forward CCGCTAGCACTCACGTTGGTAGGC

Reverse CTCATACCAGTTCGCACAGGCGGC

2min at 94˚C

35 cycles: 40secs at 94˚C, 40secs at 57˚C, 1min 30secs at 72˚C 7min at 72˚C

Wildtype band at 300 bp; floxed band at 330 bp

P0-Cre mice:

Forward GCTGGCCCAAATGTTGCTGG

Reverse CCACCACCTCTCCATTGCAC

4min at 94˚C

30 cycles: 30secs at 94˚C, 1min at 50˚C, 1min at 72˚C 10min at 72˚C

Band at 500 bp

2.7 Western blotting

2.7.1 Protein extraction

The distal stumps of transected nerves were snap frozen in liquid nitrogen and transferred to tubes containing 10-12 10B lysing matrix beads and 100 µl of lysis buffer (25 mM Tris-HCl pH 7.4, 95 mM NaCl, 10 mM EDTA, 2% SDS and proteinase and phosphatase inhibitors). The nerve samples were placed in a Fast-prep homogeniser for 45 sec at level 6, chilled on ice and then subjected to repeat homogenisation at the same setting. The resulting lysates were then centrifuged at 4˚C at 10,000 rpm for 2 min. Supernatants were transferred to new tubes and centrifuged again at the same settings. The new supernatants were collected and stored at -80˚C.

2.7.2 SDS PAGE

Protein lysate samples were separated by electrophoresis on acrylamide gels. Sample buffer was added to a final dilution of 1x, prior to gel loading:

Laemmli sample buffer (5x): 60 mM Tris pH 6.8, 2% SDS, 10% glycerol, 5% beta-mercaptoethanol and 0.01% bromophenol blue.

The protein samples (5 µg) were loaded into a 10% gel and run alongside pre-stained standard molecular weight markers (SeeBlue Plus 2, Invitrogen) to enable identification of band sizes. Gels were run using the mini Protean II gel electrophoresis apparatus (Biorad, USA) and then proteins were transferred to nitrocellulose membranes (Hybond ECL, Amersham) using the Biorad semi-dry system and transfer buffer (25 mM Tris, 192 mM glycine, 10% methanol).

2.7.3 Detection

Membranes were washed briefly in PBS after transfer and subsequently incubated in 5% fat free milk powder (Sigma) in PBS for 1 hour (RT) to block non-specific binding sites. Membranes were incubated overnight at 4˚C with primary antibodies diluted in 5% milk/PBS on a slow rotator (Gallenkamp, UK). Membranes were subsequently washed every 10 min in PBS for 30 min before addition of secondary antibodies conjugated to horseradish peroxidase (HRP) diluted in 5% milk/PBS. After secondary incubation, membranes were washed every 10 min for 40 min.

The secondary antibody signal was detected by incubating membranes in a 1:1 mixture of ECL solutions A and B for 3 min in the dark. Membranes were placed into autoradiography cassettes (Appligene, USA) and developed by brief exposure (5 sec to 5 min) to Thermo Scientific CL-XPosure film. Films were developed using an X-graph Compact X2 automatic developer (UK).

ECL solution A: 0.1M Tris, pH 8.5, 2.5 mM luminol and 0.4 mM coumaric acid

ECL solution B: 0.1M Tris, pH 8.5 and 0.02% hydrogen peroxide

Both ECL solutions were stored at 4˚C in dark conditions and mixed immediately prior to use.

2.8 Reverse transcription-quantitative polymerase chain reaction (RT-qPCR)

2.8.1 RNA extraction and reverse transcription

RNA was extracted from primary mouse Schwann cell cultures that had been subjected to infection with adeno-Cre (c-Jun KO) or adeno-GFP (control). One confluent 35-mm tissue culture dish was used for each RNA extraction, and RNA was extracted 3 times for each knockout and control (n=3). RNA was extracted using the RNeasy Micro kit (Qiagen, Venlo, Netherlands) according to the manufacturer's instructions. RNA was treated with DNAse to eliminate genomic DNA from the samples using Turbo™ DNase treatment (Life Technologies) in accordance with the manufacturer's instructions.

For reverse transcription, RNA samples were added to a nuclease-free microcentrifuge tube as follows: 1µl of oligo$(dt)_{20}$ primers (50 µM; Life Technologies), 1 µg of RNA samples, 1µl of 10 mM dNTP mix and 13 µl of sterile distilled H_2O. This mixture was heated to 65˚C for 5 min in a Biorad CFX thermalcycler and incubated on ice for 1 min. To each tube, 6 µl of the following master mix was added: 4 µl of 5 x First strand buffer, 1 µl of 0.1 M DTT and 1 µl of RNAse Out 40 U/µl (all from Life Technologies). To each sample, 1 µl of SuperScript™ II reverse transcriptase (Life Technologies) was added, heated to 42˚C for 50 min and then 70˚C for 15 min. Each 20 µl sample was divided into two and stored at -80˚C until required for RT-qPCR reactions.

2.8.2 Primer design and optimization for RT-qPCR

Primers for housekeeping genes and test genes were designed using Primer3Plus software, unless otherwise indicated. Primers were designed, where possible, to span intron-exon boundaries as an additional control for the presence of genomic DNA. Primers were optimised by testing the following concentrations of forward/reverse primers: 200 nmol/200 nmol, 300/300, 300/200 and 200/300. Primers were tested according to the following PCR conditions:

1) 95 ˚C for 3:00

2) 95 ˚C for 0:15

3) 60 ˚C for 0:30

4) 72 ˚C for 0:30

+ Plate Read

5) Gg to step 2, 39 more times

6) Melt Curve 65 to 95 ˚C, increment 1 ˚C,

0:05 + Plate Read

END

The PCR reactions contained the following components:

10 µl of Kapa SYBR green (Kapa biosystems, Wilminton, MA, USA)

0.4 µl each of Forward and Reverse Primers (if 200/200 nmol)

4 µl of cDNA (diluted 1:60 in sterile, distilled H_2O)

5.2 µl of sterile, distilled H_2O (to make a reaction total volume of 20 µl)

The PCR products of each primer pair were analysed and the primers were only accepted if they contained one melt curve peak and gave a Ct (cycle threshold)

value that was <30. PCR products were run on an agarose gel to check for the presence one band. Standard curves were carried out on the primers for each cDNA sample, and primers were only accepted if R^2>0.98 and there was a gradient of -3.2 to -3.5 (Efficiency, >95%).

2.8.3 RT-qPCR analysis

The data from the RT-qPCR were normalized to GAPDH and YWHAZ as these had the least variability of all housekeeping genes tested between the control and c-Jun knockout samples. This was done using the Biorad CFX Manager Software (version 1.6). Fold change of expression of c-Jun knockout compared to control was calculated using the $2^{-\Delta\Delta Ct}$ method using the Biorad CFX software.

2.9 Immunolabelling

2.9.1 Antibodies

Antibody	Supplier	Host Species	Application
β1-Integrin	Abcam	Mouse mono	ICC 1:500
Vinculin	Abcam	Mouse mono	ICC 1:400
c-Src	Santa Cruz	Mouse mono	WB 1:500, ICC 1:500
c-Jun	BD	Mouse mono	ICC 1:500
Cre recombinase	Merck Millipore	Rabbit poly	ICC 1:1000
GAPDH	Enzo Life Sci	Mouse mono	WB 1:2000
S100	Dako	Rabbit poly	IHC 1:500
Neurofilament	Abcam	Chick poly	IHC 1:1000

2.9.2 Fixation

Cells were fixed with 4% paraformaldehyde for 10 min at RT in all experiments. Coverslips were subsequently dipped 3 times in 5 tubes containing PBS for in order to rinse the PFA from the samples.

2.9.3 Immunolabelling

Coverslips for immunolabelling were treated for 10 min in 100% methanol for permeabilisation, for all antibodies used. Subsequently, slides and coverslips were incubated in antibody diluting solution (ADS) for 30 minutes to 1hr.

ADS: Donor Calf Serum 20 ml, Lysine 3.65 g, PBS 180 ml

Primary antibodies diluted in ADS were applied overnight at 4˚C. Coverslips were washed by dipping 3x in 5 tubes containing PBS, slides were washed in coplin jars containing PBS on a low speed platform shaker, 3x 10 minutes for 30 minutes. Secondary antibodies diluted in ADS were applied for 30 minutes and samples washed again. Coverslips containing cultured cells were inverted and mounted on glass slides using citiflour mounting medium.

2.9.4 Microscopy

Immunofluorescent cells or were visualised using either a Nikon Optiphot-2 or a Nikon Eclipse E800 fluorescent microscope. Images were captured using a digital camera (model: DXM1200, Nikon) and ACT-1 acquisition software (Nikon).

2.9.5 Nerve wholemount immunohistochemistry

The peroneal nerve was carefully cut away from the tibial nerve with small dissecting scissors, immediately prior to fixation with 4% paraformaldehyde overnight at 4˚C. The nerve sample was then rinsed with PTX (1% triton X-100 in PBS) three times for 10 min each and then incubated in blocking buffer (10% FBS in PTX) overnight at 4˚C in a 2-ml eppendorf tube. The primary antibodies (Neurofilament and S100) were diluted in 10% FBS-PTX and incubated with the sample for 72 hours at 4˚C with gentle shaking. The sample was then rinsed three times for 15 min each, followed by washing in PTX for 6 hours at 4˚C. The PTX was changed each hour and the samples left to wash overnight in the final wash. Secondary antibodies were diluted in 10% FBS-PTX and incubated for 48 hours at 4˚C with gentle shaking. The samples were then rinsed in PTX three times for 15 mins each, followed by washing overnight in PTX. The nerve was then cleared with 25%, 50% and 75% glycerol in PBS until the tissue sinks. Samples were then mounted onto a coverslip and slide using Citifluor mounting medium and nail varnish. The samples were visualised using a microscope (Leica SP2 confocal microscope), and a maximum projection of 30 stacks was created. Images were imported into Adobe Photoshop.

2.10 Statistical Analysis

All data are presented as arithmetic mean ± standard deviation (SD). Unless otherwise stated, statistical significance was estimated using the Student's t-test using Prism version 6 software (Graphpad).

Chapter 3: c-Jun controls Schwann cell morphology and migration

3.1 Introduction

Schwann cell morphology and migration are important features of the Schwann cell response to nerve injury. Schwann cell morphology is altered following injury and axonal loss in the distal nerve stump, leading to the formation of the Bands of Büngner - Schwann cell tubes that guide the regrowth of regenerating axons. The precise form of these cells is currently under investigation, however, it is known they differ greatly from mature myelinating and non-myelinating Schwann cells. The most significant difference is that the axon-Schwann cell interface is absent in Bungner Schwann cells (the myelin ring and adaxonal membrane of myelinating Schwann cells, and the invaginated plasma membrane of Remak Schwann cells is lost during transdifferentiation). Electron micrographs of Bungner cells show cells with multiple processes inside the basal lamina tube, and loss of c-Jun leads to a reduction in the number of Schwann cell processes (Arthur-Farraj et al. 2012). Furthermore, Schwann cells migration from the endoneurial tubes is necessary to bridge the gap between proximal and distal nerve stumps following a transection injury, this occurs in concert with the extension of perineurial cells, blood vessels and the influx of macrophages, as discussed in more detail in Chapter 1.

Considering that Schwann cell morphology and migration are influential during peripheral nerve regeneration, I decided to investigate how these are affected when c-Jun, a master regulator of Schwann cell transdifferentiation, is deleted in Schwann cells. Studies in other cell types, such as fibroblasts have shown that c-Jun exerts control over cell morphology and migration via several distinct pathways (Jiao et al. 2008; Jiao et al. 2010; Zenz et al. 2003).

3.2 Results

3.2.1 Loss of c-Jun induces flattening and reduces the polarity of primary Schwann cells

In order to analyze the effect of c-Jun on Schwann cells, control and c-Jun knockout cells were generated by infecting purified mouse c-Jun$^{flox/flox}$ Schwann cells with adeno-GFP and adeno-Cre respectively (as described in Chapter 2). These primary mouse Schwann cells were immunostained with an anti β1-integrin antibody in order to visualize the plasma membrane (Figure 3.1A). Additionally, c-Jun knockout cells were also generated using the P0-Cre recombinase mouse. Schwann cells were purified from P0-Cre^{+};c-Jun$^{flox/flox}$ and P0-Cre^{-};c-Jun$^{flox/flox}$ P5 littermates to obtain c-Jun knockouts and controls. I used two methods of generating the c-Jun knockout cells, firstly to demonstrate the robustness of the cell morphology phenotype, and secondly because c-Jun knockout Schwann cells proliferate slowly, making them hard to expand for use in experiments requiring large numbers of primary Schwann cells, such as migration assays. For this reason, I purified and expanded c-Jun$^{flox/flox}$ cells for all of my subsequent cell culture experiments, and infected these with adeno-Cre or adeno-GFP to generate knockout and control cells.

The results of this experiment demonstrate that the c-Jun knockout Schwann cells have an appearance significantly different to the control cells. The characteristic bi-polar and tri-polar morphology of cultured mouse Schwann cells is replaced with a flattened and rounded profile in both the adeno-Cre and P0-Cre Schwann cells. Furthermore, the expression of β1-integrin in control and c-Jun knockout cells is distributed across the entire plasma membrane and thus serves

as a useful way to delineate the cell shape (Fig. 3.1A). Quantification of cell area reveals a significant difference in the size of the c-Jun knockout cells compared to the control (Fig. 3.1B). There is a small difference in cell size between the two types of c-Jun knockout Schwann cells (P0-Cre and adeno-Cre expressing cells). Cell shape was analysed by measuring circularity with ImageJ, as described in the methods, using the formula:

$$\text{Circularity} = 4\pi \times (\text{area} / \text{perimeter}^2).$$

Quantification revealed that c-Jun deleted cells are significantly more circular than control cells (Fig. 3.1C).

Figure 3.1: Deletion of c-Jun in Schwann cells increases cell area and circularity.
(A) Immunocytochemistry of β1-integrin delineating the plasma membrane of control and c-Jun knockout mouse Schwann cells. c-Jun was deleted from primary Schwann cells using two methods; firstly by expression of Cre recombinase under the P0 promoter in c-Jun floxed mice (P0-cre; c-Jun flox/flox) and secondly by infecting c-Jun floxed purified Schwann cells with an adenovirus containing the gene for Cre-recombinase (adeno-Cre + c-Jun flox/flox). Controls were mice/Schwann cells without Cre-recombinase, and an adenovirus expressing GFP instead of Cre, respectively. Scale bar, 20μm. (B) Cell area of control and c-Jun knockout Schwann cells. (C) Circularity was measured for both control and knockout cells, as defined by $4\pi \times (\text{area} / \text{perimeter}^2)$. A value of 1 equals a circle, while a value of 0 represents a straight line. Data are means ±SD; n= a total of 180 cells from three independent experiments (90 each); $^{***}P<0.001$.

Figure 3.1

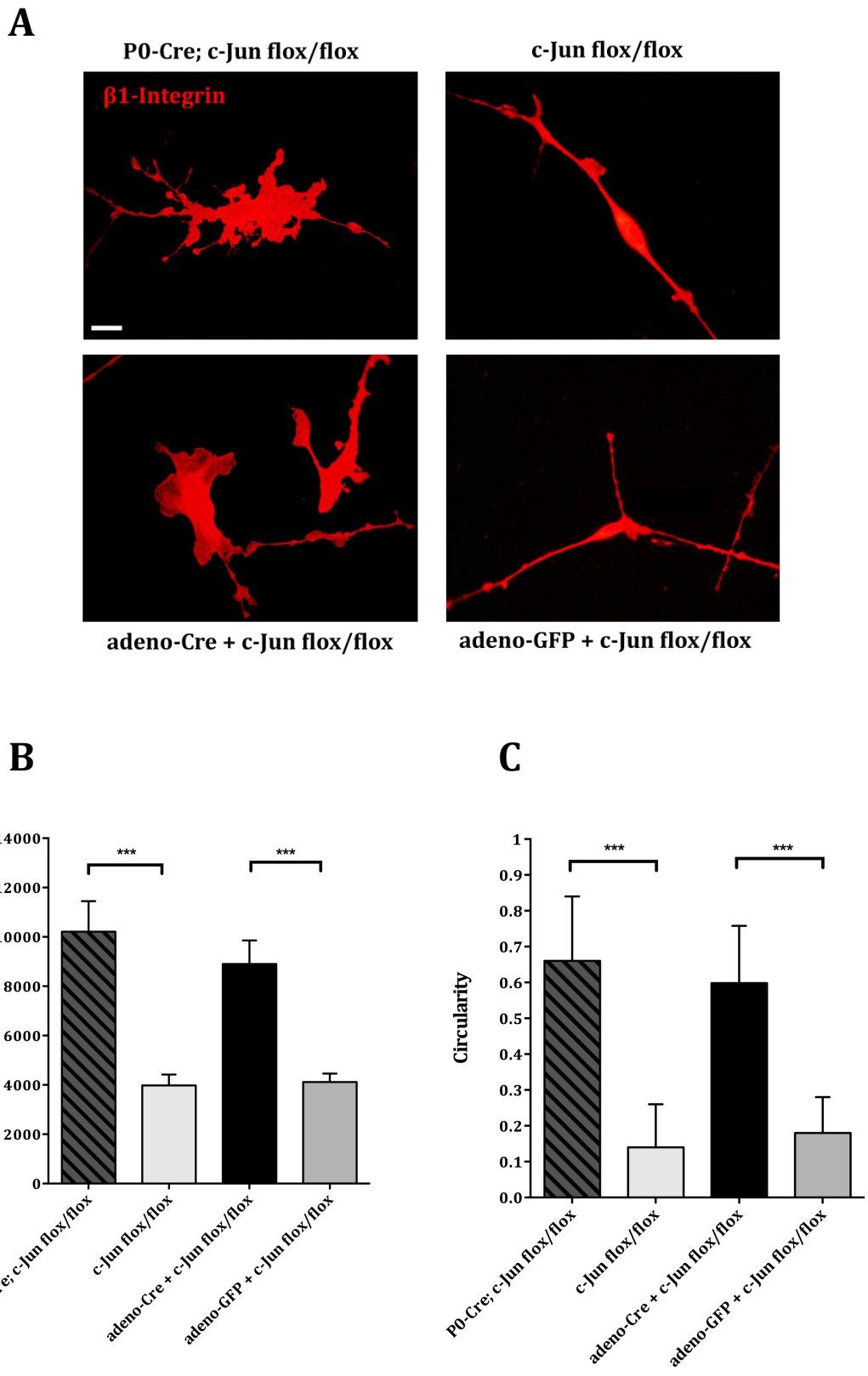
A
P0-Cre; c-Jun flox/flox
c-Jun flox/flox
β1-Integrin
adeno-Cre + c-Jun flox/flox
adeno-GFP + c-Jun flox/flox
B
Cell Area (μm²)
14000
12000
10000
8000
6000
4000
2000
0
***
***
P0-Cre; c-Jun flox/flox
c-Jun flox/flox
adeno-Cre + c-Jun flox/flox
adeno-GFP + c-Jun flox/flox
C
Circularity
1
0.9
0.8
0.7
0.6
0.5
0.4
0.3
0.2
0.1
0.0
***
***
P0-Cre; c-Jun flox/flox
c-Jun flox/flox
adeno-Cre + c-Jun flox/flox
adeno-GFP + c-Jun flox/flox

3.2.2 c-Jun deletion impairs Schwann cell migration

Changes in cell shape and the cytoskeletal rearrangement that accompanies this are frequently associated with changes in cell migration. In particular, cell flattening and a loss of polarization correlate well to a reduction in cell migration. In order to determine whether the morphological phenotype that follows the loss of c-Jun in Schwann cells also affects cell migration, I conducted transwell migration assays. As discussed above, c-Jun knockout and control cells were generated by infecting c-Jun$^{flox/flox}$ purified Schwann cells with adeno-Cre and adeno-GFP. Cell migration was induced by adding two concentrations of horse serum (0.5 and 3%) to the lower compartment of the transwell. Horse serum is a mitogen for mouse Schwann cells, so cells were pre-incubated with mitomycin-C for 2 hours before the assay in order to abolish the effects of proliferation on the results. Figure 3.2A shows that deletion of c-Jun in Schwann cells causes a reduction in cell migration through the transwell membrane (47% fewer knockout cells than wildtype, $P>0.001$). This difference is maintained in both concentrations of serum, but no significant difference was observed in the absence of any chemoattractant (defined medium only), where very few cells had migrated across the membrane for either genotype.

NRG1 is an important chemoattractant for Schwann cells, both during development and regeneration. In order to investigate its affect of the migration of c-Jun knockout Schwann cells, I repeated the assay with NRG1 (20 ng/ml) present in the lower compartment of the transwell. Again, to abolish the known affects of NRG1 on cellular proliferation, this was carried out with a pre-incubation of mitomycin-C. Figure 3.2B shows a very similar reduction in cell migration for c-Jun knockout Schwann cells to that seem in response to horse serum. In addition to examining the effect of NRG1 on cell migration, I also wanted to see if re-

introducing c-Jun into the knockout cells would restore normal cellular migration. This was achieved by infecting the knockout cells with an adenovirus expressing c-Jun and examining their migration in response to NRG1. Figure 3.3B shows that restoring c-Jun in knockout cells does indeed restore cell migration to a level similar to that of the control (no significant difference), and elevating c-Jun levels in wildtype Schwann cells leads to a slight increase in cell migration ($P<0.01$).

In order to confirm the deficient migration of c-Jun knockout Schwann cells, an additional assay measuring migration in response to NRG1 was carried out using the wound assay [described in Chapter 2 and (Meintanis et al. 2001)]. The results from this experiment confirmed that deletion of c-Jun leads to a reduction in Schwann cell migration (Fig. 3.2C).

Figure 3.2: Schwann cell c-Jun is required for cell migration.
(A) Cell migration was measured using a Transwell migration assay. Migrated cells were counted after being incubated with defined medium, or 0.5% and 3% horse serum - a known chemoattractant for Schwann cells. Data are means ±SD of three independent experiments; $^{****}P<0.0001$. (B) A Transwell migration assay showing that enforced expression of c-Jun in c-Jun KO cells using an adenovirus restores normal cell migration in response to NRG-1 (20 ng/ml) compared to control Schwann cells infected with adenoviral GFP. Control cells infected with c-Jun adenovirus show a slight increase in cell migration. (C) Wound assay showing Schwann cell migration over a period of 6, 12 and 24 hours in response to NRG-1 (20 ng/ml) for c-Jun knockout and control cells.

Figure 3.2

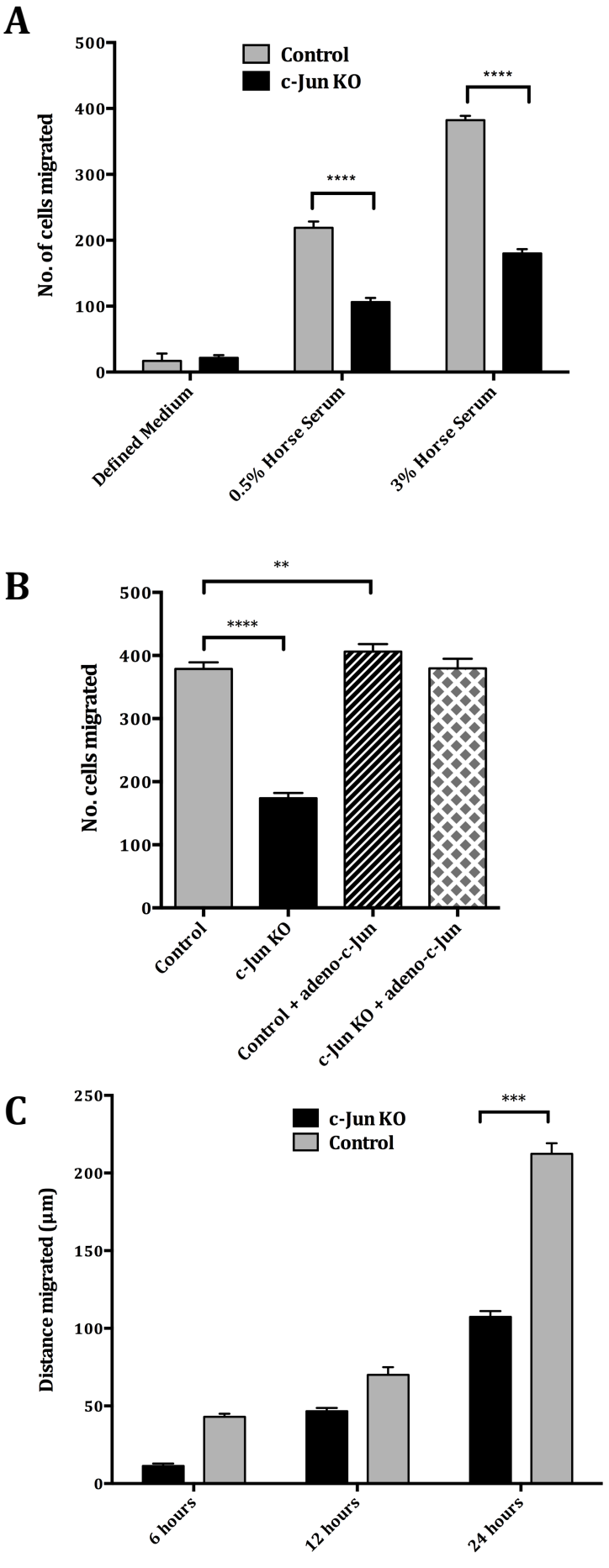
A
Control
c-Jun KO
No. of cells migrated
500
400
300
200
100
0
****
****
Defined Medium
0.5% Horse Serum
3% Horse Serum
B
**
****
No. cells migrated
500
400
300
200
100
0
Control
c-Jun KO
Control + adeno-c-Jun
c-Jun KO + adeno-c-Jun
C
c-Jun KO
Control
***
Distance migrated (µm)
250
200
150
100
50
0
6 hours
12 hours
24 hours

3.2.3 c-Jun deletion reduces cell migration on collagen and laminin

Collagen and laminin are both present in the peripheral nerve and are known to promote the migration of Schwann cells. In order to investigate the effect of these molecules on the c-Jun knockout cells, I performed transwell migration assays with collagen I-(from rat tail) and laminin 2-coated transwell membranes. Figure 3.3 shows significantly fewer Schwann cells migrate on both laminin and collagen in the c-Jun knockout compared to the control ($P<0.0001$). Control Schwann cells have significantly increased migration on laminin over collagen ($P<0.0001$), but this difference is not present when c-Jun is deleted from the cells.

Figure 3.3

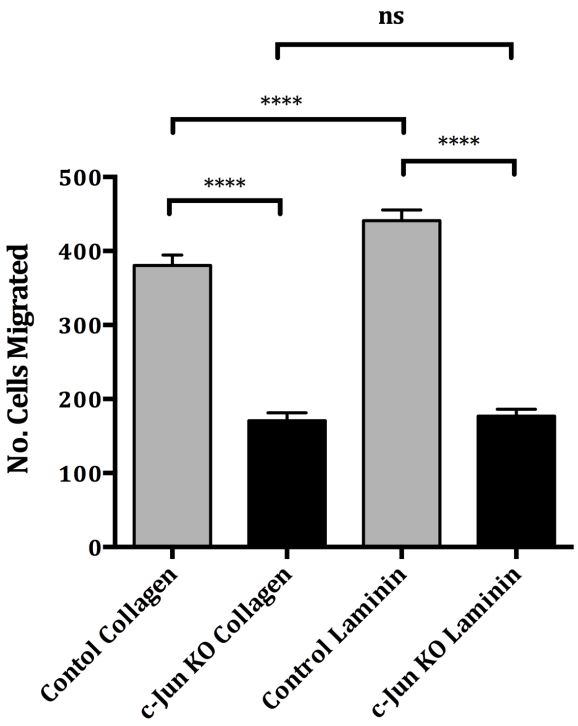

Figure 3.3: Schwann cell c-Jun is required for migration on collagen and laminin substrates.
Cell migration was measured using transwells coated with laminin or collagen for both control and c-Jun knockout Schwann cells. Data are means ±SD from three independent experiments; $^{****}P<0.0001$; ns= no significant difference.

3.2.4 c-Jun loss disrupts the Schwann cell actin cytoskeleton

The previous experiments show that c-Jun deletion causes significant morphological changes to Schwann cells, affecting their ability to migrate. This phenotype has a significant affect on the sensitivity of these cells to pro-migratory signals, such as serum, NRG1, laminin and collagen. For this reason, I decided to look at the arrangement of the actin cytoskeleton in these cells. Actin polymerization and formation of actin filaments is strongly associated with changes in cell shape, most notably the formation of stress fibers and lamellipodia. Figure 3.4 shows Schwann cells labeled with fluorescein-phalloidin, which binds to actin inside the cell. Control Schwann cells show staining throughout the cell. The Schwann cell processes are so narrow that no detailed structure to the actin positive staining can be seen. In comparison, in c-Jun knockout cells, thick actin stress fibers are visible at the periphery of the cell, often completely encircling to form an actin wreath.

Figure 3.4: Deletion of Schwann cell c-Jun induces actin cytoskeleton rearrangement.
The actin cytoskeleton of control and c-Jun null cultured Schwann cells was labeled with fluorescein-phalloidin fluorescent stain (maginification, x40; scale bar, 50μm). Nuclei were labeled with the nuclear stain, dapi.

Figure 3.4

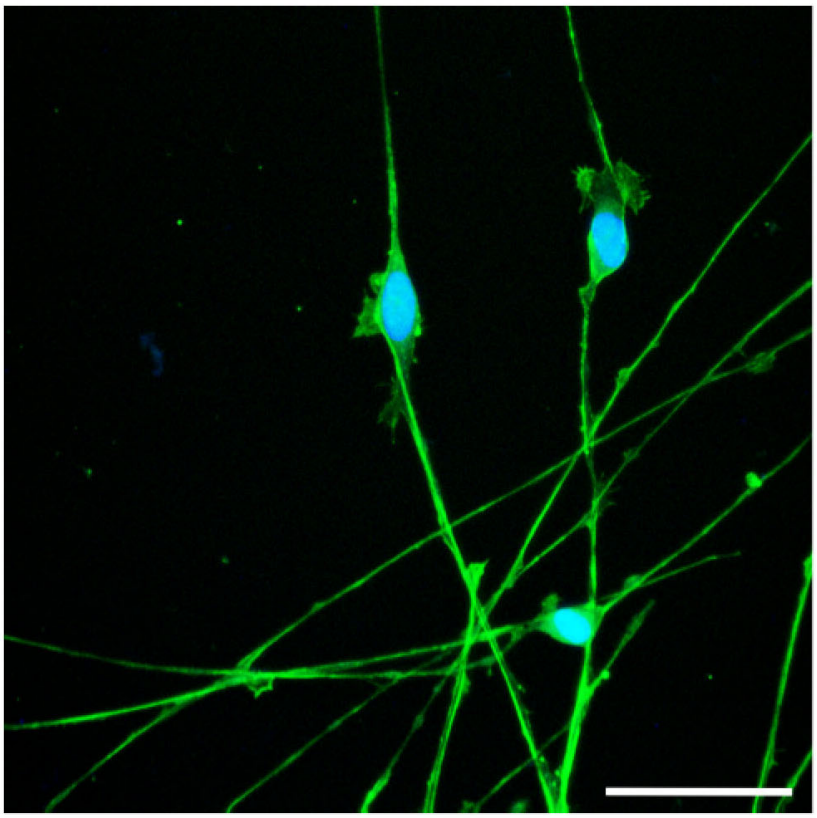

Control

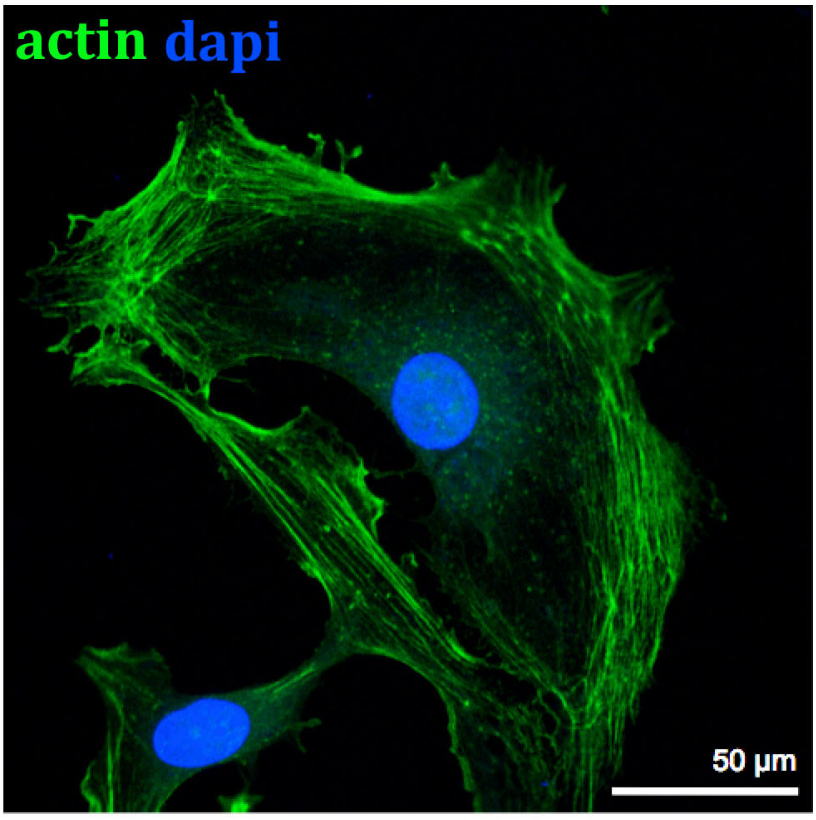

c-Jun KO

3.2.5 c-Jun deletion induces the formation of focal contacts

The presence of large focal contacts is often associated with reduced cellular migration. In order to visualize the presence or absence of focal contacts in Schwann cells, I performed immunocytochemistry of control and c-Jun knockout cells using an anti-vinculin antibody (described in Chapter 2). Figure 3.5A shows negligible cytoplasmic staining of vinculin in control Schwann cells, and it was very rare to see any aggregates of vinculin that would indicate the presence of a focal contact in the cell. Those that were present were seen at the very end of the Schwann cell process. The c-Jun knockout cell displays many more large focal contacts in the cell, typically located at the ends of actin stress fibers (mean of 15 contacts per cell, $P>0.001$).

Figure 3.5

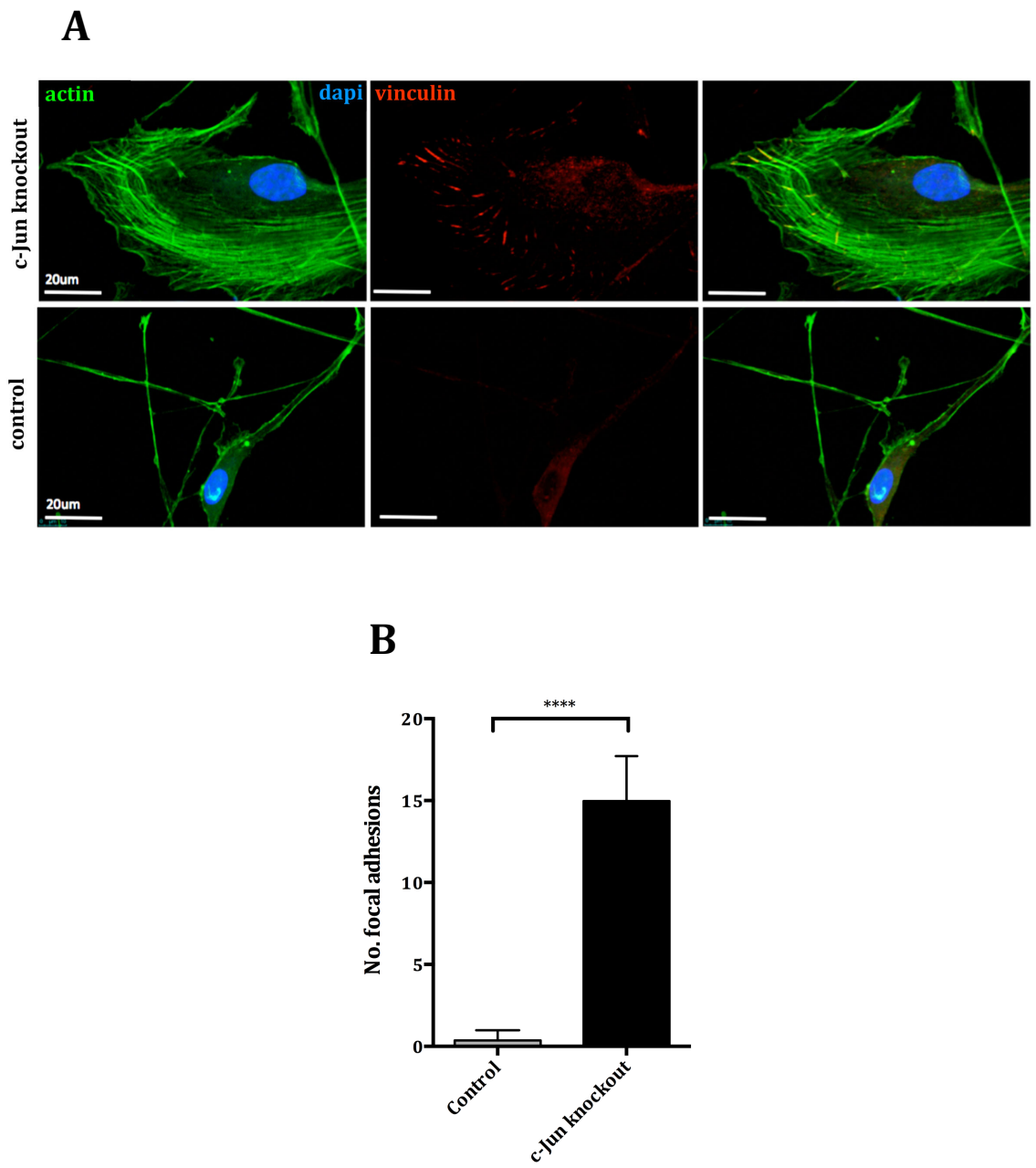

Figure 3.5: Deletion of Schwann cell c-Jun induces focal adhesions.
(A) Focal adhesions were labeled with an antibody against the focal adhesion protein vinculin. Actin was labeled with fluroscein-α-bungarotoxin. Focal adhesions are visible in the c-Jun KO at the end of large actin stress fibers. Scale bar, 20 μm .(B) Quantification of focal adhesion number per Schwann cell. c-Jun KO Schwann cells had a mean number of 14.97 ± 0.502 focal adhesions compared to 0.3667 ± 0.1123 for control cells. Data are means ±SD from three independent experiments, with a total of 150 cells. $^{****}P<0.0001$.

3.3 Discussion

Schwann cell c-Jun in important for the Schwann cell response to nerve injury, including the transdifferentiation of myelinating and Remak Schwann cells to Bungner repair cells (Arthur-Farraj et al. 2012; Fontana et al. 2012). The change in Schwann cell morphology demonstrated in Figure 3.1 may be a determinant of the poor regenerative ability of the P0-Cre^{+}; c-Jun $^{flox/flox}$ mouse following nerve crush injury. The results of the present study demonstrate that c-Jun is required for Schwann cells to migrate normally *in vitro*. The Schwann cell morphological change has been published (Arthur-Farraj et al, 2012) and forms my contribution to the study (Figure 3D and E). This paper is included at the end of this thesis.

Notably, the overexpression of c-Jun in wildtype Schwann cells leads to a slight but significant increase in migration. This finding is significant, as it is of interest to identify factors that might improve Schwann cell migration in a clinical setting, for example in enabling cells to colonize grafts of tissue or conduit more rapidly. Both horse serum and NRG1, potent Schwann cell chemoattractants, failed to compensate for the loss of c-Jun in the transwell assays. This suggests it is unlikely the cells have lost sensitivity to a specific molecule, such as NRG1, but instead show a fundamental inability to engage in persisted and directional movement. This could be due to the adeno-Cre failing to infect all the Schwann cells in the culture dish, but may also be due to genetic differences, since the c-Jun$^{flox/flox}$ Schwann cells are derived from mice of a pure C57Bl/6 background, whereas the P0-Cre derived Schwann cells have a partial FVB background (as described in Chapter 2.) To eliminate any potential phenotypic differences, c-Jun knockout Schwann cells were generated from c-Jun$^{flox/flox}$ mice infected with adeno-Cre, for all future *in vitro* experiments in this study.

The results from Figure 3.3 reveal that neither collagen or laminin substrates enhanced the migration of c-Jun knockout Schwann cells. This provides a further indication that putting the c-Jun knockout Schwann cells into an environment that favors cell migration has no effect on their ability to migrate. The results of this assay also agree with previous findings that laminin enhances control Schwann cell migration more than collagen.

The cytoskeletal phenotype of the c-Jun knockout Schwann cells, specifically, the induction of actin stress fibers and focal contacts is similar to that seen when c-Jun is ablated from mouse embryonic fibroblasts (Jiao et al, 2008). For this reason, I decided to investigate in later experiments whether the same molecular pathway downstream of c-Jun in these cells was also regulated by c-Jun in mouse Schwann cells.

In summary, the results of this chapter demonstrate that c-Jun regulates Schwann cell morphology and migration *in vitro*. This is accompanied by rearrangement of the actin cytoskeleton and the induction of focal contacts, and agrees with results in other cell types.

Chapter 4. c-Jun regulation of Schwann cell migration: Molecular mechanisms

4.1 Introduction

The results of Chapter 3 revealed the significant abnormalities in both Schwann cell morphology and migration when c-Jun is deleted from the c-Jun$^{flox/flox}$ primary Schwann cell cultures using adenoviral Cre recombinase. As a proto-oncogene, c-Jun has attracted attention for its role in the development of tumor malignancy, and studies have shown that its expression promotes cell migration in a number of cell types, including mouse embryonic fibroblasts and mammary tumor cells (Jiao et al. 2010; Jiao et al. 2008; Katiyar et al. 2007; Janowski et al. 2011).

There have been additional, earlier studies that show a role for c-Jun in inducing cell migration and tissue morphogenesis during development. The Drosophila homologue of c-Jun, DJun, has been demonstrated to play a crucial role in dorsal closure, a morphogenetic process that involves the movement of two lateral epithelial sheets towards the midline of the embryo. The Djun mutant displays a dorsal-open phenotype and therefore lacks a dorsal epidermis. In this example, DJun lies downstream of DRac and DJNK and exerts its control of cell migration via the transcriptional regulation of Decapentaplegic, a homologue of the vertebrate bone morphogenic proteins (BMPs) (Hou et al. 1997; Riesgo-Escovar & Hafen 1997a; Riesgo-Escovar & Hafen 1997b; Glise & Noselli 1997). An additional developmental process involving c-Jun mediated cell migration is murine eyelid closure. Deletion of c-Jun in keratinocytes leads to the eyes open at birth (EOB) phenotype, and in this case, c-Jun regulates the expression of EGF receptor to control cell movement and eyelid closure (Zenz et al. 2003).

The transcription factor c-Jun therefore regulates cell movement and morphology through a number of distinct pathways, and these take place during

development and pathogenesis. To date, there have been no examples of c-Jun regulating cell migration during tissue regeneration. In the present study, I aim to uncover the mechanisms by which c-Jun controls Schwann cell shape and motility using a combination of gene and protein expression analysis.

4.2 Results

4.2.1 Deletion of Schwann cell c-Jun does not alter the expression of NRG and its receptors

There exists a wealth of literature showing the important functions of NRG signaling in Schwann cell biology. Those relating to Schwann cell proliferation and motility have been discussed in detail in Chapter 1, and the reduction in migration observed when c-Jun is deleted in Schwann cells has been described in Chapter 3. To see if c-Jun deletion has an effect on the expression of NRG and its downstream receptors and effectors, and to assess whether this contributes to the deficit in migration and perturbed morphology, I performed RT-qPCR on c-Jun null and control Schwann cells in three independent experiments. These Schwann cells were purified from the neonatal nerves of c-Jun floxed mice and infected with adeno-Cre and adeno-GFP viruses to generate purified control and c-Jun knockout Schwann cell cultures. Figure 4.1 shows the fold upregulation and downregulation of the mutant mRNA compared to that of the control cells of the NRG type I, II and III isoforms, their receptors ErbB2 and ErbB3 and Shp2, a downstream activator of the MAPK pathway in many cell types (see Dance et al., 2008 for review). There are no significant differences in the C_T values of the c-Jun knockout and control Schwann cells for any of these genes when normalised to the housekeeping gene expression, indicating that similar levels of mRNA are present in both genotypes and that c-Jun does not affect the expression of key genes in the NRG1 signaling pathway.

Figure 4.1

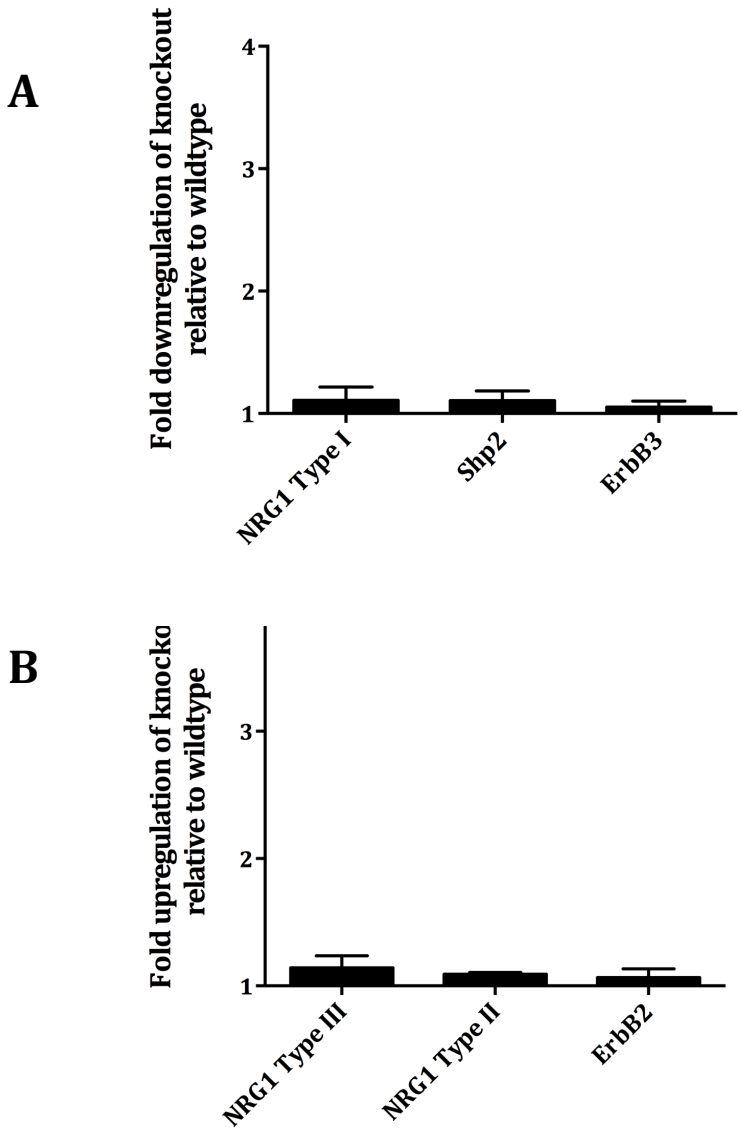

Figure 4.1: *In vitro* deletion of Schwann cell c-Jun does not alter the expression of NRG1 isoforms and their receptors

RT-qPCR was used to examine relative expression of NRG Types I, II and III, the NRG receptors ErbB2 and ErbB3, and Shp2, which is downstream of ErbB2/3. cDNA was prepared from RNA isolated from cultured control and c-Jun KO Schwann cells as described in Chapter 2. (A) Fold upregulation of genes in c-Jun knockout cells compared to wildtype control cells. (B) Fold downregulation of genes in c-Jun knockout cells compared to wildtype cells. All data show no significant difference in fold change between knockout and wildtype. All data are normalised to the reference genes GAPDH and YWHAZ. Reverse Transcriptase minus (RT-) and No Template Controls (NTCs) negative controls were used and showed that RNA was adequately treated with DNase and that no PCR products were formed from the primers in the absence of cDNA. All data are means ±SD from three independent experiments.

4.2.2 Deletion of c-Jun does not regulate Schwann cell expression of c-Src

To determine directly whether the removal of c-Jun in Schwann cells affects the expression of c-Src, I performed immunolabelling of control and c-Jun knockout cells with antibodies against c-Src. Figure 4.2A shows the distribution of c-Src and actin in the control and c-Jun knockout Schwann cells. The immunolabelling in the image shows a fairly even distribution of c-Src in the cytoplasm of the knockout cell, and it appears to be absent from the cell cortex. The control wildtype Schwann cell also shows expression of c-Src in the cytoplasm. In this case it is hard to describe a specific subcellular location of this protein as the cell processes are very narrow but the overall brightness of the c-Src labeling in the control and c-Jun knockout cells is similar. I also wished to investigate whether this observation would be replicated after nerve injury. To determine the protein level of c-Src *in vivo*, a western blot was carried out on cell lysates from the sciatic nerve distal stumps of control and *P0-Cre; c-Jun flox/flox* mice, taken 7 days following nerve transection. c-Jun is not present in the Schwann cells in the *P0-Cre; c-Jun flox/flox* mice (Arthur-Farraj et al., 2012) (see material and methods also). As expected, levels of c-Src increased in the distal stumps of control nerves following nerve transection, but no significant difference was observed between c-Src protein levels in control and knockout nerves (Fig. 4.2B). These experiments suggest that direct regulation of c-Src protein levels is unlikely to contribute the failure of migration seen in the c-Jun knockout cells.

Figure 4.2

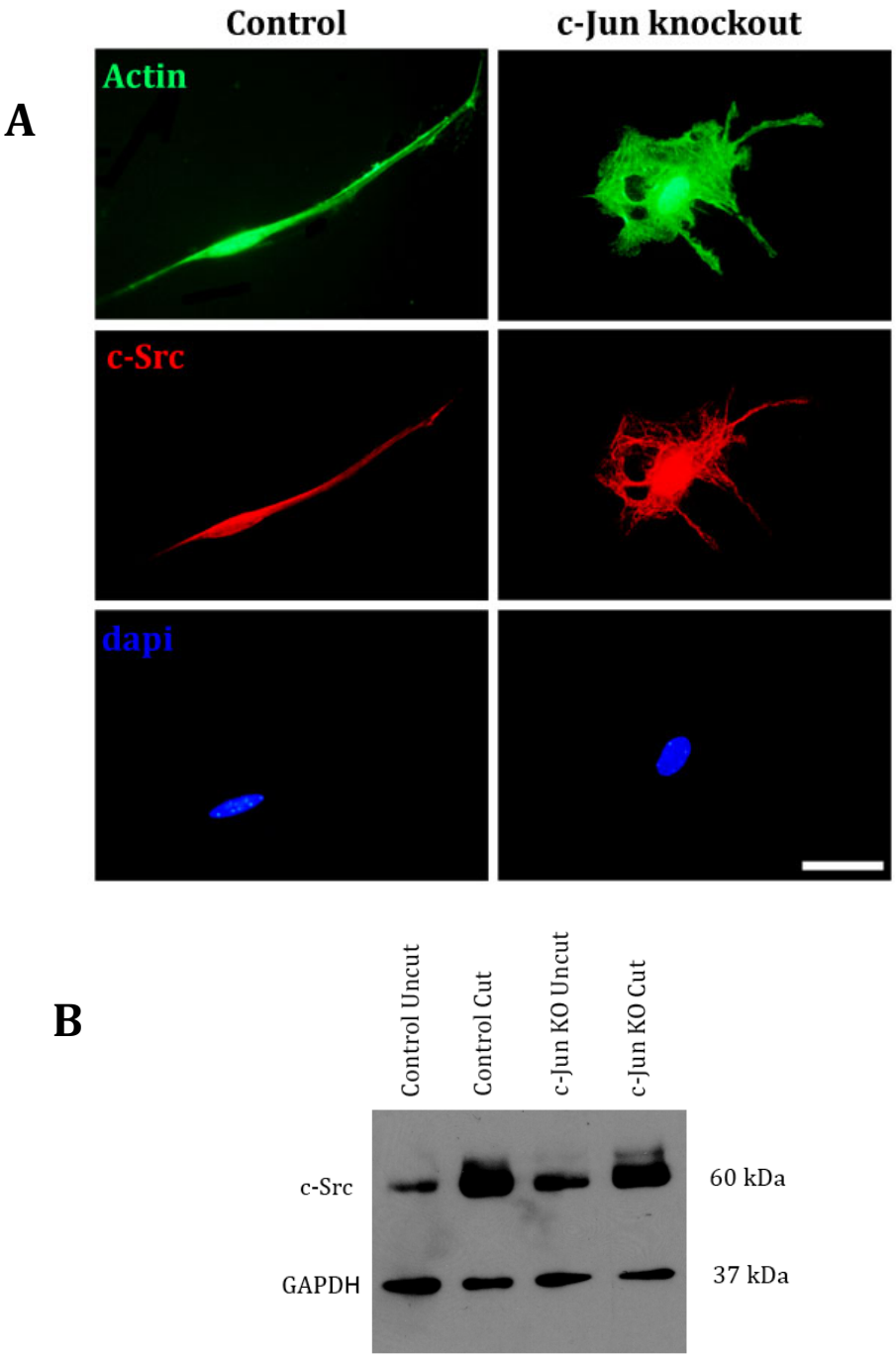

Figure 4.2: Deletion of c-Jun does not enhance Schwann cell expression of c-Src.
(A) Immunocytochemistry showing the distribution of actin and c-Src in c-Jun knockout and control Schwann cells in culture. Control and knockout cells were purified from neonatal nerves and infected with adeno-GFP and adeno-Cre respectively. Cells are co-labelled with Hoechst nuclear dye. Scale bar, 50 μm. (B) Western blot showing expression of c-Src in uncut nerves of control and c-Jun conditional knockout mice and in the distal stump of control and knockout mice, 7 days following nerve transection. Molecular weight markers were located on the PVDF membrane and not visualised on the film, and are therefore not shown.

4.2.3 Modulation of c-Src and ROCKII activity affects Schwann cell migration

Fibroblast and epithelial cell expression of the non-receptor protein tyrosine kinase c-Src is reduced in the absence of c-Jun, and this leads to the hyperactivation of ROCKII, a protein kinase that affects the cytoskeleton in several ways, including the induction cell flattening and reduction of cellular migration. This pathway is thought to contribute to the invasiveness of cancer cells that over express c-Jun and therefore lose this brake on cell motility (Jiao et al. 2008; Jiao et al. 2010). The cells lacking c-Jun described in these papers have a very similar migratory and morphological phenotype to that seen in Schwann cells lacking c-Jun, including the induction of actin stress fibers and focal adhesions (see Chapter 3).

I therefore decided to investigate whether inhibiting the activity of either of these molecules would replicate the migratory phenotype seen in the c-Jun null Schwann cells. As a first step, I set out to see if these proteins had an effect on the migration of wildtype Schwann cells in culture. Inhibition of ROCKII using the inhibitor Y27632 showed a slight but significant increase in Schwann cell migration using the transwell assay. Inhibition of c-Src with the inhibitor SU6656 produced a more significant change, with a large reduction in Schwann cell transwell migration (Figure 4.3).

Figure 4.3

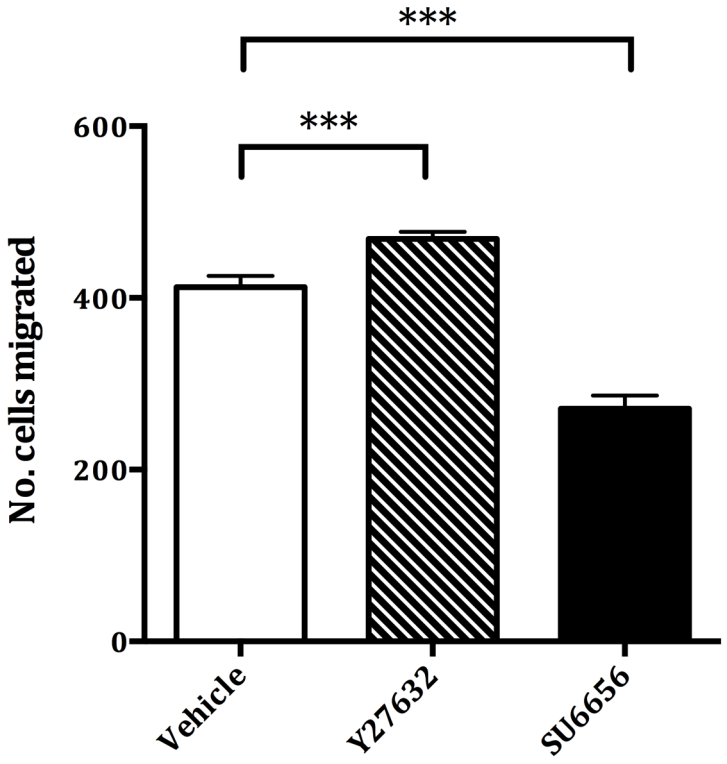

Figure 4.3: Schwann cell transwell migration in response to c-Src and ROCKII inhibitors.
Transwell migration assays were performed using wildtype mouse Schwann cells cultured in the presence of inhibitors for c-Src (SU6656, 2 μM) and ROCKII (Y27632, 10μM). Data are means ±SD from three independent experiments and $^{***}P < 0.001$.

4.2.4 Inhibition of ROCKII rescues the c-Jun knockout migration phenotype

ROCKII activity has several effects on the cytoskeleton and this is cell-type specific. In fibroblasts, increased ROCKII activity is linked to cell spreading and reduced motility. For this reason, I set out to see if inhibiting ROCKII might restore the cell migration of c-Jun knockout Schwann cells. Figure 4.4 shows the migration of c-Jun knockout Schwann cells using the wound assay, in response to the ROCKII inhibitor Y27632 in pro-migratory conditions (NRG1 20 ng/ml). The data shows that the knockout cells were able to migrate across the wound far more easily in the presence of the inhibitor compared to those incubated with vehicle alone. These cells were able to almost completely close the wound within 24 hours, at a rate similar to wildtype Schwann cells (Figure 4.5). These experiments suggest that lack of c-Jun in Schwann cells may induce activation of ROCKII, although further experiments would be required to prove this point definitively, and that this pathway is likely to be important in the reduction of migratory behavior seen in c-Jun knockout Schwann cells.

Figure 4.4

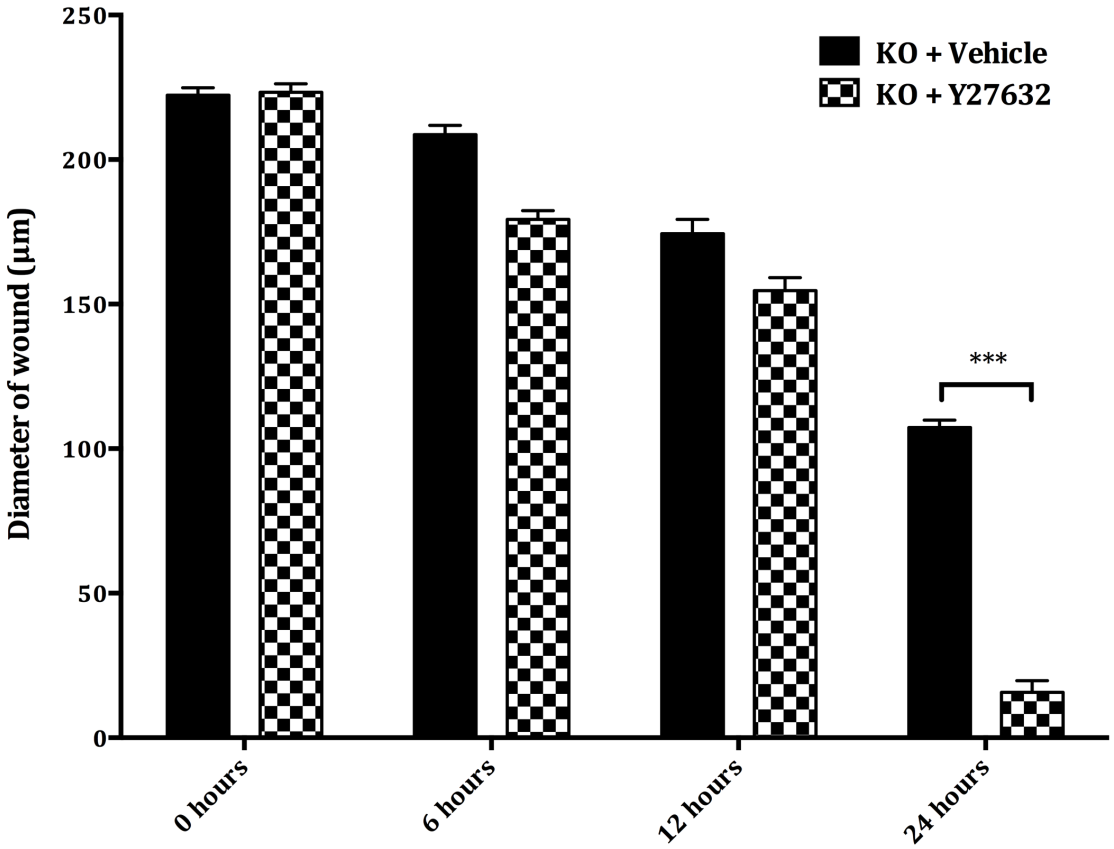

Figure 4.4: Inhibition of ROCKII rescues the c-Jun knockout migration phenotype

A wound assay was performed using c-Jun knockout Schwann cells seeded on laminin-coated coverslips. Knockout cells were incubated with inhibitor for ROCKII (Y27632, 10µM). Data are means ±SD from three independent experiments; $^{***}P < 0.001$

4.2.5 Inhibition of c-Src in wildtype Schwann cells mimics the c-Jun phenotype

As shown in Figure 4.2, c-Src inhibition slows the rate of Schwann cell migration. In order to further assess whether inhibiting c-Src has an effect on the migration of the Schwann cells, I performed the wound assay with these cells in the presence of SU6656. Figure 4.5 shows that in the presence of the inhibitor, Schwann cell migration is significantly slowed by 24 hours and does not close the wound. The rate of migration is similar to that of the c-Jun knockout Schwann cells in Figure 4.4.

Figure 4.5

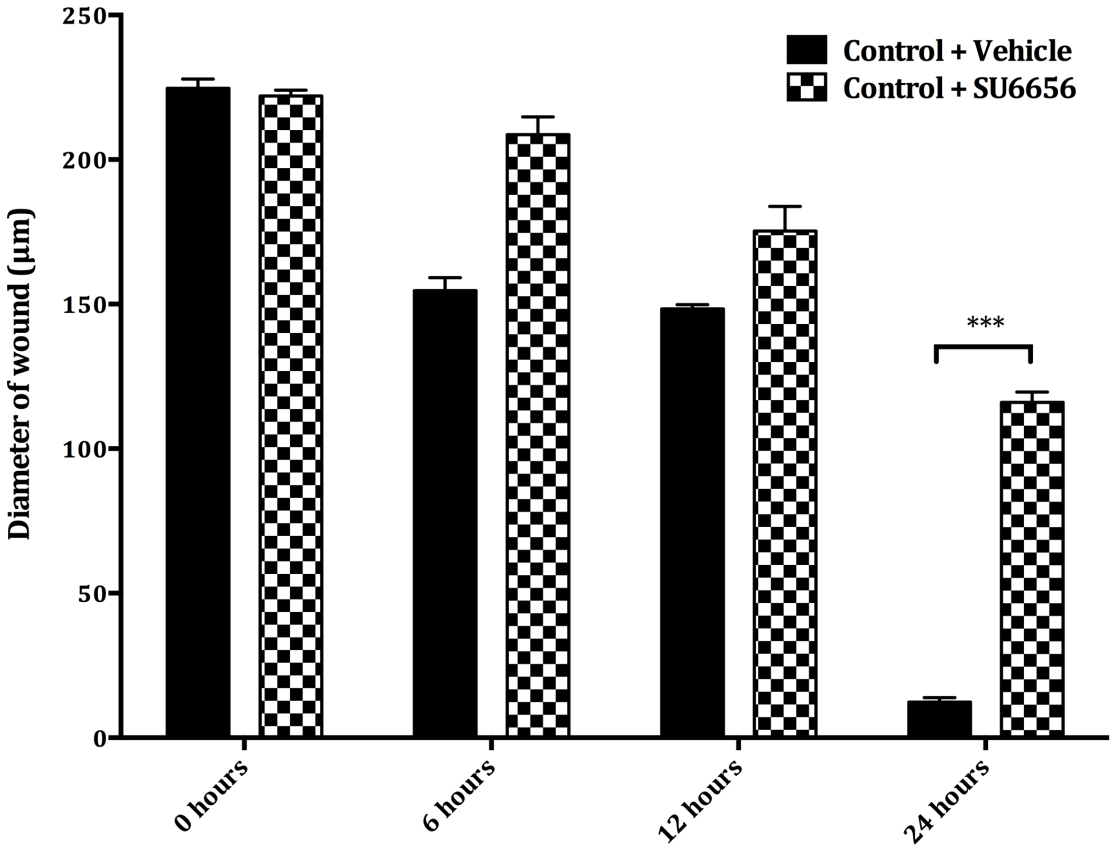

Figure 4.5: Inhibition of c-Src in wildtype Schwann cells mimics the c-Jun migration phenotype

A wound assay was performed using control Schwann cells seeded on laminin-coated coverslips. Control and c-Jun knockout cells were incubated with an inhibitor for c-Src (SU6656, 2 μM). Data are means ±SD from three independent experiments; $^{***}P < 0.001$

4.2.6 Deletion of Schwann cell c-Jun does not alter the mRNA levels of candidate genes involved in cell migration and remodeling of the cytoskeleton

In order to discover genes regulated by c-Jun that are responsible for the significant change in cell shape and migration when c-Jun is deleted in Schwann cells, I decided to conduct a gene screen by selecting candidates that fell into three groups: genes that are already known to affect these attributes in Schwann cells, genes that are both regulated by c-Jun in other cell types and regulate the cytoskeleton, and finally, genes that are major regulators of the cytoskeleton, but have not been studied in Schwann cells or have been shown to be regulated by c-Jun (discussed in Chapter 1). I performed RT-qPCR on cDNA synthesized from mRNA isolated from control and c-Jun knockout cells that had been infected with adeno-GFP and adeno-Cre respectively. Despite the careful choice of genes, the results of this candidate screen show that these genes are not significantly regulated by c-Jun at the mRNA level (Figure 4.6). The expression of the above genes was not found to be significantly altered following nerve transection between c-Jun KO and wildtype mice, according to microarray data (Arthur-Farraj et al., 2012).

Figure 4.6

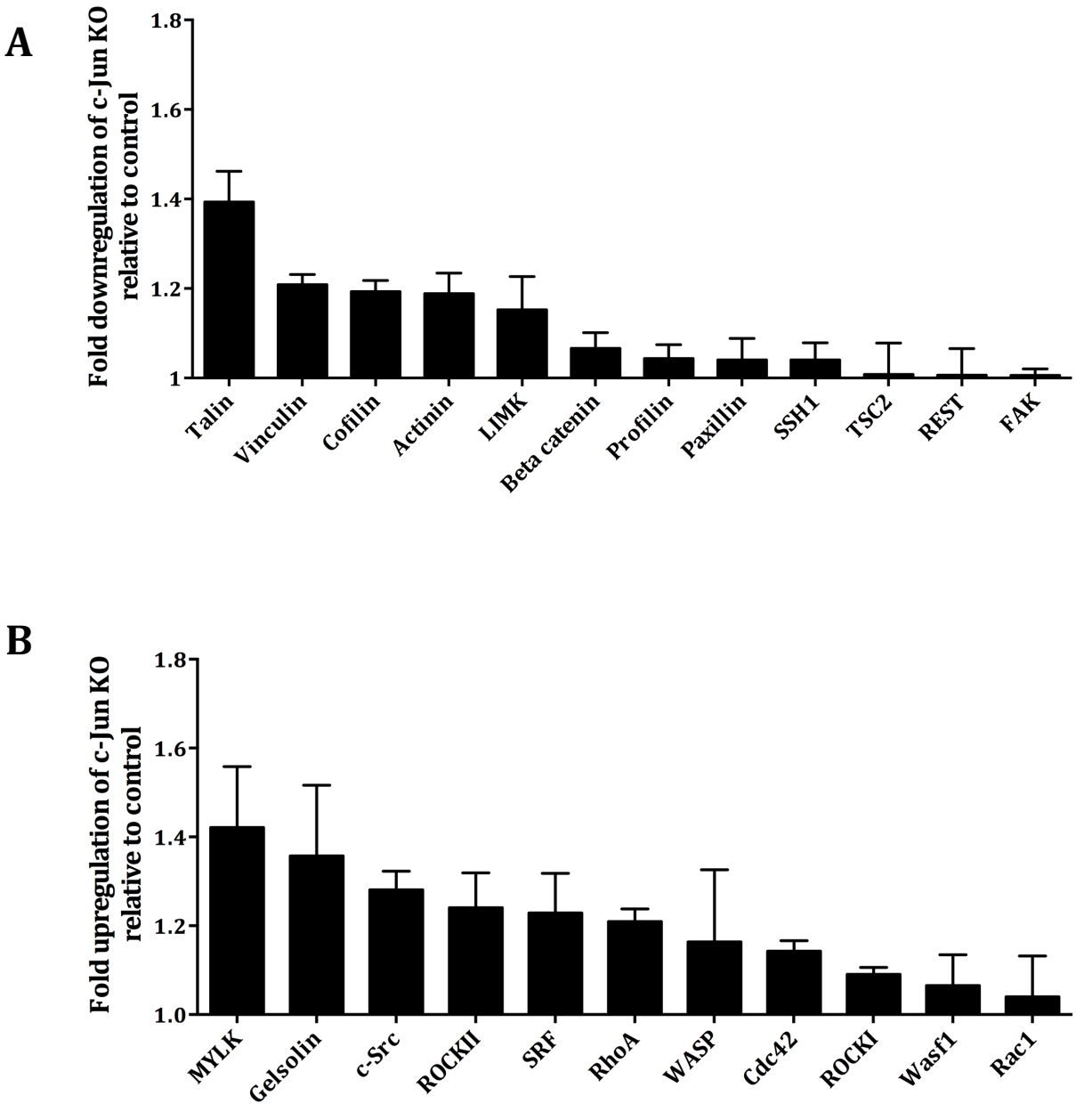

Figure 4.6 c-Jun deletion in Schwann cells does not alter the mRNA levels of genes that are known to regulate Schwann cell migration and cytoskeleton dynamics.

RT-qPCR was used to evaluate the relative mRNA expression of a number of cytoskeleton regulators. (A) Fold downregulation of c-Jun knockout compared to wildtype control. (B) Fold upregulation of c-Jun knockout compared to control. All data show no significant difference in fold change between knockout and wildtype. All data are normalised to the reference genes GAPDH and YWHAZ. Reverse Transcriptase minus (RT-) and No Template Controls (NTCs) negative controls were used and showed that RNA was adequately treated with DNase and that no PCR products were formed from the primers in the absence of cDNA. Data are means ±SD from three independent experiments.

4.2.7 Deletion of Schwann cell c-Jun regulates the expression of c-Jun, olig1, MBP and GDNF

Following a similar experimental approach as in Figure 4.6, I tested the expression of genes known to be regulated by c-Jun in the injured nerve. The results of the RT-qPCR analysis show that c-Jun is significantly downregulated (as expected), when the c-Jun floxed gene is excised from the cell by adeno-Cre (Fig. 4.7A). In this experiment, Olig1, the most regulated gene found in the microarray data (Arthur-Farraj et al. 2012) is also significantly downregulated in c-Jun knockout cells. GDNF is also downregulated, approximately 4-fold in the c-Jun knockout cells. Conversely, the myelin protein MBP and Adam23 are significantly upregulated in these cells, thus, confirming that the mRNA isolated from c-Jun knockout cells produces similar gene expression results to those of the microarray.

Figure 4.7

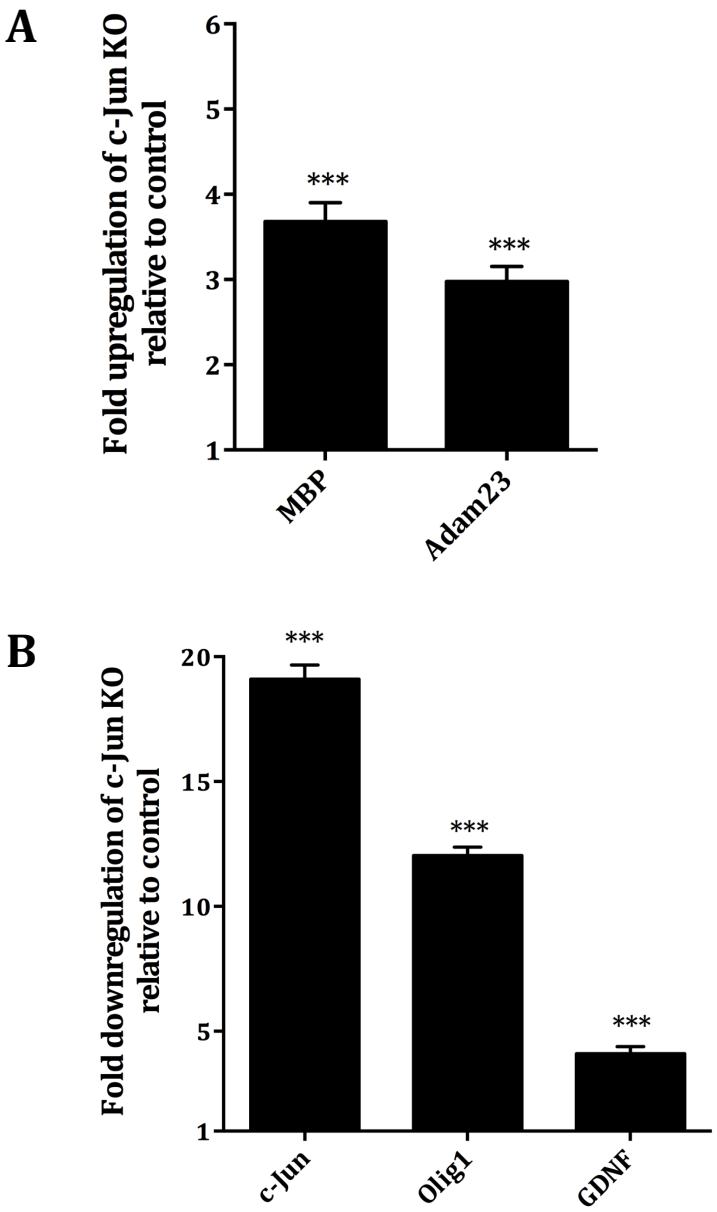

Figure 4.7 c-Jun deletion in Schwann cells does alter the mRNA levels of genes that are previously known to be regulated by c-Jun

RT-qPCR was used to evaluate the relative mRNA expression of genes known previously to be regulated by c-Jun. (A) Fold downregulation of c-Jun knockout compared to wildtype control. (B) Fold upregulation of c-Jun knockout compared to control. All data show a significant difference in fold change between knockout and wildtype. All data are normalised to the reference genes GAPDH and YWHAZ. Reverse Transcriptase minus (RT-) and No Template Controls (NTCs) negative controls were used and showed that RNA was adequately treated with DNase and that no PCR products were formed from the primers in the absence of cDNA. Data are means ±SD from three independent experiments. $^{***}P<0.01$.

4.3 Discussion

As a first step to uncovering the molecular mechanisms by which c-Jun regulates Schwann cell migration and morphology, I initially considered whether the gene expression of NRG1 signaling components was affected when c-Jun is deleted from Schwann cells. NRG1 is known to have a significant affect on Schwann cell migration, rearrangement of the cytoskeleton and the induction of focal adhesions, in addition to its crucial roles in myelination during PNS development and regeneration and remyelination following nerve injury (Stassart et al. 2013; Fricker et al. 2011; Jessen & Mirsky 2005). The results of gene expression analysis made by RT-qPCR reveal there to be no significant differences in the expression of NRG1 isoforms and their receptors between the c-Jun knockout Schwann cells and control cells (Fig. 4.1) This finding supports the idea that the reduced cell migration observed between c-Jun knockout cells and controls in response to NRG1 in both wound and transwell migration assays (Fig. 3.2 B and C) was not due to a lack of expression of these components of NRG1 signaling in the mutant cells. In addition, the RT-qPCR data shown here agrees with gene expression analysis of the distal stump of the injured Sciatic nerve, where microarray analysis revealed no significant change in expression of these genes between c-Jun conditional knockout mice and controls at 7 days following nerve transection (Arthur-Farraj et al. 2012). The actin-severing protein cofilin-1 has recently been identified to act downstream of NRG1 to affect many of these cellular changes. In the present study, I observed a similar flattened morphology and induction of actin stress fibers when c-Jun is deleted in mouse Schwann cells (Fig. 3.1A) as compared to the cofilin-1-deficient rat Schwann cells generated using short hairpin RNA interference (shRNAi) (Sparrow et al. 2012). Whilst these data suggest that c-Jun expression does not regulate the upstream components of the NRG1 pathway to

control Schwann cell morphology and migration, it is possible that proteins known to be regulated by NRG1 signaling and expressed by Schwann cells, such as cofilin-1 may also be regulated by c-Jun, and for this reason I performed further gene expression analysis in the later part of this Chapter.

I proceeded to investigate potential molecular pathways that might be regulated by c-Jun in Schwann cells. A previous study has shown that in mouse embryonic fibroblasts, c-Jun deletion reduces the expression of c-Src (see above), which allows for the hyperactivation of Rho kinase II (ROCKII), immunocytochemistry of c-Src (Fig. 4.2A) shows that expression of the protein is abundant in both c-Jun knockout and control Schwann cells. I attempted to examine c-Src expression levels in the cultured mouse Schwann cells using western blotting, however this experiment was unsuccessful due to the large numbers of primary cells required to give a signal for this protein. I was unable to resolve this in this time constraints of the study. I was, however, able to perform western blotting to examine levels of c-Src in the 7 day-old distal stump of transected sciatic nerves of the c-Jun conditional knockout mouse and its control. The results of this assay showed no demonstrable effect of deleting c-Jun on c-Src levels between the control and c-Jun conditional knockout nerves (Fig. 4.2 B). There was, however, a significant induction in c-Src expression following injury, and this agrees with observations by Zhao *et al*. (2003), who identified a three-fold increase in c-Src expression following both nerve crush and transection injuries to the rat sciatic nerve. Expression of c-Src mRNA was measured using RT-qPCR for c-Jun knockout and control Schwann cells and again, there was no significant difference between the two samples (Fig. 4.6A). While the data in the present study does not suggest a role for c-Jun in regulating the expression of c-Src protein or mRNA, the possibility exists that c-Jun might control c-Src activity through an

intermediate that can activate/deactivate c-Src through phosphorylation or protein-protein interactions, rather than by the direct transcriptional upregulation as demonstrated by Jiao *et al*. (2008) It would therefore be informative to conduct a c-Src kinase activity assay and ROCKII activity assay in the future to see if c-Jun does in fact modulate the c-Src-ROCKII signaling axis in Schwann cells.

To further probe a possible involvement of c-Src and ROCKII in c-Jun-dependent Schwann cell migration, I first conducted a transwell assay with wildtype primary mouse Schwann cells to see if inhibiting their activity would have an affect on cell migration. The results of this experiment showed that inhibition of c-Src leads to a significant reduction in Schwann cell migration compared to the vehicle control. Conversely, inhibiting ROCKII caused an increase in cell migration when compared to Schwann cells treated with vehicle alone (Fig 4.3). These results must be treated with caution, since within the timeframe of this study I was not able to measure the effects of the inhibitors on c-Src and ROCKII with an activity assay. The inhibitors for c-Src (SU6656) and ROCKII (Y27632) were used at concentrations (2 μM and 10 μM respectively) reported in the literature (Jiao et al. 2008) to inhibit the activity of these proteins, and I observed no effect on the cell viability in this experiment (data not shown). However, it seems reasonable to conclude from these results that c-Src activity promotes and ROCKII activity inhibits primary mouse Schwann cell migration. The ROCKII finding is supported by data from rat Schwann cell transwell migration assays, where Y27632 increases cell migration by ~20% (Yamauchi et al. 2004).

In light of the findings that c-Src and ROCKII activity can change wildtype Schwann cell migratory behavior, I conducted additional migration assays (Figs. 4.4 and 4.5) to address whether the activity of these proteins can alter the cell migration of the c-Jun knockout Schwann cells. Application of ROCKII inhibitor to

the c-Jun knockout cells in the wound assay led to a significant increase in closure of the wound (Fig. 4.4), and significantly, at 24 hours, the diameter of the wound for c-Jun knockout Schwann cells at 24 h (Fig. 4.4) was comparable to that of control Schwann cells at the same time point (Fig. 5.5). This finding implies that inhibition of ROCKII in c-Jun knockout Schwann cells is sufficient to rescue the rate of migration to that of c-Jun-expressing Schwann cells. There are two possible explanations for this; firstly the activity of ROCKII is abnormally high in these cells, and reducing this with an inhibitor can restore normal rates of migration, or secondly that c-Jun deletion affects Schwann cell migration by a ROCKII-independent pathway, but inhibiting ROCKII activity can compensate for this alternative brake on Schwann cell migration and return it to normal. This present study does not resolve this, but determining the activity of ROCKII in c-Jun knockout Schwann cells would shed some light onto this in the future. It has been shown previously that negative regulation of Rho/ROCK signaling in Schwann cells can promote the extension of radial lamellipodia via the activation of Profilin1. Cultured primary mouse Schwann cells were treated with shRNA directed at Profilin1, and switched to a bi-polar morphology from the original ROCK-induced flattened morphology (Montani et al. 2014). It would be informative to treat the c-Jun knockout Schwann cells with shRNA against Profilin1 in future experiments to determine whether its activity has an affect on the morphological phenotype of these cells.

Further to these results, I also conducted a wound assay in which control Schwann cells were incubated with the c-Src inhibitor. These results show that c-Src inhibition mimics the loss of c-Jun, as the SU6656-treated cells have a similar rate of wound-closure to the c-Jun knockout Schwann cells (Fig. 4.5). Again, determining the phosphorylation state of c-Src and its kinase activity of the two

cell populations, and transfecting c-Jun knockout cells with recombinant c-Src as a rescue experiment would help to resolve whether a c-Jun-c-Src-ROCKII axis exists in Schwann cells to control cell morphology and migration.

Finally, I conducted a gene expression screen using RT-qPCR on selected candidate genes to identify proteins associated with the cytoskeleton and/or cell migration that might in turn be regulated by c-Jun (Fig 4.6). This analysis was conducted in three independent experiments and failed to identify any significant differences in gene expression of the candidates. Differences in the expression of proteins already known to be mis-expressed (c-Jun, olig1, GDNF and MBP) in Schwann cell-specific c-Jun knockout distal nerve stumps were identified and these agreed with the microarray data of Arthur-Farraj *et al*.(2012). Since these certain genes, that are known to be upregulated or downregulated in the microarray are also regulated in the same manner in my RT-qPCR analysis, this gives confidence that none of these candidate genes are significantly regulated at a transcriptional level when c-Jun in removed from mouse primary Schwann cells.

While the strategy (see Table 4.1) in the present study was to carefully select candidate genes that have a basis in the literature for being transcriptionally regulated by c-Jun to control cell migration, or regulate cytoskeleton dynamics, and/or are known to regulate Schwann cell migration, this approach was ultimately unsuccessful in finding a target of c-Jun. Future studies might identify proteins downstream of c-Jun by using microarray analysis of the c-Jun knockout Schwann cells. A more informative method might be to conduct proteomic analysis of the cytoskeletome to study post-translational modifications such as phosphorylation, since many of proteins involved in cytoskeletal rearrangement can have their activity modified by the addition of phosphates or the exchange of nucleotides such as GTP/GDP. Attempts were made to quantify the activities of

Rac1 and Cdc42 in this study. I isolated cellular protein from primary mouse Schwann cells for use in an immunoprecipitation assay, but this failed due to sensitivity of the assay and the lack of protein available from the primary cell cultures, despite the use of pooled samples. Furthermore, attempts were made to use rat Schwann cell primary cultures transfected with siRNA targeted at c-Jun for the Rac1 and Cdc42 pull down assays, since these primary cells can be expanded more easily than mouse Schwann cells, however due to time constraints I could not optimise these assays to generate data for use in this report.

In conclusion, it seems unlikely that NRG1 signaling is regulated by c-Jun and therefore the response of c-Jun knockout Schwann cells to NRG1 is most likely not due to the lack of expression or recognition of NRG1-ErbB1/2 in these cells. Additionally, the downstream target of NRG1 signaling, Cofilin-1, that modulates the Schwann cell cytoskeleton is not seen here to be transcriptionally regulated by c-Jun, but could be aberrant from control Schwann cell cofilin-1 in terms of protein expression, phosphorylation or additional post-translational modifications. The expression of c-Src mRNA and protein does not appear altered, but this may also have a different phosphorylation status in the c-Jun knockout Schwann cells. While modulating the activity of c-Src and ROCKII has affects on cell migration consistent with the presence of a c-Jun-c-Src-ROCKII signaling axis, further experiments are required to confirm this. Gene expression analysis using RT-qPCR was unable to detect regulation by c-Jun, and so additional experiments are required to find a target of c-Jun, should the c-Jun-c-Src-ROCKII pathway prove not to be active in controlling Schwann cell morphology and migration.

Table 4.1 Candidate genes for RT-qPCR screen

Involved in cell migration and known to be regulated by c-Jun in other cells.	Involved in Schwann cell migration, but not known to be regulated by c-Jun	Known to be regulated by c-Jun in Schwann cells
c-Src, ROCKII, Vinculin, Paxillin, TSC2, REST	MYLK, Gelsolin, SRF, RhoA, WASP, Cdc42, ROCKI, Wasf1, Rac1, Talin, Cofilin, LIMK, Beta catenin, Profilin, SSH1, FAK, NRG1 isoforms, ErbB1/2, Shp2	c-Jun, Olig1, GDNF, MBP, Adam23

Chapter 5: A novel assay for measuring axonal and Schwann cell outgrowth in a nerve transection injury

5.1 Introduction

Nerve injury is a common problem encountered by physicians, with many of these involving the complete transection of a peripheral nerve. A robust and repeatable model of these injuries is needed in order to understand the precise events of nerve injury and regeneration and also to develop therapies that enhance the normal regeneration programme in place in the peripheral nerve. To date, the most commonly used assay for quantifying axonal regrowth following peripheral nerve transection involves complete transection of the sciatic nerve at the level of the sciatic notch. This assay requires improvement in several ways. Firstly, it effectively involves severing the tibial, common peroneal and sural branches of the sciatic nerve and therefore results in significant morbidity to the animal. For experiments that do not require results of sensory or motor function from all three branches, this procedure could be refined to cause less harm to the animals in line with Home Office guidelines. In order to study axonal regrowth from the proximal nerve stump into the distal stump, it is in principle sufficient to transect a single branch of the sciatic nerve, and doing so would reduce pain and mobility problems for the animal.

Secondly, complete sciatic nerve transection results in gaps between the proximal and distal nerve stumps that differ significantly in length from animal to animal, and generates variable alignment between the two stumps, therefore the complete transection model requires improvement to generate more accurate and reliable results. This improvement would have the added benefit of requiring fewer animals to produce statistically significant results, and therefore satisfying the ‘reduce’ criteria of the guiding principles of animal research in the UK. In this

chapter I will show the lack of reducibility in the current model of nerve transection injury in the mouse and provide evidence for a more reliable method that I have devised, involving the transection of only the peroneal branch of the sciatic nerve.

5.2 Results

5.2.1 Transection of the sciatic nerve does not produce a consistent nerve bridge

During my initial experiments in studying the role that Schwann cell c-Jun plays in nerve regeneration, I quickly realised the standard protocol that had been established in the laboratory for studying the effects of transection on the distal nerve stump would not yield consistent results when looking at growth of axons and Schwann cells across the nerve bridge. Experiments by others in the laboratory had looked at the events following nerve transection in the distal stump in isolation, such as demyelination and changes in protein expression and mRNA expression. This was possible by ensuring the proximal stump was sutured to muscle far away from the distal stump, so that reconnection was not possible. For my studies, I required an assay that would provide a consistent gap between the proximal and distal stumps from which the axons and Schwann cells could outgrow. Figure 5.1 shows the average gap between proximal and distal nerve stumps measured at 5 days following transection. At this time the nerve bridge is still translucent and is easy to measure by light microscopy. The measurement showed that the gap between the nerve stumps varied from 1 to 6 mm in the case of control mice and 2 to 6 mm in the case of c-Jun cKO mice. The substantial variation in bridge length resulted in large error bars for the averages in both genotypes (SEM = 0.87 mm and 0.78 mm for control and c-Jun cKO samples respectively).

Figure 5.1

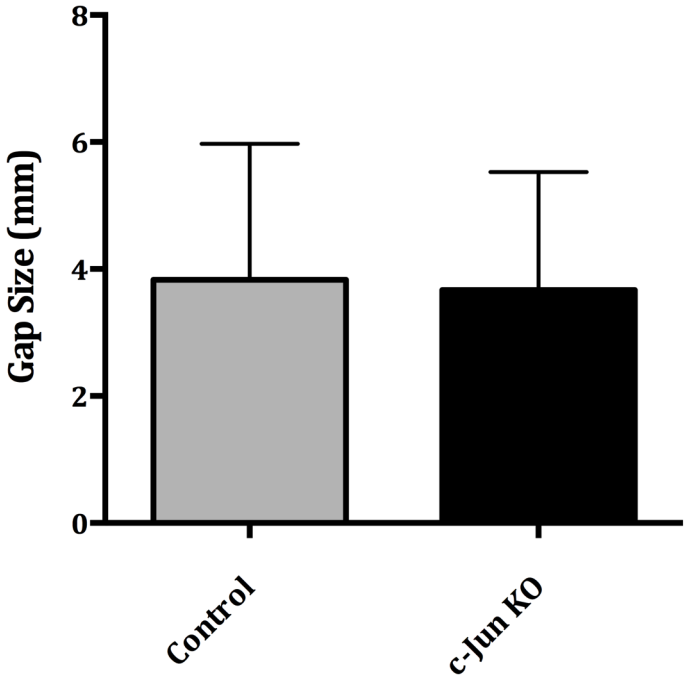

Figure 5.1 Complete Sciatic nerve transection produces a variable nerve bridge size.
Quantification of nerve bridge distance at 5 days post transection. There was no significant difference between the two mouse genotypes. Significantly there is the large variation in bridge size for the given number of mice, as shown by the large error bars. Results shows are the mean ± SEM of three independent experiments performed in triplicate. A total of 9 mice were used for each of the control and c-Jun KO samples.

5.2.2 Transection of solely the peroneal branch, leaving the tibial branch intact produces a consistent nerve bridge size

Due to the lack of repeatability from the complete sciatic nerve transection, I needed to develop an assay that would generate more consistent results and allow me to test whether Schwann cell c-Jun deletion has an effect on axon and Schwann cell outgrowth and the formation of the nerve bridge. To achieve this, I decided to transect only the common peroneal branch of the sciatic nerve, as this would leave the larger tibial branch intact and in position to provide support for the proximal and distal nerve stumps with the aim of creating a more consistent gap between them. The sural branch was not suitable for this due to its smaller size making it harder to visualize during surgery. Figure 5.2 is an illustration of the 'partial transection' model of sciatic nerve injury. A full explanation of the method for this assay is described in Chapter 2.

As shown in Figure 5.3 there was a much more consistent size of bridge between the nerve stumps for both control and c-Jun cKO mice. The gap between the proximal and distal common peroneal nerve stumps ranged between 1 and 1.5 mm for both the control and c-Jun cKO mice. The standard error of the mean for these samples was 0.087 mm and 0.083 mm for control and cKO mice respectively. This compares to 0.87 mm and 0.78 mm for the complete sciatic nerve transection results shown in Figure 5.1. This shows clearly that using the partial transection model generates much more consistent replicates than the complete sciatic nerve transection model, and therefore requires fewer animals in each experiment. In line with the results shown from Figure 5.1, there was no significant difference in bridge length between the two genotypes.

Figure 5.2

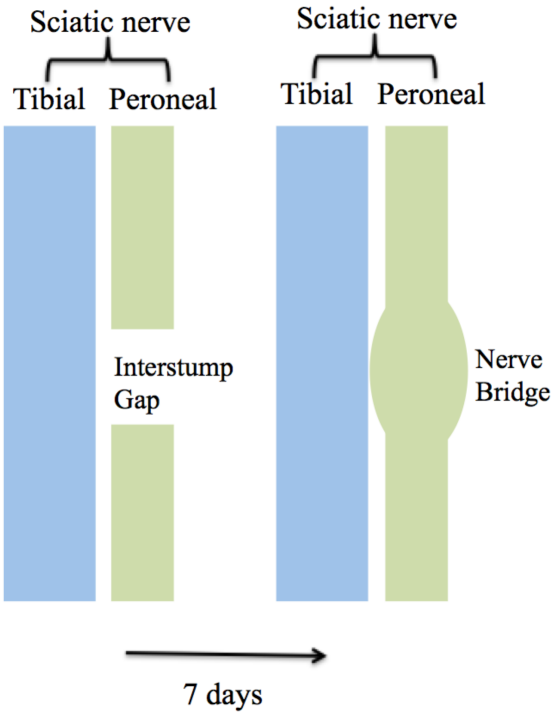

Figure 5.2 An illustration of the Sciatic nerve partial transection model
The peroneal branch of the Sciatic nerve is transected using surgical scissors to create a clean cut of the tissue. Minimal disturbance of the nerve is required in order for the nerve stumps to remain in place and supported by the tibial branch. After 7 days, outgrowth of tissue from the two stumps has formed a stable nerve bridge that is suitable for wholemount immunostaining.

Figure 5.3

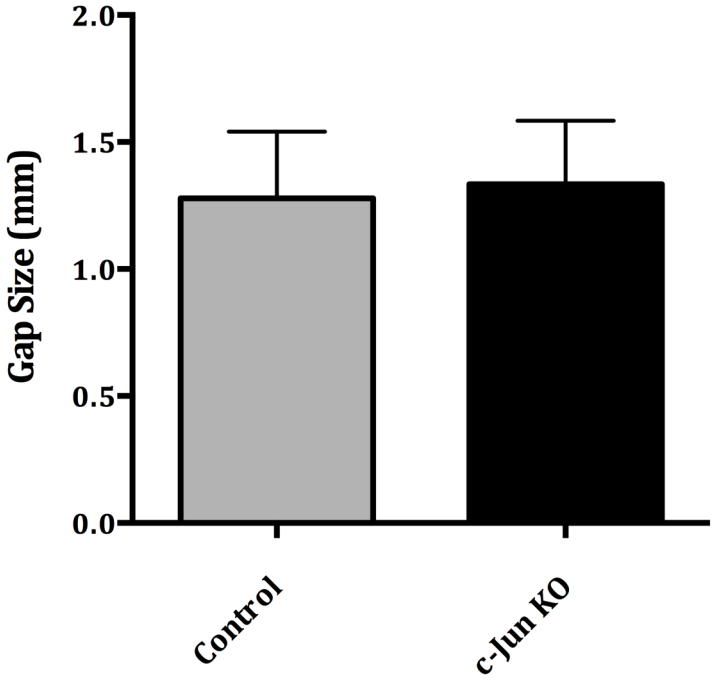

Figure 5.3 Partial transection of the Sciatic nerve produces a more consistent nerve bridge

Quantification of nerve bridge size at 5 days post transection. Results shows are the mean ±SEM of three independent experiments performed in triplicate. A total of 9 mice were used for each of the control and c-Jun KO samples. There is no significant difference between the two mouse genotypes.

5.2.3 c-Jun null Schwann cells are able to cross the nerve bridge by 7 days

I used the partial transection model to compare control and c-Jun cKO Schwann cells in the nerve bridge. This was done by carrying out wholemount immunostaining of the samples to show localization of the Schwann cell marker S100 at 7 days post transection. The images in Figure 5.4 show that S100 positive cells were distributed along the entire length of the nerve bridge. This experiment was repeated in 3 animals per genotype and the images in Figure 5.4 are representative of these. Surprisingly, in view of the difference in morphology between control and c-Jun KO Schwann cells *in vitro* (Chapter 3) the morphology of individual cells in the c-Jun cKO appeared to be similar to the control, showing a long slender profile with similar sized nuclei (see inset of Figure 5.4).

Figure 5.4

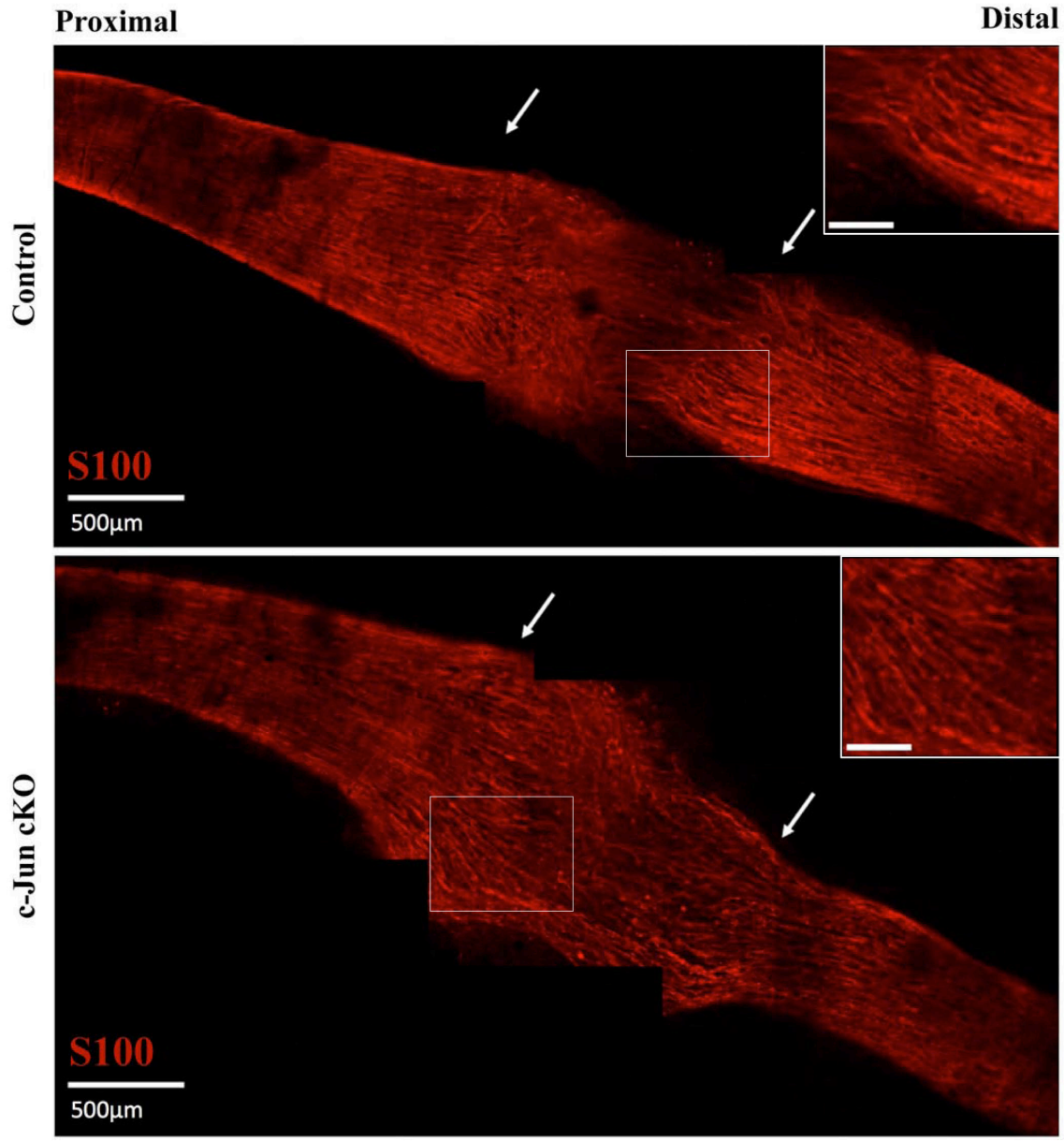

Figure 5.4 Immunohistochemistry shows Schwann calls in control and c-Jun cKO mice can traverse the nerve bridge by 7 days
Immunohistochemical labeling of sciatic nerve wholemounts using anti-S100 antibody to visualise Schwann cells at 7 days following transection. Images were taken by a Leica confocal as described in Chapter 2 at x20 magnification. Arrows indicate the approximate ends of the proximal and distal nerve stumps. This figure is a composite of 8 separate confocal images (per sample) stitched together to reveal the whole nerve sample. Z-stacks were taken at an interval of 1 µm, with a total of 40 slices to a depth of 40 µm.

5.2.4 Both control and c-Jun cKO nerves show regrowth of axons across the bridge at seven days after injury, but control axons penetrate much farther into the distal stump than axons from c-Jun cKO nerves.

I compared axon outgrowth from control and c-Jun cKO mice using a similar experimental approach. In this case, the same wholemount samples shown in Figure 5.4 were double labeled with anti-neurofilament antibody to visualise axons. Similar results were obtained in three separate experiments. The double labeling protocol is described in Chapter 2 and was optimised for this experiment by performing a no first layer control to check for non-specific staining. I also carried out the necessary second-layer controls to check for cross-reactivity between the chick anti-neurofilament antibody and anti-rabbit-Cy3 antibodies and the rabbit anti-S100 and anti-Chick-488 antibodies. Several antibodies for axonal markers were tested, including mouse anti-neurofilament, rabbit anti-neurofilament, anti-galanin and anti-CGRP antibodies, but the anti-chick neurofilament yielded the best staining for both wholemount and cryosection sample preparations.

Figure 5.5 shows that at 7 days post injury, axons in the control nerve had grown through the nerve bridge and into the distal stump. In the c-Jun cKO nerve, on the other hand axons had barely penetrated the distal stump. This effect was quantified by measuring the length of the longest axon in the distal stump in the two mouse genotypes using additional 7 day partial transection samples. Injured nerves from three separate pairs of mice were embedded in OCT and serial sections were made at fixed 100 μm intervals up to the sample length of 5 mm (Figure 5.6). This showed that axons reached a maximum distance of 0.8 mm after 7 days in the c-Jun cKO mice, compared to at least 5 mm in the control mice.

Figure 5.5

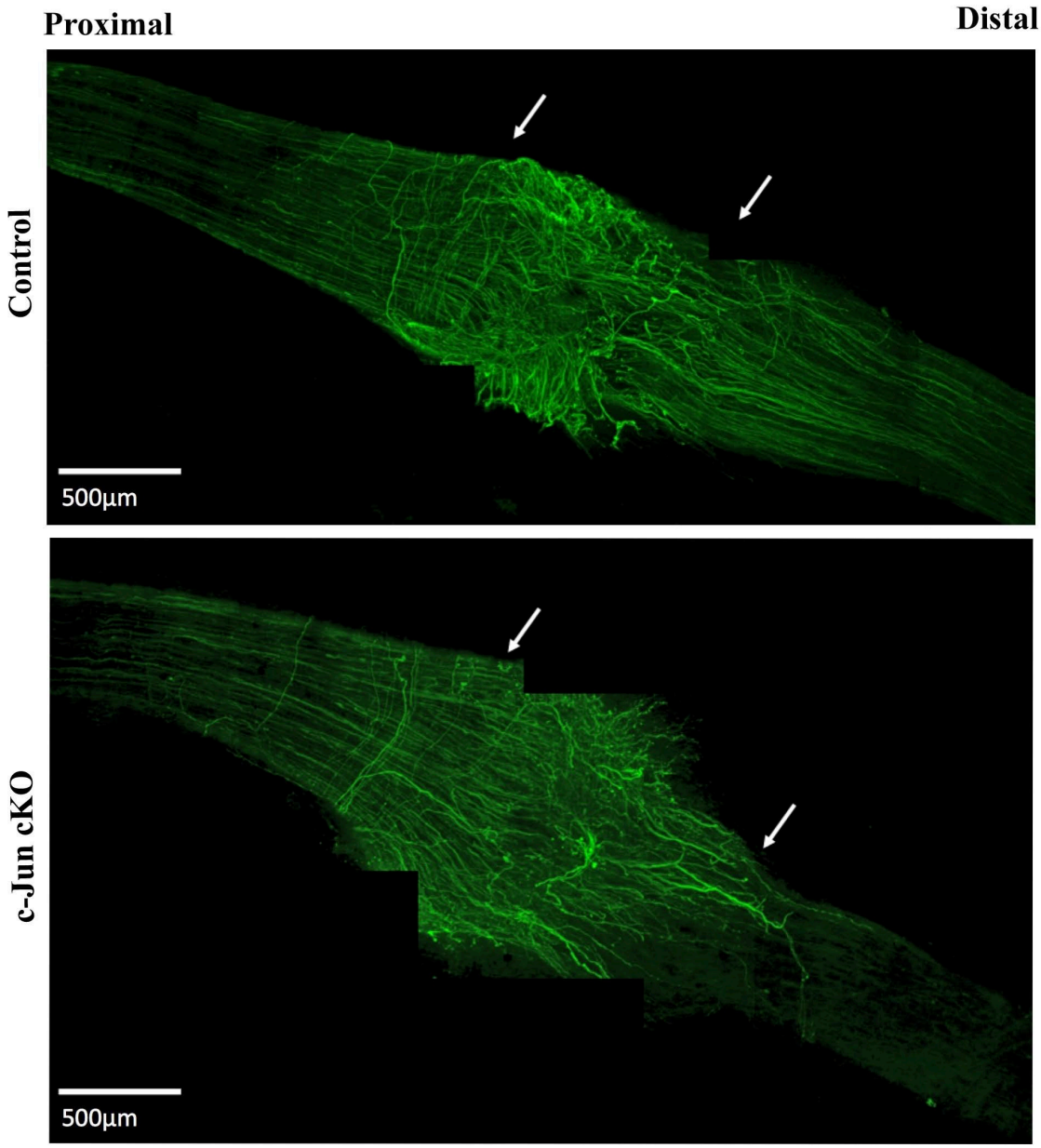

Figure 5.5 Axonal regrowth into the distal stump is deficient in the c-Jun KO mouse at 7 days.
Immunohistochemical labeling of nerve wholemounts using anti-neurofilament antibody to visualise axons at 7 days following transection. Images were taken by Leica confocal microscope as described in Chapter 2, at x20 magnification. Arrows indicate the approximate ends of the proximal and distal nerve stumps. This figure is a composite of 8 separate confocal images (per sample) stitched together to reveal the whole nerve sample. Z-stacks were taken at an interval of 1 µm, with a total of 40 slices to a depth of 40 µm.

5.3 Discussion

My results show that it is possible to form a consistent size of nerve bridge by using the partial transection injury model that I have developed. This proves to be more useful than a complete transection due to the increased repeatability of the results and reduced morbidity for the animals. This method could also be adopted for similar experiments in rats. Whilst there is a higher degree of skill necessary to perform this surgery over the complete transection model, this is fairly easily overcome with appropriate surgical scissors, a higher magnification when using the dissecting microscope and practicing the technique on cadavers. It is important to note that the partial transection of the sciatic nerve was performed far away from the sacral plexus, at mid-thigh level. In this region, the peroneal and tibial nerves are held together by loose tissue from their respective outermost layers (epineurium) and with a precise transection of the peroneal nerve, it is unlikely that significant damage would be inflicted upon the tibial nerve fibers, however to confirm this, immunohistochemistry could be done in the future to ensure the tibial nerve fibers remain intact and there is no interaction of Schwann cells and axons from the tibial nerve into the newly formed peroneal nerve bridge.

Although I found no difference between c-Jun and control mice in the length of the bridge between the proximal and distal stumps using the conventional transection assay, it might be possible to find a statistically significant difference if enough animals were used. However this would be both impractical and expensive. But for both mouse lines, the sciatic nerve complete transection model is problematic for the purpose of assaying outgrowth of Schwann cells and axons from the nerve stumps due to the high variability of the nerve bridge that is formed. There are a number of reasons that may contribute to the lack of consistency in the complete transection method. The behavior of the mice may

contribute to gap size as neither the proximal or distal stumps are anchored inside the thigh cavity and are free to move. Stretching of the hind limb could move the stumps apart and impede the formation of the nerve bridge or create a larger gap for the bridge to cross. While the mice used in this experiment were matched for age and sex, some physiological differences between the mice exist, and these might further contribute to the gap size. The amount of stress applied to the intact nerve in normal conditions is unlikely to be precisely the same between different mice. Therefore, when the nerve is severed, the force that pulls the nerves apart would also not be identical and would result in varying distances between the nerve stumps.

In contrast, a comparison of my results using the improved method of creating the bridge (Figure 5.2) with those achieved using the conventional method (Figure 5.1) shows that the assay I devised can produce highly repeatable results for the nerve bridge size, giving confidence to the results shown in Figure 5.3, indicating that there is no difference in nerve bridge size between the control and c-Jun knockout nerves. *In vitro*, c-Jun knockout Schwann cells show a much reduced rate of migration in the wound and transwell migration assays (Chapter 3) and this might affect formation of the nerve bridge, but for now I can conclude that c-Jun null Schwann cells do not affect the formation of the bridge, in terms of the amount of tissue between the nerve stumps. This is somewhat expected since the initial formation of the bridge is carried out mostly by perineurial fibroblasts and see discussion below. The outgrowing fibroblasts possess the same type of collagen fibrils as perineurial and endoneurial fibroblasts, distinct from those fibroblasts of the epineurium (Thomas 1966).

To see whether the Schwann cell emigration from the proximal and distal stumps that normally occurs after injury is affected by the loss of c-Jun, I next

performed immunohistochemistry on peroneal nerve wholemount preparations using antibodies to S100, a Schwann cell marker, to visualise the Schwann cells (Figure 5.4). These experiments showed that at 7 days after injury in both control and Schwann cell c-Jun KO nerves, Schwann cells have migrated to fill the gap between the proximal and distal stumps. Interestingly, as shown in the higher power insert to Figure 5, the elongated bipolar shape of the Schwann cells in the bridge appears similar in both control and c-Jun KO nerves. As mentioned above this is surprising, given the reduced rate of Schwann cell migration in culture assays and the marked difference in cell shape between freshly isolated Schwann cells from c-Jun and control mice (Chapter 3). Possible reasons for the c-Jun KO Schwann cells in the nerve bridge exhibiting a normal shape and migration at 7 days after injury include the very different environment of the bridge which consists of a gel-like extracellular matrix, fibroblasts, macrophages, newly formed blood vessels and other immune system cells (Parrinello 2012, Chen et al. 2007) compared with the more defined conditions used in the culture assays. In addition, there are interactions between the regenerating axons and the c-Jun KO Schwann cells that are not present in the Schwann cell cultures. It would be informative to carry out future experiments in neuron-Schwann cell co-cultures to see if axons can rescue the aberrant c-Jun KO cell morphology *in vitro*. To establish definitively whether the migration rate into the bridge is affected, experiments at shorter time points after nerve transection would need to be carried out. Several attempts were made to do this, but technical problems involving the fragility of the bridge tissue at three and five days after transection when performing immunohistochemistry would need to be solved in the future before a definitive answer could be obtained.

Seven days after transection my experiments show that axonal growth into the distal stump is severely retarded, although axons in both control and Schwann

cell c-Jun KO nerves have crossed the bridge from the proximal to the distal stump. It is therefore possible that removing c-Jun from Schwann cells provides an unfavourable environment for axons to grow through the distal stump that is different from the environment present in the bridge. Before coming to this conclusion however it would be important to establish whether the rate of initial outgrowth of axons from the proximal stump into the bridge and the rate of growth across the bridge once the axons start to grow is identical in the wild type and Schwann cell c-Jun KO nerve, since a slower outgrowth of axons from the proximal stump in the knockout will also contribute to the lower overall growth of axons at 7 days shown in Figures 5.5 and 5.6. As mentioned above it would be necessary to repeat the axonal experiments at shorter time points when technical problems have been solved. This would enable me to determine firstly whether the initial outgrowth of axons from the proximal stump is delayed in the c-Jun cKO, and secondly whether the rate of elongation across the bridge is slower once axonal growth is initiated compared with control nerves. It would also allow me to determine whether the rate of growth after entry into the distal stump is the same as the rate of growth across the bridge both in c-Jun cKO and control nerve transected nerves. Preliminary results in the laboratory have shown that some regeneration associated genes (RAGs) in sensory neurons are activated more slowly when c-Jun is removed from Schwann cells (Shaline Fazal, unpublished data) suggesting that c-Jun controls signals from Schwann cells that contribute to the activation of axonal growth after injury.

Nevertheless it is also possible that the Schwann cells in the distal stump also provide an unfavourable environment for axonal growth that is not present in the different environment of the bridge. The fact that the axons in the Schwann cell c-Jun KO nerves are still able to cross the nerve bridge could be related to the

different molecular and cellular composition of the two tissues. The nerve bridge architecture is less developed than that of the distal stump and lacks the basal lamina endoneurial tubes of the distal stump. The nerve bridge also contains an abundance of fibroblasts, inflammatory cells and growing blood vessels at this early stage of regeneration. Nerve bridge formation and axonal regrowth occur concurrently, and it is possible that events that take place in the nascent nerve bridge but not in the distal stump, such as fibroblast-Schwann cell sorting and guiding of axonal growth cones by Schwann cell processes are sufficient to aid axon regrowth across the bridge, but that this regeneration stalls in the very different environment of the distal stump (Zochodne 2010; Parrinello et al. 2010).

Previous experiments in the laboratory using Schwann cell c-Jun KO mice have shown that Schwann cells in the distal stumps of these mice fail to make trophic factors for axons such as GDNF, BDNF and artemin at 7 days after transection, that axonal regeneration after crush injury is slower and that expression of cell surface molecules such as N-Cadherin, p75NTR and L1 is down-regulated. The rate of myelin breakdown is also slower in the c-Jun cKO nerve (Parkinson et al. 2008; Arthur-Farraj et al. 2012). A myelin-rich environment is generally considered inhibitory to axonal regrowth, and this may be a further factor in the slow regrowth of the axons into the c-Jun cKO distal nerve stump (Vargas & Barres 2007).

It is also known that the bands of Bungner in the c-Jun cKO nerves have an abnormal morphology at 4 weeks after nerve transection injury (Arthur-Farraj et al., 2012) with flatter Bungner cells and fewer cellular profiles. As I have already shown in Chapter 2, Schwann cells freshly isolated from P9 c-Jun cKO nerves already display a similar phenotype to the Bungner cells. This morphological phenotype may stop axons from growing normally into the endoneurial tubes of

the distal stump and help to account for the retarded axonal regrowth, although this seems unlikely since there is no sign of axon build up at the junction between the bridge and the distal stump in the c-Jun cKO nerve samples similar to that seen when regenerating axons become trapped by the over-expression of neurotrophic factors such as GDNF in nerve grafts, the so-called “candy store effect” (Blits et al. 2004) (Fig 5.5). The morphological abnormalities may, however, have a significant effect on axonal growth once the axons have to grow through the environment of the distal stump.

In summary, in the future it will be important in conduct further experiments to distinguish between the contributions of each of the possibilities mentioned above. A future experimental approach to confirm this includes the grafting of a wildtype distal stump to wildtype and c-Jun cKO proximal stumps to assay for the regrowth of axons from neurons that have not been affected by Schwann cell c-Jun via the possible induction of RAGs.

Chapter 6: General Discussion

The earliest studies carried out on peripheral nerves were quick to identify Schwann cells as being highly motile cells, both during development and in the degenerating nerve. This migratory behavior has been studied since, however, mostly in the context of uncovering the mechanisms of Schwann cell precursor migration using cultured, neonatal Schwann cells. These cells were referred to in the past as dedifferentiated Schwann cells, however, work from our lab indicates that a more appropriate term would be 'transdifferentiated', since the Schwann cell formed following nerve injury functions as a specialized repair cell, and does not resemble the immature Schwann cell progenitor, aside from the lack of myelin and the expression of some cell markers. Cells undergoing an epithelial-to-mesenchymal transition lose their polarity and contacts with neighbouring cells and adopt a migratory behavior. This is comparable to the behavior of Schwann cells following nerve injury, where they lose contact with axons and where possible, can migrate from nerve stumps.

The aim of this thesis was to investigate whether the transcription factor c-Jun, a key player in the generation of transdifferentiated (Bungner) Schwann cells, also played a role in their adoption of a migratory phenotype. The results of this study clearly show that c-Jun does regulate Schwann cell motility and morphology in vitro. Initial results in this thesis, using an in vivo model of nerve transection injury suggest that c-Jun is not required for Schwann cells to cross the bridge between the proximal and distal stumps. This is surprising, given the significant migratory deficit of c-Jun knockout cells in two migration assays, however the fact that Schwann cells of the proximal stump are in contact with regrowing axons may point to an explanation for this difference. It is possible that axonal contact

activates signalling pathways inside the proximal stump Schwann cells that allow them to overcome a brake on migration caused by the absence of c-Jun. Performing migration assays from DRG explants to observe the affect of growing axons on c-Jun knockout Schwann cell migration might resolve this question. It would also be informative to perform the nerve bridge assay from Chapter 5 at earlier time points to reveal whether the Schwann cells that are able to traverse the nerve bridge are predominantly from the proximal stump. It is clear that further studies are required to understand the molecular control of Schwann cell migration in vivo, and the precise involvement of c-Jun in this. The finding that c-Jun regulates Schwann cell migration in vitro may be important in the development of therapies for nerve injury, in particular for nerve conduit experiments. Chemical or genetic modulation of c-Jun activity may allow for control over the colonization or immobilization of Schwann cells in this environment.

The work presented in this thesis also demonstrates that disruption of c-Jun has significant affects on the Schwann cell cytoskeleton, with the formation of actin stress fibers and the induction of focal adhesions. This is similar to the effects of c-Jun deletion in other cell types (Jiao et al. 2008; Katiyar et al. 2007), however in the present case it is not apparent that c-Jun directly regulates the protein expression of c-Src. It is possible that c-Jun regulates the phosphorylation of this protein, and given more time, further experiments would be carried out to examine the activity and phosphorylation of c-Src, ROCKII and downstream effectors such as LIMK and cofilin-1. It would also be informative to examine the expression and activation of Lck tyrosine kinase, as the expression of this Src family member is associated with the formation of Schwann cell lamellipodia and the induction of focal adhesions (Ness et al. 2012). Analysis of gene expression of a number of candidates known to be involved in cell cytoskeleton regulation and Schwann cell migration did not

demonstrate any significant differences between control and c-Jun knockout Schwann cells. Further investigation using a microarray gene screen might uncover some genes that are regulated by c-Jun, that directly regulate the cytoskeleton, however it is also possible that c-Jun might regulate the expression of proteins with functions far removed from the cytoskeleton, that can interact with cytoskeleton proteins via signalling cascades. It is therefore probably more informative to carry out further analysis of protein activity and protein modifications in order to determine the mechanism by which c-Jun controls Schwann cell migration. I attempted to measure Rac1 and cdc42 activity using a pull-down assay, but this was unsuccessful due to technical difficulties and time constraints. The activity of these Rho GTPases might provide valuable clues into the regulation of Schwann cell morphology and migration by c-Jun.

Finally, the results herein demonstrate that the sciatic nerve partial transection model provides a reproducible and reliable method for creating a nerve gap and ensuing bridge between proximal and distal nerve stumps. Whilst this assay did not reveal any differences in Schwann cell migration between genotypes, wholemount immunostaining of the nerve stumps and bridge did allow visualisation of axonal regrowth, and showed clearly that axonal growth into the c-Jun knockout distal stump is defective. This nerve injury model may be useful in future experiments that consider outgrowth from the nerve stumps, in particular to examine how the nerve bridge is formed from migrating fibroblasts from the perineurium.

In conclusion, through the investigations described in this thesis, I have identified c-Jun as a regulator of Schwann cell migration and morphology and have demonstrated a new model of sciatic nerve transection that offers a significant improvement over the original complete transection model.

References

Abercrombie M: The outwandering of cells in tissue cultures of nerves undergoing Wallerian degeneration. J Exp Biol 19: 266-283, 1942.

Abercrombie M and Johnson ML: Quantitative histology of Wallerian degeneration; nuclear population in rabbit sciatic nerve. J Anat 80: 37-50, 1946.

Abercrombie M, Johnson ML and Thomas GA: The influence of nerve fibres on Schwann cell migration investigated in tissue culture. Proc R Soc Lond (Biol) 136: 448-460, 1949.

Abernethy DA, Thomas PK, Rud A and King RH: Mutual attraction between emigrant cells from transected denervated nerve. J Anat 184: 239-249, 1994.

Akagi K, Sandig V, Vooijs M, Van der Valk M, Giovannini M, Strauss M and Berns A: Cre-mediated somatic site-specific recombination in mice. Nucleic Acids Res 25: 1766-1773, 1997.

Anton ES, Sandrock AW Jr and Matthew WD: Merosin promotes neurite growth and Schwann cell migration *in vitro* and nerve regeneration *in vivo*: Evidence using an antibody to merosin, ARM-1. Dev Biol 164: 133-146, 1994a.

Anton ES, Weskamp G, Reichardt LF and Matthew WD: Nerve growth factor and its low-affinity receptor promote Schwann cell migration. Proc Natl Acad Sci USA 91: 2795-2799, 1994b.

Armati P: The Biology of Schwann Cells: development, differentiation and immunomodulation. Cambridge University Press, 2007.

Arthur-Farraj PJ, Latouche M, Wilton DK, Quintes S, Chabrol E, Banerjee A, Woodhoo A, Jenkins B, Rahman M, Turmaine M, Wicher GK, Mitter R, Greensmith L, Behrens A, Raivich G, Mirsky R and Jessen KR: c-Jun reprograms Schwann cells of injured nerves to generate a repair cell essential for regeneration. Neuron 75: 633-647, 2012.

Baron-Van Evercooren A, Kleinman HK, Seppä HE, Rentier B and Dubois-Dalcq M: Fibronectin promotes rat Schwann cell growth and motility. J Cell Biol 93: 211-216, 1982.

Bear JE and Gertler FB: Ena/VASP: Towards resolving a pointed controversy at the barbed end. J Cell Sci 122: 1947-1953, 2009.

Behrens A, Sibilia M, David JP, Möhle-Steinlein U, Tronche F, Schütz G and Wagner EF: Impaired postnatal hepatocyte proliferation and liver regeneration in mice lacking c-jun in the liver. EMBO J 21: 1782-90, 2002.

Beirowski B, Adalbert R and Wagner D: The progressive nature of Wallerian degeneration in wild-type and slow Wallerian degeneration (WldS) nerves. BMC Neurosci 6: Feb 2005.

Benninger Y, Thurnherr T, Pereira JA, Krause S, Wu X, Chrostek-Grashoff A, Herzog D, Nave KA, Franklin RJ, Meijer D, Brakebusch C, Suter U and Relvas JB: Essential and distinct roles for cdc42 and rac1 in the regulation of Schwann cell biology during peripheral nervous system development. J Cell Biol 177: 1051-1061, 2007.

Benowitz LI, Routtenberg A. GAP-43: an intrinsic determinant of neuronal development and plasticity. Trends Neurosci 20: 84-91, 1997.

Bentley CA and Lee KF: p75 is important for axon growth and schwann cell migration during development. J Neurosci 20: 7706-7715, 2000.

Bhattacharyya A, Frank E, Ratner N and Brackenbury R: P0 is an early marker of the Schwann cell lineage in chickens. Neuron 7: 831-844, 1991.

Bhattacharyya A, Brackenbury R and Ratner N: Axons arrest the migration of Schwann cell precursors. Development 120: 1411-1420, 1994.

Blits B, Carlstedt TP, Ruitenberg MJ, de Winter F, Hermens WT, Dijkhuizen PA, Claasens JW, Eggers R, van der Sluis R and Tenenbaum L: Rescue and sprouting of motoneurons following ventral root avulsion and reimplantation combined with intraspinal adeno-associated viral vector-mediated expression of glial cell line-derived neurotrophic factor or brain-derived neurotrophic factor. Exp Neurol 189: 303-316, 2004.

Bradley, WG and Jenkinson, M: Abnormalities of peripheral nerves in murine muscular dystrophy. J Neurol Sci 18: 227-247, 1973.

Britsch S, Li L, Kirchhoff S, Theuring F, Brinkmann V, Birchmeier C and Riethmacher D: The ErbB2 and ErbB3 receptors and their ligand, neuregulin-1, are essential for development of the sympathetic nervous system. Genes Dev 12: 1825-1836, 1998.

Brockes JP, Fields KL, Raff MC. Studies on cultured rat Schwann cells. I. Establishment of purified populations from cultures of peripheral nerve. Brain Res 165: 105-118, 1979.

Bugyi B and Carlier M-F: Control of actin filament treadmilling in cell motility. Annu Rev Biophys 39: 449-470, 2010.

Bunge RP, Bunge MB and Bates M: Movements of the Schwann cell nucleus implicate progression of the inner (axon-related) Schwann cell process during myelination. J Cell Biol 109: 273-284, 1989.

Cajal, RY: Degeneration and Regeneration of the Nervous system. Oxford University Press, London. 1928; reissued 1982.

Cajal, RY: Consideraciones crıticas sobre la teorıa de acerca de la estructura y conexiones de las celulas nerviosas. Trab Lab Invest Biol 2: 129–221, 1903. [In Spanish]

Chaudhry V and Cornblath DR: Wallerian degeneration in human nerves: Serial electrophysiological studies. Muscle Nerve 15: 687-693, 1992.

Chen Z-L, Yu W-M and Strickland S: Peripheral regeneration. Annu Rev Neurosci 30: 209-233, 2007.

Chesarone MA and Goode BL: Actin nucleation and elongation factors: Mechanisms and interplay. Curr Opin Cell Biol 21: 28-37, 2009.

Cho Y, Sloutsky R, Naegle KM and Cavalli V: Injury-induced HDAC5 nuclear export is essential for axon regeneration. Cell 155: 894-908, 2013.

Chong MS, Woolf CJ, Turmaine M, Emson PC, Anderson PN. Intrinsic versus extrinsic factors in determining the regeneration of the central processes of rat dorsal root ganglion neurons: the influence of a peripheral nerve graft. J Comp Neurol 370: 97-104, 1996.

Chong MS, Woolf CJ, Haque NS, Anderson PN. Axonal regeneration from injured dorsal roots into the spinal cord of adult rats. J Comp Neurol 410: 42-54, 1999.

Coleman MP, Conforti L, Buckmaster EA and Perry VH. An 85-kb tandem triplication in the slow Wallerian degeneration (Wlds) mouse. Proc Natl Acad Sci USA 95: 9985-9990. 1998

Conforti L, Tarlton A, Mack TGA, Mi W, Buckmaster EA, Wagner D and Coleman MP: (2000). A Ufd2/D4Cole1e chimeric protein and overexpression of Rbp7 in the slow Wallerian degeneration (WldS) mouse. Proc Natl Acad Sci USA 97: 11377-11382, 2000.

Conklin EG: Effects of centrifugal force on the structure and development of the eggs of Crepidula. J Exp Zool 22: 311-419, 1917.

Cramer LP: Mechanism of cell rear retraction in migrating cells. Curr Opin Cell Biol 25: 591-599, 2013.

Curtis R, Stewart HJ, Hall SM, Wilkin GP, Mirsky R and Jessen KR: GAP-43 is expressed by nonmyelin-forming Schwann cells of the peripheral nervous system. J Cell Biol 116: 1455-1464, 1992.

David S and Aguayo AJ: Axonal elongation into peripheral nervous system "bridges" after central nervous system injury in adult rats. Science 214: 931-933, 1981.

De Robertis E and Schmitt FO: The effect of nerve degeneration on the structure of neurotubules. J Cell Physiol 32: 45-56, 1948.

Dong Z, Brennan A, Liu N, Yarden Y, Lefkowitz G, Mirsky R and Jessen KR: Neu differentiation factor is a neuron-glia signal and regulates survival, proliferation, and maturation of rat Schwann cell precursors. Neuron 15: 585-596, 1995.

Dong Z, Sinanan A, Parkinson D, Parmantier E, Mirsky R and Jessen KR: Schwann cell development in embryonic mouse nerves. J Neurosci Res 56: 334-348, 1999.

Egeblad M and Werb Z: New functions for the matrix metalloproteinases in cancer progression. Nat Rev Cancer 2: 161-174, 2002.

Erdman R, Stahl RC, Rothblum K, Chernousov MA and Carey DJ: Schwann cell adhesion to a novel heparan sulfate binding site in the N-terminal domain of alpha 4 type V collagen is mediated by syndecan-3. J Biol Chem 277: 7619-7625, 2002.

Erez H, Malkinson G, Prager-Khoutorsky M, De Zeeuw CI, Hoogenraad CC and Spira ME: Formation of microtubule-based traps controls the sorting and concentration of vesicles to restricted sites of regenerating neurons after axotomy. J Cell Biol 176: 497-507, 2007.

Etienne-Manneville S and Hall A: Rho GTPases in cell biology. Nature 420: 629-635, 2002.

Feltri ML and Wrabetz L: Laminins and their receptors in Schwann cells and hereditary neuropathies. J Peripher Nerv Syst 10: 128-143, 2005.

Feltri ML, Graus Porta D, Previtali SC, Nodari A, Migliavacca B, Cassetti A, Littlewood-Evans A, Reichardt LF, Messing A, Quattrini A, Mueller U and Wrabetz L: Conditional disruption of beta 1 integrin in Schwann cells impedes interactions with axons. J Cell Biol 156: 199-209, 2002.

Feltri ML, Suter U and Relvas JB: The function of RhoGTPases in axon ensheathment and myelination. Glia 56: 1508-1517, 2008.

Feltri ML, Poitelon Y, Previtali SC. How Schwann Cells Sort Axons: New Concepts. Neuroscientist pii: 1073858415572361 [Epub ahead of print], 2015.

Fernandez-Valle C, Gorman D, Gomez AM and Bunge MB: Actin plays a role in both changes in cell shape and gene-expression associated with Schwann cell myelination. J Neurosci 17: 241-250, 1997.

Fernandez-Valle C, Gwynn L, Wood PM, Carbonetto S and Bunge MB: Anti-beta 1 integrin antibody inhibits Schwann cell myelination. J Neurobiol 25: 1207-1226, 1994.

Flemming W: Beiträge zur Kenntniss der Zelle und Ihrer Lebenserscheinungen. Arch Mikroskopische Anat 18: 151-259, 1880.

Fontana X, Hristova M, Da Costa C, Patodia S, Thei L, Makwana M, Spencer-Dene B, Latouche M, Mirsky R, Jessen KR, Klein R, Raivich G and Behrens A: c-Jun in Schwann cells promotes axonal regeneration and motoneuron survival via paracrine signaling. J Cell Biol 198: 127-141, 2012.

Freud S: Über den Bau der Nervenfasern und Nervenzellen beim Flusskrebs. Sitzungsberichte der kaiserliche Akademie der Wissenschaften (Vienna) 85:9-46, 1882. [In German]

Fricker FR, Antunes-Martins A, Galino J, Paramsothy R, La Russa F, Perkins J, Goldberg R, Brelstaff J, Zhu N, McMahon SB, Orengo C, Garratt AN, Birchmeier C and Bennett DL: Axonal neuregulin 1 is a rate limiting but not essential factor for nerve remyelination. Brain 136: 2279-2297, 2013.

Fricker FR, Lago N, Balarajah S, Tsantoulas C, Tanna S, Zhu N, Fageiry SK, Jenkins M, Garratt AN and Birchmeier C: Axonally derived neuregulin-1 is required for

remyelination and regeneration after nerve injury in adulthood. J Neurosci 31: 3225-3233, 2011.

Friede RL and Bischhausen R: The fine structure of stumps of transected nerve fibers in subserial sections. J Neurol Sci 44: 181-203, 1980.

Frixione E: Recurring views on the structure and function of the cytoskeleton: A 300-year epic. Cell Motil Cytoskeleton 46: 73-94, 2000.

Funakoshi H, Frisén J, Barbany G, Timmusk T, Zachrisson O, Verge VM and Persson H: Differential expression of mRNAs for neurotrophins and their receptors after axotomy of the sciatic nerve. J Cell Biol 123: 455-465, 1993.

Gaudet AD, Popovich PG and Ramer MS: Wallerian degeneration: Gaining perspective on inflammatory events after peripheral nerve injury. J Neuroinflammation 8: 110, 2011.

Gilles C, Polette M, Zahm JM, Tournier JM, Volders L, Foidart JM and Birembaut P: Vimentin contributes to human mammary epithelial cell migration. J Cell Sci 112: 4615-4625, 1999.

Gilmour DT, Maischein H-M and Nüsslein-Volhard C: Migration and function of a glial subtype in the vertebrate peripheral nervous system. Neuron 34: 577-588, 2002.

Glise B and Noselli S: Coupling of Jun amino-terminal kinase and Decapentaplegic signaling pathways in Drosophila morphogenesis. Genes Dev 11: 1738-1747, 1997.
Gray EG and Guillery RW: The basis for silver staining of synapses of the mammalian spinal cord: A light and electron microscope study. J Physiol 157: 581-588, 1961.

Grim M, Halata Z and Franz T: Schwann cells are not required for guidance of motor nerves in the hindlimb in Splotch mutant mouse embryos. Anat Embryol (Berl) 186: 311-318, 1992.

Grossmann KS, Wende H, Paul FE, Cheret C, Garratt AN, Zurborg S, Feinberg K, Besser D, Schulz H and Peles E: The tyrosine phosphatase Shp2 (PTPN11) directs Neuregulin-1/ErbB signaling throughout Schwann cell development. Proc Natl Acad Sci USA 106: 16704-16709, 2009.

Grove M, Komiyama NH, Nave KA, Grant SG, Sherman DL and Brophy PJ: FAK is required for axonal sorting by Schwann cells. J Cell Biol 176: 277-282, 2007.

Guo L, Moon C, Niehaus K, Zheng Y and Ratner N: Rac1 controls Schwann cell myelination through cAMP and NF2/merlin. J Neurosci 32: 17251-17261, 2012.

Hall A: Rho GTPases and the actin cytoskeleton. Science 279: 509-514, 1998.

Hayworth CR, Moody SE, Chodosh LA, Krieg P, Rimer M and Thompson WJ: Induction of neuregulin signaling in mouse schwann cells *in vivo* mimics responses to denervation. J Neurosci 26: 6873-6884, 2006.

Heumann R, Lindholm D, Bandtlow C, Meyer M, Radeke MJ, Misko TP, Shooter E and Thoenen H: Differential regulation of mRNA encoding nerve growth factor and its

receptor in rat sciatic nerve during development, degeneration, and regeneration: Role of macrophages. Proc Natl Acad Sci USA 84: 8735-8739, 1987.

Holmes W and Young JZ: Nerve regeneration after immediate and delayed suture. J Anat 77: 63-96, 1942.

Holmes W, Sanders F and Young J: Nerve regeneration: Importance of the peripheral stump and the value of nerve grafts. Lancet, 1940.

Hou XS, Goldstein ES and Perrimon N: Drosophila Jun relays the Jun amino-terminal kinase signal transduction pathway to the Decapentaplegic signal transduction pathway in regulating epithelial cell sheet movement. Genes Dev 11: 1728-1737, 1997.

Howard MJ, David G and Barrett JN: Resealing of transected myelinated mammalian axons *in vivo*: Evidence for involvement of calpain. Neuroscience 93: 807-815, 1999.

Hulkower KI and Herber RL: Cell Migration and Invasion Assays as Tools for Drug Discovery. Pharmaceutics 3: 107-124, 2011.

Huxley, TH: An introduction to the study of zoology, illustrated by the crayfish. Appleton, New York (reissued by MIT Press, 1974), 1880.

Ingebrigtsen R: Studies of the degeneration and regeneration of axis cylinders *in vitro*. J Exp Med 17: 182-191, 1913.

Ishikawa H, Bischoff R and Holtzer H: Formation of arrowhead complexes with heavy meromyosin in a variety of cell types. J Cell Biol 43: 312-328, 1969.

Janowski E, Jiao X, Katiyar S, Lisanti MP, Liu M, Pestell RG and Morad M: c-Jun is required for TGF-β-mediated cellular migration via nuclear Ca^{2+} signaling. Int J Biochem Cell Biol 43: 1104-1113, 2011.

Jessen KR and Mirsky R: The origin and development of glial cells in peripheral nerves. Nat Rev Neurosci 6: 671-682, 2005.

Jessen KR, Brennan A, Morgan L, Mirsky R, Kent A, Hashimoto Y and Gavrilovic J: The Schwann cell precursor and its fate: A study of cell death and differentiation during gliogenesis in rat embryonic nerves. Neuron 12: 509-527, 1994.

Jiao X, Katiyar S, Willmarth NE, Liu M, Ma X, Flomenberg N, Lisanti MP and Pestell RG. c-Jun induces mammary epithelial cellular invasion and breast cancer stem cell expansion. J Biol Chem 12: 8218-8226, 2010.

Jiao X, Katiyar S, Liu M, Mueller SC, Lisanti MP, Li A, Pestell TG, Wu K, Ju X and Pestell RG: Disruption of c-Jun reduces cellular migration and invasion through inhibition of c-Src and hyperactivation of ROCK II kinase. Mol Biol Cell 19: 1378-1390, 2008.

Katiyar S, Jiao X, Wagner E, Lisanti MP and Pestell RG: Somatic excision demonstrates that c-Jun induces cellular migration and invasion through induction of stem cell factor. Mol Cell Biol 27: 1356-1369, 2007.

Klämbt C: Modes and regulation of glial migration in vertebrates and invertebrates. Nat Rev Neurosci 10: 769-779, 2009.

Le Douarin N and Kalcheim C: The Neural Crest. Cambridge University Press, 1999.

Lefcort F, Venstrom K, McDonald JA and Reichardt LF: Regulation of expression of fibronectin and its receptor, alpha 5 beta 1, during development and regeneration of peripheral nerve. Development 116: 767-782, 1992.

Lo CM, Wang HB, Dembo M and Wang YL. Cell movement is guided by the rigidity of the substrate. Biophysical Journal 79: 144-152, 2000.

Lohman FP, Gibbs S, Fischer DF, Borgstein AM, van de Putte P and Backendorf C: Involvement of c-Jun in the regulation of terminal differentiation genes in normal and malignant keratinocytes. Oncogene 14: 1623-1627, 1997.

Lubińska L: Early course of Wallerian degeneration in myelinated fibres of the rat phrenic nerve. Brain Res 130: 47-63, 1977.

Lunn ER, Perry VH, Brown MC, Rosen H and Gordon S: Absence of Wallerian Degeneration does not Hinder Regeneration in Peripheral Nerve. Eur J Neurosci 1: 27-33, 1989.

Lyon MF, Ogunkolade BW, Brown MC, Atherton DJ, Perry VH: A gene affecting Wallerian nerve degeneration maps distally on mouse chromosome 4. Proc Natl Acad Sci USA 90: 9717-9720, 1993.

Lyons DA, Pogoda HM, Voas MG, Woods IG, Diamond B, Nix R, Arana N, Jacobs J and Talbot WS: Erbb3 and erbb2 are essential for schwann cell migration and myelination in zebrafish. Curr Biol 15: 513-524, 2005.

Machesky LM, Mullins RD, Higgs HN, Kaiser DA, Blanchoin L, May RC, Hall ME and Pollard TD: Scar, a WASp-related protein, activates nucleation of actin filaments by the Arp2/3 complex. Proc Natl Acad Sci USA 96: 3739-3744, 1999.

Mack TG, Reiner M, Beirowski B, Mi W, Emanuelli M, Wagner D, Thomson D, Gillingwater T, Court F, Conforti L, Fernando FS, Tarlton A, Andressen C, Addicks K, Magni G, Ribchester RR, Perry VH, Coleman MP. Wallerian degeneration of injured axons and synapses is delayed by a Ube4b/Nmnat chimeric gene. Nat Neurosci 12: 1199-1206, 2001.

Mahanthappa NK, Anton ES and Matthew WD: Glial growth factor 2, a soluble neuregulin, directly increases Schwann cell motility and indirectly promotes neurite outgrowth. J Neurosci 16: 4673-4683, 1996.

Mandolesi G, Madeddu F, Bozzi Y, Maffei L and Ratto GM: Acute physiological response of mammalian central neurons to axotomy: ionic regulation and electrical activity. FASEB 18: 1934-1936, 2004.

Maro GS, Vermeren M, Voiculescu O, Melton L, Cohen J, Charnay P and Topilko P: Neural crest boundary cap cells constitute a source of neuronal and glial cells of the PNS. Nat Neurosci 7: 930-938, 2004.

Martín-Blanco E, Gampel A, Ring J, Virdee K, Kirov N, Tolkovsky AM and Martinez-Arias A: puckered encodes a phosphatase that mediates a feedback loop regulating JNK activity during dorsal closure in Drosophila. Genes Dev 12: 557-570, 1998.

Masson P: Experimental and Spontaneous Schwannomas (Peripheral Gliomas): I. Experimental Schwannomas. Am J Pathol 8: 367-388, 1932.

Mayor R, Carmona-Fontaine C. Keeping in touch with contact inhibition of locomotion. Trends in Cell Biology 20: 319-328, 2010.

Meintanis S, Thomaidou D, Jessen KR, Mirsky R and Matsas R: The neuron-glia signal beta-neuregulin promotes Schwann cell motility via the MAPK pathway. Glia 34: 39-51, 2001.

Meyer M, Matsuoka I, Wetmore C, Olson L and Thoenen H: Enhanced synthesis of brain-derived neurotrophic factor in the lesioned peripheral nerve: Different mechanisms are responsible for the regulation of BDNF and NGF mRNA. J Cell Biol 119: 45-54, 1992.

Milner R, Wilby M, Nishimura S, Boylen K, Edwards G, Fawcett J, Streuli C, Pytela R and ffrench-Constant C: Division of labor of Schwann cell integrins during migration on peripheral nerve extracellular matrix ligands. Dev Biol 185: 215-228, 1997.

Mirsky R, Parkinson, DB, Dong, Z, Meier, C, Calle, E, Brennan, A, Topilko, P, Harris, BS, Stewart, HJS, Jessen, KR: Regulation of genes involved in Schwann cell development and differentiation. In: Progress in Brain Research. Progress in Brain Research 132: 3-11, 2001.

Montani L, Buerki-Thurnherr T, de Faria JP, Pereira JA, Dias NG, Fernandes R, Gonçalves AF, Braun A, Benninger Y, Böttcher RT, Costell M, Nave KA, Franklin RJ, Meijer D, Suter U, Relvas JB. Profilin 1 is required for peripheral nervous system myelination. Development 141: 1553-1561, 2014.

Moore PB, Huxley HE and DeRosier DJ: Three-dimensional reconstruction of F-actin, thin filaments and decorated thin filaments. J Mol Biol 50: 279-295, 1970.

Morgan, L, Jessen KR, and Mirsky R: The effects of cAMP on differentiation of cultured Schwann cells: Progression from an early phenotype (04+) to a myelin phenotype (P0+, GFAP–, N-CAM–, NGF-receptor–) depends on growth inhibition. J Cell Biol 112: 457–467, 1991.

Morris, JH, Hudson, AR and Weddell, G: A study of degeneration and regeneration in the divided rat sciatic nerve based on electron microscopy: Changes in the axons of the proximal stump. Z Zellforschung Mik Ana 124: 131-164, 1972.

Morris JK, Lin W, Hauser C, Marchuk Y, Getman D and Lee KF: Rescue of the cardiac defect in ErbB2 mutant mice reveals essential roles of ErbB2 in peripheral nervous system development. Neuron 23: 273-283, 1999.

Ness JK, Snyder KM, Tapinos N. Lck tyrosine kinase mediates β1-integrin signalling to regulate Schwann cell migration and myelination. Nat Commun 4: 1912, 2012,

Neumann S and Woolf CJ: Regeneration of dorsal column fibers into and beyond the lesion site following adult spinal cord injury. Neuron 23: 83-91, 1999.

Nodari A, Zambroni D, Quattrini A, Court FA, D'Urso A, Recchia A, Tybulewicz VL, Wrabetz L and Feltri ML: Beta1 integrin activates Rac1 in Schwann cells to generate radial lamellae during axonal sorting and myelination. J Cell Biol 177: 1063-1075, 2007.

Oudega M, Varon S, Hagg T. Regeneration of adult rat sensory axons into intraspinal nerve grafts: promoting effects of conditioning lesion and graft predegeneration. Exp Neurol 129: 194-206, 1994.

Parkinson DB, Bhaskaran A, Arthur-Farraj P, Noon LA, Woodhoo A, Lloyd AC, Feltri ML, Wrabetz L, Behrens A, Mirsky R and Jessen KR: c-Jun is a negative regulator of myelination. J Cell Biol 181: 625-637, 2008.

Parkinson DB, Dong Z, Bunting H, Whitfield J, Meier C, Marie H, Mirsky R and Jessen KR: Transforming growth factor beta (TGFbeta) mediates Schwann cell death *in vitro* and *in vivo*: Examination of c-Jun activation, interactions with survival signals, and the relationship of TGFbeta-mediated death to Schwann cell differentiation. J Neurosci 21: 8572-8585, 2001.

Parrinello S, Napoli I, Ribeiro S, Wingfield Digby P, Fedorova M, Parkinson DB, Doddrell RD, Nakayama M, Adams RH and Lloyd AC: EphB signaling directs peripheral nerve regeneration through Sox2-dependent Schwann cell sorting. Cell 143: 145-155, 2010.

Pellegrin S and Mellor H: Actin stress fibres. J Cell Sci 120: 3491-3499, 2007.

Pereira JA, Benninger Y, Baumann R, Gonçalves AF, Ozçelik M, Thurnherr T, Tricaud N, Meijer D, Fässler R, Suter U and Relvas JB: Integrin-linked kinase is required for radial sorting of axons and Schwann cell remyelination in the peripheral nervous system. J Cell Biol 185: 147-161, 2009.

Perlin JR, Lush ME, Stephens WZ, Piotrowski T, Talbot WS. Neuronal Neuregulin 1 type III directs Schwann cell migration. Development 138: 4639-4648, 2011

Perry VH, Tsao JW, Fearn S and Brown MC: Radiation-induced reductions in macrophage recruitment have only slight effects on myelin degeneration in sectioned peripheral nerves of mice. Eur J Neurosci 7: 271-280, 1995.

Perry VH, Brown MC and Lunn ER: Very Slow Retrograde and Wallerian Degeneration in the CNS of C57BL/Ola Mice. Eur J Neurosci 3: 102-105, 1991.

Peters RA: Surface structure in the integration of cell activity. Trans Faraday Soc 26: 797-807, 1930.

Politis MJ, Ederle K and Spencer PS: Tropism in nerve regeneration *in vivo*. Attraction of regenerating axons by diffusible factors derived from cells in distal nerve stumps of transected peripheral nerves. Brain Res 253: 1-12, 1982.

Pollard TD and Borisy GG: Cellular motility driven by assembly and disassembly of actin filaments. Cell 112: 453-465, 2003.

Pring M, Evangelista M, Boone C, Yang C and Zigmond SH: Mechanism of formin-induced nucleation of actin filaments. Biochemistry 42: 486-496, 2003.

Quinlan ME, Heuser JE, Kerkhoff E and Mullins RD: Drosophila Spire is an actin nucleation factor. Nature 433: 382-388, 2005.

Raivich G, Bohatschek M, Da Costa C, Iwata O, Galiano M, Hristova M, Nateri AS, Makwana M, Riera-Sans L, Wolfer DP, Lipp HP, Aguzzi A, Wagner EF and Behrens A: The AP-1 transcription factor c-Jun is required for efficient axonal regeneration. Neuron 43: 57-67, 2004.

Raftopoulou M and Hall A: Cell migration: Rho GTPases lead the way. Dev Biol 265: 23-32, 2004.

Remak R: Neurologische Erläuterungen. Arch Anat Physiol Wiss Med 12: 463–472, 1844. [In German]

Revenu C, Athman R, Robine S and Louvard D: The co-workers of actin filaments: From cell structures to signals. Nat Rev Mol Cell Biol 5: 635-646, 2004.

Rexed B: Uber die Aktivitat der Schwannschen Zellen bei der Nervenregeneration. I. Dieuberbrucking neuritloser Nervenlucken. Z Mik Forsch 51: 177-183, 1942. [In German]

Richardson PM and Issa VM: Peripheral injury enhances central regeneration of primary sensory neurones. Nature 309: 791-793, 1984.

Richardson PM, McGuinness UM and Aguayo AJ: Axons from CNS neurons regenerate into PNS grafts. Nature 284: 264-265, 1980.

Riesgo-Escovar JR and Hafen E: Common and distinct roles of DFos and DJun during Drosophila development. Science 278: 669-672, 1997a.

Riesgo-Escovar JR and Hafen E: Drosophila Jun kinase regulates expression of decapentaplegic via the ETS-domain protein Aop and the AP-1 transcription factor DJun during dorsal closure. Genes Dev 11: 1717-1727, 1997b.

Riethmacher D, Sonnenberg-Riethmacher E, Brinkmann V, Yamaai T, Lewin GR and Birchmeier C: Severe neuropathies in mice with targeted mutations in the ErbB3 receptor. Nature 389: 725-730, 1997.

Rishal I and Fainzilber M: Axon-soma communication in neuronal injury. Nat Rev Neurosci 15: 32-42, 2014.

Rubino S, Fighetti M, Unger E and Cappuccinelli P: Location of actin, myosin, and microtubular structures during directed locomotion of Dictyostelium amebae. J Cell Biol 98: 382-390, 1984.

Schmitt FO and Geren BB: The fibrous structure of the nerve axon in relation to the localization of "neurotubules". J Exp Med 91: 499-504, 1950.

Sepp KJ and Auld VJ: RhoA and Rac1 GTPases mediate the dynamic rearrangement of actin in peripheral glia. Development 130: 1825-1835, 2003.

Sepp KJ, Schulte J and Auld VJ: Developmental dynamics of peripheral glia in Drosophila melanogaster. Glia 30: 122-133, 2000.

Shin JE, Cho Y, Beirowski B, Milbrandt J, Cavalli V and DiAntonio A: Dual leucine zipper kinase is required for retrograde injury signaling and axonal regeneration. Neuron 74: 1015-1022, 2012.

Shy ME, Shi Y, Wrabetz L, Kamholz J and Scherer SS: Axon-Schwann cell interactions regulate the expression of c-jun in Schwann cells. J Neurosci Res 43: 511-525, 1996.

Sparrow N, Manetti ME, Bott M, Fabianac T, Petrilli A, Bates ML, Bunge MB, Lambert S and Fernandez-Valle C: The actin-severing protein cofilin is downstream of neuregulin signaling and is essential for Schwann cell myelination. J Neurosci 32: 5284-5297, 2012.

Speidel C: Studies of living nerves. I. The movements of individual sheath cells and nerve sprouts correlated with the process of myelin-sheath formation in amphibian larvae. J Exp Zool 61: 279-331, 1932.

Stassart RM, Fledrich R, Velanac V, Brinkmann BG, Schwab MH, Meijer D, Sereda MW and Nave KA: A role for Schwann cell-derived neuregulin-1 in remyelination. Nat Neurosci 16: 48-54, 2013.

Stewart HJ: Expression of c-Jun, Jun B, Jun D and cAMP response element binding protein by Schwann cells and their precursors *in vivo* and *in vitro*. Eur J Neurosci. 7: 1366-1375, 1995.

Straub FB: Actin, II. Stud Inst Med Chem Univ Szeged, 1943.

Takatori A, Geh E, Chen L, Zhang L, Meller J and Xia Y: Differential transmission of MEKK1 morphogenetic signals by JNK1 and JNK2. Development 135: 23-32, 2008.

Takeda S, Minakata S, Koike R, Kawahata I, Narita A, Kitazawa M, Ota M, Yamakuni T, Maéda Y and Nitanai Y: Two distinct mechanisms for actin capping protein regulation--steric and allosteric inhibition. PLoS Biol 8: e1000416, 2010.

Taskinen HS, Röyttä M. Increased expression of chemokines (MCP-1, MIP-1alpha, RANTES) after peripheral nerve transection. J Peripher Nerv Syst 5: 75-81, 2000.

Thomas PK: The cellular response to nerve injury. 1. The cellular outgrowth from the distal stump of transected nerve. J Anat 100: 287-303, 1966.

Tojkander S, Gateva G and Lappalainen P: Actin stress fibers--assembly, dynamics and biological roles. J Cell Sci 125: 1855-1864, 2012.

Valerius NH, Stendahl OI, Hartwig JH, Stossel TP and Keller HU: Distribution of actin-binding protein and myosin in neutrophils during chemotaxis and phagocytosis. Adv Exp Med Biol 141: 19-28, 1982.

Vargas ME and Barres BA: Why is Wallerian degeneration in the CNS so slow? Annu Rev Neurosci 30: 153-179, 2007.

Vleugel MM, Greijer AE, Bos R, van der Wall E and van Diest PJ: c-Jun activation is associated with proliferation and angiogenesis in invasive breast cancer. Hum Pathol 37: 668-674, 2006.

Vuoriluoto K, Haugen H, Kiviluoto S, Mpindi JP, Nevo J, Gjerdrum C, Tiron C, Lorens JB and Ivaska J: Vimentin regulates EMT induction by Slug and oncogenic H-Ras and migration by governing Axl expression in breast cancer. Oncogene 30: 1436-1448, 2011.

Wakatsuki S, Araki T, Sehara-Fujisawa A. Neuregulin-1/glial growth factor stimulates Schwann cell migration by inducing α5 β1 integrin-ErbB2-focal adhesion kinase complex formation. Genes Cells 19: 66-77, 2014.

Waller, A: Experiments on the section of the glossopharyngeal and hypoglossal nerves of the frog, and observations of the alterations produced thereby in the structure, Philos Trans R Soc Lond 140, 423-429, 1850.

Wang H, Tewari A, Einheber S, Salzer JL and Melendez-Vasquez CV: Myosin II has distinct functions in PNS and CNS myelin sheath formation. J Cell Biol 182: 1171-1184, 2008.

Wanner IB, Guerra NK, Mahoney J, Kumar A, Wood PM, Mirsky R and Jessen KR: Role of N-cadherin in Schwann cell precursors of growing nerves. Glia 54: 439-459, 2006a.

Wanner IB, Mahoney J, Jessen KR, Wood PM, Bates M and Bunge MB: Invariant mantling of growth cones by Schwann cell precursors characterize growing peripheral nerve fronts. Glia 54: 424-438, 2006b.

Webster H and Favilla JT: Development of peripheral nerves. In: Peripheral neuropathy. Dyck PJ (ed). W B Saunders Co., Philadelphia, 1984.

Williams PL and Hall SM: Prolonged in vivo observations of normal peripheral nerve fibres and their acute reactions to crush and deliberate trauma. J Anat 108: 397-408, 1971.

Woldeyesus MT, Britsch S, Riethmacher D, Xu L, Sonnenberg-Riethmacher E, Abou-Rebyeh F, Harvey R, Caroni P, Birchmeier C: Peripheral nervous system defects in erbB2 mutants following genetic rescue of heart development. Genes Dev 13: 2538-2548, 1999.

Yamauchi J, Miyamoto Y, Chan JR and Tanoue A: ErbB2 directly activates the exchange factor Dock7 to promote Schwann cell migration. J Cell Biol 181: 351-365, 2008.

Yamauchi J, Chan JR and Shooter EM: Neurotrophin 3 activation of TrkC induces Schwann cell migration through the c-Jun N-terminal kinase pathway. Proc Natl Acad Sci USA 100: 14421-14426, 2003.

Yamauchi J, Chan JR and Shooter EM: Neurotrophins regulate Schwann cell migration by activating divergent signaling pathways dependent on Rho GTPases. Proc Natl Acad Sci USA 101: 8774-8779, 2004.

Yang DP, Zhang DP, Mak KS, Bonder DE, Pomeroy SL and Kim HA: Schwann cell proliferation during Wallerian degeneration is not necessary for regeneration and remyelination of the peripheral nerves: Axon-dependent removal of newly generated Schwann cells by apoptosis. Mol Cell Neurosci 38: 80-88, 2008.

Zenz R, Scheuch H, Martin P, Frank C, Eferl R, Kenner L, Sibilia M and Wagner EF: c-Jun regulates eyelid closure and skin tumor development through EGFR signaling. Dev Cell 4: 879-889, 2003.

Zochodne D: Nerve regeneration and repair. JPNS, 8: 59-60, 2003.

Zochodne D: Experimental Neurology: The nerve regenerative microenvironment: Early behavior and partnership of axons and Schwann cells. Exp Neurol, 2010.

Zochodne D. Neurobiology of Peripheral Nerve Regeneration. First Edition Cambridge University Press, New York. 2008.

Appendix

Primer	Sequence (5' to 3')	Conc., nmol rev/fw	Source
GAPDH fwd	AGGTCGGTGTGAACGGATTTG	200/300	D. Wilton, Jessen lab
GAPDH rev	TGTAGACCATGTAGTTGAGGTCA		
YWHAZ fwd	TAAATGGTCTGTCACCGTCT	200/300	Sigma-Aldrich OligoArchitect™
YWHAZ rev	GGAAATACTCGGTAGGGTGT		
c-Jun fwd	AATGGGCACATCACCACTACAC	200/200	M.L-Hartmann Jessen lab
c-Jun rev	TGCTCGTCGGTCACGTTCT		
Vinculin fwd	CTTCGATGAGGCTGAGGTTC	200/300	Primer 3 Plus
Vinculin rev	TGGTGAGTCAACTCCTGCTG		
FAK fwd	CGTGAAGCCTTTTCAAGGAG	200/200	Primer 3 Plus
FAK rev	TCCATCCTCATCCGTTCTTC		
Src fwd	TGTAGCCATGACAGGCTGAG	300/200	Primer 3 Plus
Src rev	CATGGTCCTGGCTGATAGGT		
Profilin fwd	TGACCTCATCTGTCCCTTCC	200/200	Primer 3 Plus
Profilin rev	ACAGGAGGGGGTATGGGTAG		
Cofilin1 fwd	TGCTGCCAACTTCTAACC	200/300	Primer 3 Plus
Cofilin1 rev	GTCATTTCCACATTTCATTTACAC		
Paxillin fwd	CAACTTCGTATGGCTCAA	200/300	Primer 3 Plus
Paxillin rev	CAAGGACAGACCAGAGTA		
MYLK fwd	GACGTGTTCACCCTGGTTCT	150/200	Sigma-Aldrich OligoArchitect™
MYLK rev	GTCACCATCACCATGAGCAC		
LIMK1 fwd	TGCTCAAGTTCATCGGAGTG	300/200	Primer 3 Plus
LIMK1 rev	TTCATCGAATGGAGGTAGGC		
WASP fwd	CCTGGCCCAACTGATAAGAA	200/200	Sigma-Aldrich OligoArchitect™
WASP rev	AGACCTCCCTGGTCCTCAAT		
Actn1 fwd	GGCAAGATGAGAGTGCACAA	200/200	Primer 3 Plus
Actn1 rev	AGATGTCCTGGATGGCAAAG		
SRF fwd	ATGCCCCATCCCTTAAAATC	200/300	Primer 3 Plus
SRF rev	CGCAGAAGTAGGCTTGTTCC		
ROCK2 fwd	CTGAATGAAATGCAGGCTCA	300/200	Sigma-Aldrich OligoArchitect™
ROCK2 rev	CACAGGCAATGACAACCATC		
NRG1 I fwd	GGGAAGGGCAAGAAGAAGG	200/300	Stassart et al., 2012
NRG1 I rev	TTTCACACCGAAGCACGAGC		
NRGI II fwd	CCTCGTTTCCTCCGCTG	200/200	Stassart et al., 2012
NRGI II rev	GACTCCTGGCTTTTCATCTCTT		
NRGI III fwd	ACTCAGCCACAAACAACAGAAAC	200/200	Stassart et al., 2012
NRGI III rev	GAAGCACTCGCCTCCATT		
ErbB2 fw	GAGACAGAGCTAAGGAAGCTGA	300/200	Primer 3 Plus
ErbB2 rew	ACGGGGATTTTCACGTTCTCC		
ErbB3 fw	AAGTGACAGGCTATGTACTGGT	200/200	Primer 3 Plus
ErbB3 rev	GCTGGAGTTGGTATTGTAGTTCA		
Shp2 fw	CATGGCAGCTTCCTCGTTC	200/200	Primer 3 Plus
Shp2 rev	TCCCCTTTGTCGTCACCAGT		
GDNF fw	GATTCGGGCCACTTGGAGTT	200/200	M.L-Hartmann Jessen lab
GDNF rev	GACAGCCACGACATCCCATA		
Olig1 fw	CCGCCCCAGATGTACTATGC	200/300	M.L-Hartmann Jessen lab
Olig1 rev	AACCCACCAGCTCATACAGC		
MBP fw	TCACAGCGATCCAAGTACCTG	300/200	Primer Bank
MBP rev	CCCCTGTCACCGCTAAAGAA		
MAL fw	TTTGTGAGTTTGTCTTTGGAGGC	200/300	PrimerBank

MAL rev	CCGCCATGAGTACCAATTATGT		
SSH1 fw	ACCTTCTGCGTTGCGAAGAC	200/200	PrimerBank
SSH1 rev	AGGTGGATTTTCGTGTCGCTC		
Gelsolin fw	TCACGGGTGATGCCTATGTCA	200/300	Primer 3 Plus
Gelsolin rev	AGCCAATAGTGGAGGTCATACTG		
NF2 fw	GCTCCCGAAAAGGGTGATAAA	200/300	Primer 3 Plus
NF2 rev	GCATACCAAGCCGTAATTCTCTC		
WASF1 fw	ATGCCGTTGGTGAAAAGAAACA	300/200	Primer 3 Plus
WASF1 rev	ACACTAACAGACAATCGGTCCA		
ARP3 fw	CGCTGACGGGTACAGTAATAGA	200/300	Primer 3 Plus
ARP3 rev	TCCTGCGATTGGAATGTGTTTA		
Krox20 fw	GCCAAGGCCGTAGACAAAATC	300/200	M.L-Hartmann Jessen lab
Krox20 rev	CCACTCCGTTCATCTGGTCA		
Talin1 fw	TACTACATGCTCCGAAATGGGG	200/200	Primer 3 Plus
Talin1 rev	CACCGTTCCGTCTAACATCCG		
Villin1 fw	TCAAAGGCTCTCTCAACATCAC	200/200	Primer 3 Plus
Villin1 rev	AGCAGTCACCATCGAAGAAGC		
Beta-catenin f	ATGGAGCCGGACAGAAAAGC	200/200	Primer 3 Plus
Beta catenin r	CTTGCCACTCAGGGAAGGA		
Adam23 fw	CTTTCGGCTCCAAGTTCATTCT	300/200	Primer 3 Plus
Adam23 rev	TCCCGTCTTCATAGTGGATCTC		
TSC2 fw	TGCCGCAGCATCAGTGTATC	200/300	Sigma-Aldrich OligoArchitect™
TSC2 rev	TGCCAGGAGGAACTCTCCC		
REST fw	GGCAGATGGCCGAATTGATG	300/200	Sigma-Aldrich OligoArchitect™
REST rev	CTTTGAGGTCAGCCGACTCT		
Cadherin1 fw	CAGGTCTCCTCATGGCTTTGC	200/200	Primer 3 Plus
Cadherin1 rv	CTTCCGAAAAGAAGGCTGTCC		
RhoA fw	AGCTTGTGGTAAGACATGCTTG	200/200	PrimerBank
RhoA rev	GTGTCCCATAAAGCCAACTCTAC		
Rac1 fw	GAGACGGAGCTGTTGGTAAAA	300/200	Primer 3 Plus
Rac1 rev	ATAGGCCCAGATTCACTGGTT		
Cdc42 fw	CCCATCGGAATATGTACCAACTG	200/300	Primer 3 Plus
Cdc42 rev	CCAAGAGTGTATGGCTCTCCAC		

Gene	C(t) value
GAPDH	26
YWHAZ	24
c-JUN	24
Vinculin	23
FAK	28
SRC	26
Profilin	27
Cofilin1	27
Paxillin	23
MYLK	26
LIMK	23
WASP	21
Actn1	24
SRF	24
ROCK1	20
ROCK2	25
NRG1 I	34

NRG1 II	33
NRG1 III	25
ErbB2	29
ErbB3	28
Shp2	25
GDNF	26
Olig1	21
MBP	23
MAL	23
SSH1	29
Gelsolin	27
NF2	29
WASF1	29
ARP3	25
Krox20	24
Talin1	23
Villin1	27
Beta-catenin	26
Adam23	26
TSC2	21
REST	24
Cad1	26
RhoA	29
Rac1	24
Cdc42	23